UNIVERSITÀ DEGLI STUDI DI PADOVA

DIPARTIMENTO DI INGEGNERIA DELL'INFORMAZIONE

DEPARTMENT OF INFORMATION ENGINEERING

MASTER'S DEGREE IN ICT FOR INTERNET AND MULTIMEDIA

Quantifying Sprint Determinants: Development of Motion Capture Analysis tools to support elite coaching.

Supervisor:
Prof. NICOLA PETRONE

Co-Supervisor:
Prof. GIUSEPPE MARCOLIN

Candidate:
MARCO BUCCIOL
2026503

ACADEMIC YEAR 2023-2024

Senza una famiglia, l'uomo, solo nel mondo, trema di freddo.

Ai miei cari.

Abstract

Sports science is a field that has successfully leveraged the potential of Motion Capture technologies in the past years. Detailed real-time data allows us to carry precise analysis over the captured movements, potentially leading to new findings, insights or corrections. By observing mocap technologies at work, it was noticed that there is a gap between the captured data and the results. The Vicon Nexus software, paired with reflective markers and force plates, allows to render a skeleton and visualize its gait and the forces expressed on the ground. These, however, are lacking both in terms of clarity and proper analysis. The purpose of this work is twofold.

First, to define a set of parameters and elements that characterize performance in sprinting. This was done by: referring to the prevailing literature, studying the parameters chosen by leading analysts in the field, and by discussing with experienced athletics coaches. 22 able bodied athletes of different levels participated in this study, performing block starts and sprinting trials. An analysis framework was created to extract relevant information about such efforts. The collected dataset on kinematic and kinetic parameters was investigated, and the latter were found to be more related to performance. Further analysis is required to better understand the weight of specific parameters in the sprinting performance.

Second, to program an automatic tool capable of extracting raw data according to the framework and analyze it. Such software tool, developed in Matlab, provides a detailed report about the performance of the athlete, bridging the gap between the running effort and its objective details. This pipeline with automated analysis reduces processing time from hours to minutes and allows us to perform more running sessions and gather more data, with potential applications to Paralympic athletes. The report structure and content was based on the analysis conducted on the full dataset and on feedback by experts. Its graphs and organized tables strongly enhance the limited visualization provided by the tools previously available.

Abstract in italiano

La scienza dello sport è un campo che, negli ultimi anni, ha saputo sfruttare con successo il potenziale delle tecnologie di Motion Capture. Dati dettagliati e in tempo reale permettono di analizzare con precisione i movimenti acquisiti, aprendo la strada a nuove scoperte, intuizioni o correzioni. Osservando l'uso delle tecnologie di mocap, è emerso un divario tra i dati acquisiti e i risultati ottenuti. Il software Vicon Nexus, in combinazione con marcatori riflettenti e piattaforme di forza, consente di generare uno scheletro virtuale, visualizzandone l'andatura e le forze espresse sul terreno. Tuttavia, tali rappresentazioni risultano carenti sia in termini di chiarezza che di analisi approfondita. Lo scopo di questo lavoro è duplice.

In primo luogo, definire un insieme di parametri ed elementi che caratterizzano la performance nella corsa veloce. Ciò è stato realizzato attraverso: il riferimento alla letteratura prevalente, lo studio dei parametri scelti dai principali analisti del settore e il confronto con allenatori di atletica esperti. A tale studio hanno partecipato 22 atleti normodotati di diversi livelli, eseguendo partenze dai blocchi e prove di sprint. È stato creato un framework di analisi per estrarre informazioni rilevanti da tali prestazioni. Il dataset raccolto sui parametri cinematici e cinetici è stato analizzato, evidenziando come questi ultimi siano maggiormente correlati alla performance. Ulteriori analisi saranno necessarie per comprendere meglio il peso specifico dei singoli parametri nella prestazione di sprint.

In secondo luogo, programmare uno strumento automatico in grado di estrarre i dati grezzi secondo il framework e analizzarli. Tale strumento software, sviluppato in Matlab, fornisce un rapporto dettagliato sulle prestazioni dell'atleta, colmando il divario tra la prova di corsa e i suoi dettagli oggettivi. Questa pipeline con analisi automatizzata riduce il tempo di elaborazione da ore a minuti e permette di eseguire più sessioni di corsa e raccogliere più dati, con potenziali applicazioni agli atleti paralimpici. La struttura e il contenuto del report si basano sull'analisi condotta sull'intero set di dati e sul feedback degli esperti. I grafici e le tabelle organizzate migliorano notevolmente la visualizzazione limitata fornita dagli strumenti precedentemente disponibili.

Contents

List of Figures

Chapter 1

Literature review

1.1 Topic overview

Motion Capture

3D motion capture (also known as mocap) is a technology that allows precise recording of human movement in three-dimensional space. This technology has revolutionized the study of biomechanics, allowing for a more detailed analysis of motion than ever before. The basic principle of motion capture is to track the positions of reflective markers or sensors placed on specific points of the body, such as joints or limbs. These markers are recorded in real-time by multiple cameras or infrared sensors, which use triangulation to determine the exact position of each marker in 3D space. The data is then processed by specialized software, which reconstructs the recorded movements into a digital model. In essence, motion capture provides a way to convert physical movement into quantifiable data. The applications of this data are vast, especially in fields like sports science, rehabilitation, animation, and even ergonomics. What makes 3D motion capture so powerful is its ability to measure really detailed aspects of movement—things that would be difficult to observe with the naked eye. These measurements can include joint angles, limb velocities, ground reaction forces, and more.

One of the key reasons motion capture is so widely used in sports science is because it offers objective, quantifiable data. For instance, in sprinting, understanding the angle at which a sprinter's foot strikes the ground, or the exact timing of their push-off phase, can provide insights into how to optimize performance. These types of details, captured through motion analysis, help athletes and coaches make data-driven decisions, rather than relying just on intuition or experience. Motion capture is also heavily used in injury prevention and rehabilitation. For example, in running biomechanics, motion capture can highlight imbalances or deviations from optimal form. In rehabilitation, motion capture can track an athlete's progress over time, comparing their movement patterns before and after an injury.

Athletics and sprinting

Athletics is a sport that centers on precision, efficiency, and optimal performance, particularly in events like sprinting, where fractions of a second define the winners. As one of the oldest and most foundational sports, sprinting is one of the purest tests of human speed and power. To excel in sprinting, athletes have to master the technical details of their biomechanics, maximize their physical capabilities, and refine their technique. Not all athletes are equal (Brutsaert et al., 2006 [1]).

At the heart of sprinting is the need for maximum velocity in the shortest time possible. Unlike endurance events, which require pacing and energy management, sprints are about explosive power and the ability to sustain that power over short distances. Sprint races, covering distances from 60 meters to 200 meters, require athletes to push their bodies to the limits of speed, acceleration, and technique. In this context, the performance of sprinters is often defined by how efficiently they can convert muscular energy into forward motion, power into speed.

Sprinting can be broken down into different phases, each of which plays a critical role in determining overall performance. The start phase is crucial as it can set the outcome of the entire race. Once the sprinter has exited the starting blocks, they enter the acceleration phase, which typically lasts for the first 30 meters of the race. During this phase, the athlete gradually builds up to his maximum speed. Effective acceleration requires a balance between maintaining forward lean and gradually straightening the body as velocity increases. The goal is to minimize resistance while maximizing power output. In the next sections we will go over the studies mentioning some of these aspects. The maximum velocity phase occurs once the sprinter has fully accelerated, and it is in this phase that maintaining speed becomes the goal. Achieving and sustaining top speed requires a fine balance between stride length and stride frequency. Elite sprinters are able to increase both variables simultaneously, reaching speeds of up to 12 meters per second or more. The mechanics of this phase are critical, as even minor inefficiencies can cause a sprinter to lose valuable time. For example, over striding can lead to greater braking forces as the foot strikes too far in front of the center of mass, reducing momentum and increasing the likelihood of injury.

As sprinters approach the finish line they enter the deceleration phase, where fatigue begins to take its toll, and maintaining speed becomes increasingly difficult. Even the best sprinters experience some level of deceleration towards the end of a race, and the goal is to minimize it as much as possible. The ability to maintain form under fatigue is crucial here, as poor mechanics can exacerbate deceleration and result in a slower finish time. In addition to physical factors, mental aspects play a significant role in sprint performance. Sprinting demands intense focus and concentration, particularly during the start and acceleration phases. Even small distractions or lapses in focus can result in slower reaction times or suboptimal technique, ultimately affecting

the outcome of the race

In conclusion, sprinting within athletics is a sport defined by precision, power, and efficiency. Each phase of the race requires careful attention to biomechanics and technique, with even minor deviations from optimal form potentially costing valuable time. 3D motion capture and other technological advancements have allowed researchers and coaches to analyze sprinting mechanics in great detail, providing athletes with the data needed to optimize their performance.

Current literature

In the next sections we go over the meaningful literature concerning sprinting performance. Dozens of papers have been shared in the last years: some tackle the acceleration phase, other the max velocity phase; a few consider the muscular implications and ground forces, and other give advice on how to train for performance. Given the nature of our study, we will now consider separately the general notions, the acceleration phase notions, and the max velocity notions. After this, it will be clear what the current literature deems relevant for the sprinting performance. Once such literature parameters are categorized, we explain why our research is justified.

1.1.1 Literature: general notions

We start with some general notions, not limited to acceleration or max velocity phase. Literature agrees on many points, although some are still up for debate. On other topics, we now see how there are divergent opinions. First of all, we should note that speed abilities are strongly determined by genetics (Maćkała et al.,2015 [2]). In sprinters, the presence of long lower extremities is found to be advantageous in achieving top performance (Vucetic et al., 2008 [3]). The favorable genetic constitution plays an important role as found by (Brutsaert et al., 2005 [1]), however elite athlete still need years of focused training to realize their full potential. This is consistent with what mentioned by Mann and Sprague (1980) along with Simonsen et al. (1985), that recognised other factors besides leg length including the force of the extensor muscles of the ankle and knee joints since they produce the push-off impulse in the contact phase. Other studies, however, claim that the is no clear correlation between the anthropometric variables studied and 100-m performance (Jean Benoit et al., 2012 [4]). While it is important to mention that it seems that literature is inclined to consider advantageous to have a taller body. As cited in (Majumdar et al., 2011 [5]), "*Body height has a greater impact on maintaining speed and stride length. Faster men are, in general, taller than slower men. An extensive study conducted by Paruzel-Dyja et al. ([6]) on a large number of elite 100 m dash sprinters, found stride length, not stride frequency, to have the most dominant impact on success in the 100 m dash for the male gender. Interestingly, the opposite was true for top female sprinters, whose excellence in*

sprint performance was based on high stride frequency rather than long strides. This analysis suggests a distinction for gender-specific technical training, as different parameters of the 100 m dash are characteristic to each gender." It should be noted that the optimal relationship between these factors (stride length, stride frequency) for an individual sprinter could depend on his standing height, leg length, crural index (ratio of calf length to thigh length), explosiveness of muscular contractions and speed of movement of his limbs. (H. KUNZ et al., 1981 [7]). Therefore, we may say that its not automatic to be faster if one is taller or has higher stride frequency. We may consider this as a potential, but work must be done to reach it. Another crucial aspect, as pointed out by (Jean Benoit et al., 2012 [4]), is that many studies involved high-level athletes but not world-class subjects. It is questionable how much of the findings can be applied to the top athletes in the sport. Some generalizations can be made, but it's not clear how perfect of a match they are. On a previous study, (Jean-Benoit et al., 2011 [8]) found that the way runners apply force onto the ground (technical ability) seems to be more important to field sprint performance than the amount of total force they are able to produce (physical capability). Because this may be considered a technical ability, further studies should investigate whether it could be trained/improved. Greater muscular strength underpins many physical and performance attributes and can be vastly influential in improving an individual's overall performance. (Suchomel et al., 2016 [9]). The ground reaction forces play a crucial round, as found by Rabita et al. in 2014: elite sprinters are able to produce higher horizontal force at any given velocity than sub-elite sprinters. There are clear biomechanical differences during the stance phase of acceleration and maximum velocity sprint running. Longer ground contact times exist during acceleration with a greater requirement for explosive concentric strength, directed more horizontally. Shorter ground contact times exist during maximum velocity with a greater requirement for reactive eccentric strength, and vertically directed forces. (James Wild et al., 2013 [10]) Other factors correlated with the sprinting performance concerning athletic training, are: strength (back squat) and jumping ability (standing long jump, standing five-jumps, standing ten-jumps). The different horizontal jumps are strongly correlated with time and stride characteristics in the sprinters. Horizontal jumps can be used in the training process because they are correlated with the starting acceleration. Besides, there is a correlation between one repetition of back squat, jumps and speed in the first 10 meters. (Maćkała et al., 2015 [2])

Despite the voluminous body of research devoted to sprint training, our understanding of the training process leading to a world-class sprint performance is limited. (Haugen et al. 2019 [11], [12]). In other words, while literature does indicate state of the art techniques and approaches like resistance training, over-speed, progressive overload, tapering and so on, there is no unique training method for achieving top performance. On one side, this allows coaches and athletes to explore personalized and maybe innovative approaches; on the other side, many inefficien-

cies are present in a lot of training programs. The chances that an athlete will change training approach when switching coach are very high.

1.1.2 Literature: acceleration phase notions

When talking about acceleration we imply in order: reaction to the gun, block clearance, first steps from 1 to 10 meters, and subsequent steps until 30 to 40m when acceleration ends, and max velocity is achieved.

Gun and reaction

Currently, there is a lack of scientifc evidence for the 100 ms false start threshold. This has been consistently criticized in the literature for more than 10 years without resulting revisions to the rules. (Milloz et al., 2021 [13]) It has become more frequent to see elite athletes reach with faster than allowed times. Studies as the one carried out by Milloz show how it is theoretically possible to apply force on the footplates in under a tenth of a second. It should also be known that the average reaction time (RT) of the elite sprinters is not significantly different from that of the well-trained sprinters (Slawinski et al., 2010 [14]).

Set position; block setting

In terms of the choice of "set" position, it is likely that no single, universally optimum combination of lower body joint kinematics exists when in the "set" position (Bezodis et al., 2019 [15]). The bunched start has been demonstrated to be the least efficient from a biomechanical perspective because less force is exerted on the starting blocks with a reduction in block velocity. Bunched is typically <0.3 m, medium between 0.3 and 0.5 m, and elongated>0.5 m. The increase in inter-block distance is associated with improved performance in several kinetic and kinematic variables linked to the sprint start. (Cavedon et al., 2019 [16]) It was found that modifying the anteroposterior block distances from bunched to medium distance, allowed for an immediate improvement of performance in the sprinters with no period of familiarization. The findings presented in this study show that a block setting position, calculated on the basis of a proportion of the leg length allows sprinters to improve performance in both the block phase and early acceleration, thereby confirming the hypothesis that considering the athlete's body dimensions when calculating block setting is beneficial to the sprint start (Cavedon et al., 2019 [16]). The above is confirmed by (Slawinski et al., 2012 [14]): increasing the antero-posterior distance between the foot plates leads to increased push phase duration and total impulse and therefore greater block exit velocities. This is likely due to greater rear leg forces, which lead to greater rear leg segmental kinetic energies. While maximizing the output of the rear leg is crucial, the

front leg contributes 66–76% of the total horizontal impulse due to 1.9–2.4 times longer block contact than the rear leg. (Bezodis et al., 2019 [15]). The extension of both hips appears important for performance during the push phase against the blocks. Regarding foot plates, a steeper rear foot plate is associated with a greater mean rear block horizontal force between sprinters. The extension of both hips appears important for performance during the push phase against the blocks. (Bezodis et al., 2019 [15]) This can be achieved by moving from a bunched position to a medium position. Another more recent confirmation, comes from (Valamatos et al., 2022 [17]). The choice of an anteroposterior block distance relative to the sprinter's leg length may be beneficial for some individuals, promoting greater block start performance. The use of footplate inclinations that individually facilitate initial dorsiflexion should be encouraged—footplate angles around the 40 degrees are recommended and block angles steeper than 65 degrees should be avoided. A different opinions comes from (Nagahara et al. 2019 [18]): no correlation between horizontal GRF and block angles is found, and no effects of habitual block angle on block power are found.

Steps

At first touchdown, higher performing sprinters typically land with their center of mass (CM) further along the track. The foot is behind the CM at first touchdown (i.e., a negative touchdown distance and moves progressively forwards relative to the CM at touchdown as a sprint progresses. (Bezodis et al., 2019 [15]). In terms of CM another study confirms a difference between elite and non-elite athletes: elite sprinters put their CM closer to the start line than the well-trained sprinters. Positioning the CM as close as possible to the start line is important in reducing the distance by which the athlete must displace his CM and in creating a greater velocity of the CM during the pushing phase (Slawinski et al., 2010 [14]) Another interesting aspect is that step frequencies from the first fight and stance are already up to 90–95% of their respective values during maximum velocity (Nagahara et al. 2014 [19]). This is consistent with the findings of (Rabita et al., 2014 [20]): while step length increases regularly during the acceleration phase, step frequency is almost instantaneously leveled at the maximal possibility of elite athletes. This is followed by the claim that World-class 100 m sprinters can achieve around one-third of their maximum velocity in around only 5% of total race time by the instant they leave the blocks, and sprint start performance is strongly correlated with overall 100 m time (Bezodis et al. ,2019 [15]).

Between males and females, the only clear sex differences are that males have a shorter push phase duration, higher block exit velocity and shorter contact times for the first two steps (Bezodis et al., 2019 [15]).

Ground Reaction Forces (GRF)

Regarding ground reaction forces literature is clear and agrees on the importance of anteroposterior forces, and the capacity of producing forward propulsion rather than the maximum GRF expressed. As found in a study by (F. Kugler et al., 2010 [21]), the faster subjects attained higher running speeds by applying more forward oriented, but not greater forces to the ground. Greater GRF seem not to be the cause but the effect of higher running speed. The relevance of the impulse is underlined by (Slawinski et al., 2010 [14]), claiming that no difference in the duration of force application has been found between elite and well-trained sprinters. Indeed, the time block was not significantly different between elite and well-trained sprinters. The rate of force development was greater in elite sprinters. Elite sprinters are able to exert greater forces in the same amount of time. This is confirmed by (Jean-Benoit Morin et al., 2013 [22]): "[…] *as subjects' performance level in the 100m increased, their ability to orient the resultant GRF generated by the lower limbs with a forward orientation, i.e. to produce higher amounts of horizontal net force at each step, also increased*." Again, confirmation by (Rabita et al., 2014 [20]): the effectiveness of force application greatly accounts for the difference in the performance between highly trained athletes. The vertical forces are necessary to avoid falling, but the focus should be put on the anteroposterior forces. The effectiveness of force application during the acceleration phase, represented by the averaged ratio of force, is one of the abilities most closely linked to performance. This was not the case for the total amount of force that a sprinter can produce (Rabita et al., 2014 [20]) Another study is partially in contrast with the above claims by deeming more important reducing the braking phase: "*in the later part of the acceleration, the horizontal propulsive impulse can be 4 times greater than the horizontal braking impulse. This result may indicate that the greater acceleration during the acceleration phase was achieved by a lower horizontal braking force, not a larger horizontal propulsive force*" (Jiabin Yu et al., 2015 [23]).

1.1.3 Literature: max velocity phase notions

During top speed phase vertical forces are much higher than acceleration because of the upright position of the body. Now that top speed (or max velocity) is achieved, the focus is to keep it and reduce as much as possible the decline in speed. During maximal sprinting, it is both biomechanically and aerodynamically favorable for a sprinter to have a slight forward lean in the body (Majumdar et al., 2011 [5]). In term of forces, a significant and clear correlation between 100-m performance and average or maximal mechanical power normalized to body mass in the horizontal direction was found by (Jean Benoit et al., 2012 [4]). They claim the higher importance of the capability of the neuromuscular system to keep producing high levels

of horizontal force at high and very high velocities, rather than to produce very high levels of maximal force (Jean Benoit et al., 2012 [4]).

Therefore, the vertical component of GRF has the aim of keeping the body upright, while the horizontal GRF component keeps the high speed achieved in the acceleration phase: during the maximum velocity phase, the horizontal propulsive impulse is slightly larger than the horizontal braking impulse. Once the running speed approaches the maximum velocity, the horizontal braking force reaches the maximum value (Jiabin Yu et al., 2015 [23]). An interesting finding by Weyand et al. (2000 [24]) puts things in a time perspective: at top speed, every sprinter takes around a third of a second to pick their foot up and put it down again. It can be concluded that maximum running speed is largely determined by how much force a sprinter can apply to the ground during each step. Crucially, each step should be both quick and powerful. It was found that elite sprinters can produce steps that are less than 100 ms long.

An interesting point is made by (Miyashiro et al., 2019 [25]) regarding stature and leg length: as moment of inertia theoretically increases with the square of the length for a given mass, a long leg length will make it difficult to rotate fast, resulting in a decrease in step frequency. Faster running speed is associated with higher step frequency and greater swing (flight)/support ratio regardless of leg length. This is confirmed by (Kenneth P. Clark, 2022 [26]): longer legs may allow for fast speeds to be attained with reduced mechanical requirements (i.e., prolonged ground contact times, decreased vertical forces, reduced thigh angular velocities and accelerations). However, longer legs may also require increases in other physical parameters such as torque generating capacity.

1.1.4 Literature: studied parameters

At the end of the chapter are found the two tables (1.1, 1.2) representing the current parameters accepted and studied by literature. They are organized by column: Parameters - optimal value - literature reference.

1.1.5 Justifications for our study

There are multiple reasons that justify our research. First, many studies in the past were conducted on instrumented treadmills in laboratory conditions. This approach allows to capture meaningful data, both kinematic and kinetic, but there is a substantial difference between treadmill and track. The most crucial aspect is that the maximum speed reached on treadmill is lower than what can be achieved on track. How can we analyze top-speed and top-performance patterns on treadmills? Some studies correctly mention that generalizations can be made, but treadmill analysis is a limitation. Moreover, as we can see from the parameter tables, it seems

hard to produce some standardized value intervals that can be followed to improve performance. One of the few examples are the footplates angles. Our study is conducted on track, with an *in vivo* setup. Force plates are placed under the tartan, in a seamless setup.

Another point is the quality of the subjects. There are studies that analyze subjects running at 7-8 m/s: we believe that these speeds are nowhere close enough to the sub-maximal effort required in sprinting, therefore it's hard to generalize results obtained from those observation. We argue that the dynamics of an Olympic athlete running at more that 11 m/s are different that those running at 8 m/s. Our study had around 20 male participants of various levels, from regional to national italian level, and then Olympic level. We believe this is key to discover why there's a difference between athletes and which parameters may explain it. We don't assume we will find these parameters, but we believe this to be the correct approach.

Another point is the quality of the system. 9 force plates embedded into the ground under the tartan allow athletes to run in a straight line in an indoor facility that is race-ready. Athletes have little to no disruption in their running effort. 12 Vicon cameras of latest generation were placed high above the track thanks to an aluminum supporting structure. This allowed us to place cameras on 4 sides of the volume, ensuring maximum capability of capturing the passive markers.

After careful consideration of the considered parameters by literature, we discussed with high-level coaches what they look for when pushing athletes to their best. We defined two lists of parameters that we analyzed for Max velocity and Block Start phases. Some of these are found in literature, some are - to our knowledge - new. Our aims are:

- to get confirmation of the most solid parameters in literature;
- to discover potential new keys to read performance;
- to verify if the parameters suggested by coaches have an actual impact in distinguishing elite athletes from the rest.

Lastly, having two subjects of Olympic level, we want to seek confirmation of whether the literature parameters apply to them when expressing their potential on track, without holding back or being hindered by treadmills or similar. The Olympic subjects performed the trials in may, which coincided with their final preparation for the summer season, implying that their performance was about to peak in the following months.

1.2 Notions of running

In this section a series of concepts is discussed to help the unexperienced reader understand the subsequent chapters. We talk about coordinate system, ground reaction forces, biomechanical

factors in start and max velocity phases. [29]

1.2.1 Kinematic conventions

Human body can be approximated by rigid body segments connected by joints. A coordinate system (CS) is an orthonormal right-handed triad composed of three unit vectors. To describe the position and orientation of a rigid body in space, a stationary Cartesian coordinate system first must be defined. Such a system is Global Coordinate System (GCS) and corresponds to the coordinate system of the laboratory. In order to describe accurately a movement, clear terminology must be used. We define the three anatomical planes as:

- transverse plane: it divides the body into cranial (head) and caudal (tail) portions. It is parallel to the ground, which (in humans) separates the superior from the inferior.
- frontal plane: it is perpendicular to the ground and divides the body into dorsal (posterior or back) and ventral (anterior or front) portions
- sagittal plane: it is perpendicular to the ground and divides the body into left and right.

When describing anatomical motion, these planes describe the axis along which an action is performed. An axis is a straight line around which an object rotates and movement at the joint takes place in a plane about an axis. As well as for anatomical planes, three axes of rotation can be defined:

- vertical axis: it passes vertically from inferior to superior and is formed by the intersection of the sagittal and frontal planes;
- sagittal axis: it passes horizontally from posterior to anterior and is formed by the intersection of the sagittal and transverse planes;
- frontal axis: it passes horizontally from left to right and is formed by the intersection of the frontal and transverse planes.

The three anatomical planes and axes of movement can be visualized in figure 1.1

Considering the sagittal plane [30], flexion and extension can be defined. Flexion occurs when the angle between two adjacent segments in the body decreases as the ventral surfaces of the segments approximate each other and occurs in a sagittal plane about a frontal axis. Extension occurs when the angle between two adjacent segments in the body increases as the ventral surfaces of the segments move away from each other and occurs in a sagittal plane about a frontal axis. Then abduction and adduction can be defined. These are movements in the frontal plane about the sagittal axis and involve moving the body part away or towards an imaginary center

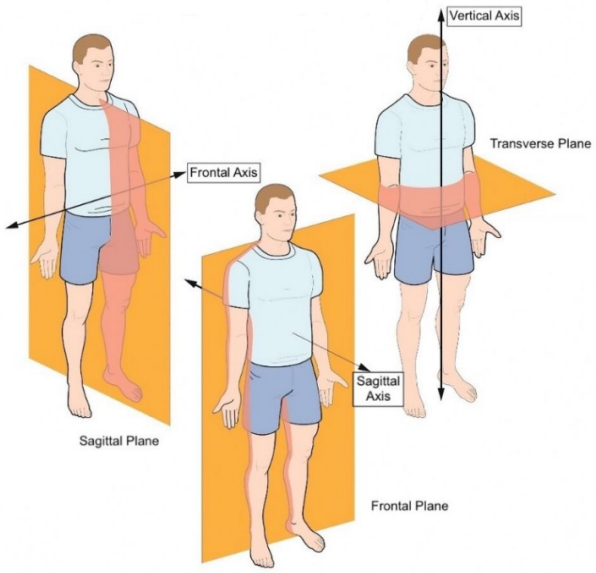

Figure 1.1: Sagittal planes

line. Abduction is taking the body part away from the central line and adduction is moving it towards. Adduction can also be moving the body part across the center line and to the other side of the body. Among the joints capable of abduction and adduction are the shoulder and hip. Other abduction and adduction movements include the fingers. Finally internal and external rotations can be defined (see figure 2.7). Rotation movements are in the transverse plane and include any twisting motion. Joints which permit rotation include the shoulder and hip. These are both ball and socket joints. We can also rotate our necks and backs due to a series of smaller joints, including the atlantoaxial joint which is a pivot joint in the neck between the first two vertebrae (C1 and C2).

1.2.2 Kinetics and Ground reaction forces

Kinetics examines the forces and movements of the body, specifically focusing on how ground reaction forces influence joint movements and muscle power. Strength and power parameters can be predictors of performance (Smirniotou et al., 2008 [31]). While kinematics analyzes movement patterns, kinetics explains the causative forces behind these movements. Analyzing movement patterns alone (kinematics) without understanding the underlying forces can lead to incorrect conclusions. When the foot contacts the ground during locomotion, the ground exerts an equal and opposite force, known as the Ground Reaction Force (GRF). This force can be measured along three axes: vertical (up-down), anterior-posterior (forward-backward), and medial-lateral (side-to-side). Specialized equipment called force plates measures these forces and determines the precise point of force application, termed the Center of Pressure. Multiple

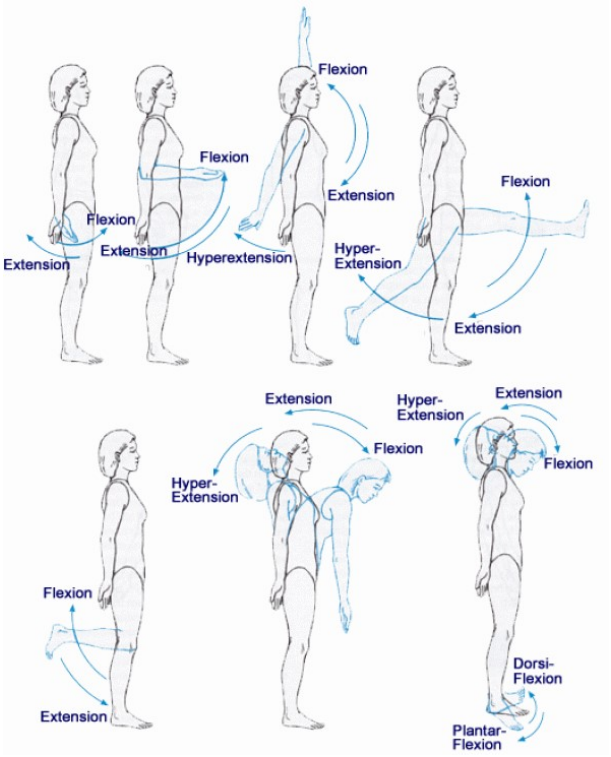

Figure 1.2: Flexion and extension

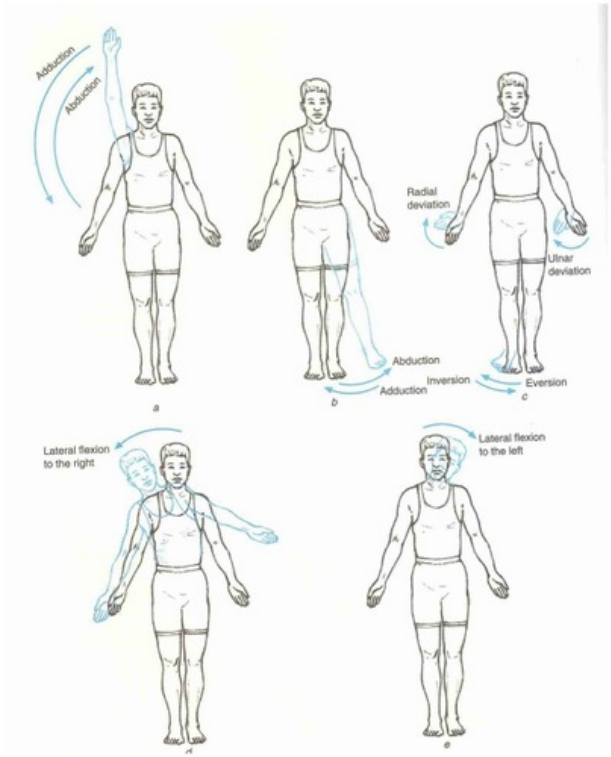

Figure 1.3: Adduction and abduction

variables influence ground reaction forces. The foot strike pattern significantly impacts force distribution. Additionally, shoes may alter force patterns, and running velocity directly affects force magnitude. The vertical force component represents the most substantial contribution to the total force vector. During sprinting activities, vertical forces can reach magnitudes of approximately four times body weight, significantly higher than walking, which typically generates forces equal to body weight. The method of foot strike demonstrates notable influence on force patterns - forefoot strikers generally exhibit superior shock absorption characteristics compared to heel strikers. The anterior-posterior force component illustrates the braking and propulsive phases of gait. Initial ground contact generates a posterior force (braking), followed by an anterior force during push-off. Heel strike patterns typically generate greater braking forces compared to forefoot strike patterns. Note that due to the nature of sprinting and the subjects in this study, only forefoot strikes have been observed. The medial-lateral force component, while smallest in magnitude, correlates with foot pronation and supination movements. This force component particularly influences ankle and knee joint stability in the frontal plane. The magnitude and direction of these forces depend on foot position and the specific region of foot-ground contact during the stance phase.

1.2.3 The phases of sprint running

The 100 meters sprint can be divided into phases. Athletes, coaches and researches may have different opinions on how many phases and how long each phase lasts, but a general distinction is: acceleration (0-30 meters), maximal velocity (30-90 meters) and deceleration (90-100 meters). (Maćkała et al., 2015 [2]).

The acceleration phase

The start phase comprises the first 10 meters of any sprinting race. In the 100 meters dash this is crucial. When the judge commands ”on your marks” (see image 1.4) the athletes move into the block, setting into a static position. Once all athletes are still, the judge orders the ”set” position. All athletes rise, pushing with their feet on the footplates and holding a static position, ready to burst out of the blocks. Once the starting gun fires, the athletes can finally leave the blocks. Usually, elite athletes have a reaction time of 110 to 140 milliseconds, which is deemed good. However, it doesn’t correlate with performance levels. (Mero et al., 1992) (Bezodis et al., 2019 [15]). The rear block is cleared first, and as the back leg moves forward the front leg keeps pushing on the block. Once the front leg exits the block, the rear leg will touch down on the track, pushing the body forward. And the movement will repeat. Sprint start has been studied in the biomechanics field with great attention since decades (M.J.Harland and J.R. Steele, 1997 [32]).

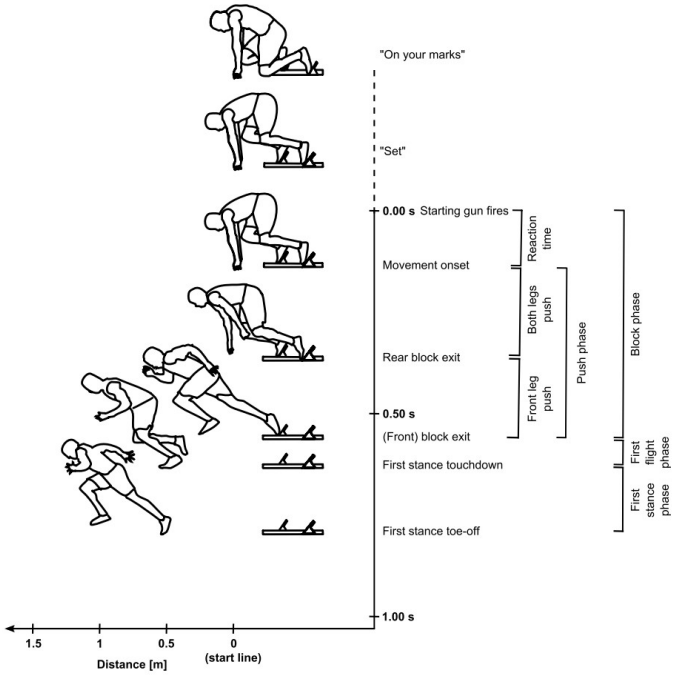

Figure 1.4: The phases of block clearance

The late acceleration phase

This phase was added to underline how, at one point, the accelerating phase comes to an end. Usually this happens at the 30 meter mark, although it varies based on anthropometric characteristics. As the acceleration comes to an end, the vertical GRF are more evident, as the horizontal GRF diminish; the athlete moves into the max velocity phase with upright posture.

The max velocity phase

The maximum velocity phase, occurring approximately between 30-90 m in elite sprinters, represents the peak of sprint performance where several biomechanical factors work together for optimal speed production. (See image 3.5). The body maintains a near-vertical alignment with a slight forward lean, ground contact occurs on the ball of the foot, directly under the center of mass. Contact times are minimal (approximately 90-95 ms in elite sprinters, as found in our data) to maintain horizontal velocity. The stance leg exhibits a stiff spring-like action, minimizing vertical oscillation. During ground contact, the knee flexes slightly to absorb force before extending rapidly for propulsion. Arms move in opposition to leg movement to balance their action.

The deceleration phase

The final portion of the race is known as the deceleration phase or speed endurance phase. Due to neuromuscular fatigue and the depletion of energy systems, athletes typically experience a slight decrease in velocity. The ability to minimize this speed loss through speed endurance is crucial for performance. Maintaining proper mechanics becomes increasingly challenging during this phase. An athlete that is seen recovering in the last part of the race means that he was able to reduce the loss of speed more than the others.

1.3 The Study: an overview

It's now time to discuss our study. Given the literature shown in the previous sections, we decided to study sprinting and block starts among athletes of different levels. The approach is experimental, and the study was conducted *in vivo*. The goal of the study is to determine whether certain parameters and quantities can be related to performance; to find if some single parameters - or groups - can justify the difference in ability among athletes. The study will try and find any correlation between these variables and sprint time or velocity, exploring if and how a combination of these parameters can account for variations in time and speed. The choice of parameters was influenced by multiple sources: first of all, literature. The starting point was to consider what the current state of research is, and find some baseline parameters to track, either to confirm their validity or to further investigate them. Second, books and papers written by coaches or sport analysts were considered as a source of experience from the field. These helped identify what international coaches follow. Third, we cooperated with high-level coaches: Marco Airale, Mario Del Giudice, Federico Candeo. They achieved national and international recognition in the field of athletics. They contributed to the definition of the final parameters, subject to our observation.

The study involved 22 athletes, of which 18 males and 4 females - of varying skill level. The age range was 17-35 years old. The specific events were 100-200-400 m, as only sprinters were considered in the study. Their skill levels were determined using the World Athletics (formerly IAAF) scoring system, with scores ranging from 713 to 1217 points. The athletes were recruited from various local athletics clubs (Gruppo Atletico Aristide Coin, Cus Padova, Assindustria Sport, Atletica Vicentina, Bracco Atletica, etc.) as well as from the United Kingdom. For statistical purposes, the analysis primarily focuses on male subjects. All athletes signed the informed consent form, and willingly carry the trials. Any data related to athletes and trials has been treated with care and privacy (see table 1.3).

The study is part of the Pro-Olympia project, led by Professor Petrone from the University of Padua and Engineer Cutti from INAIL. The project focuses on the biomechanical analysis

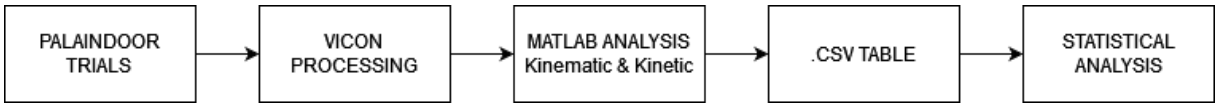

Figure 1.5: Study Flowchart

of athletes of varying levels, specifically based on their running performance. Data collection sessions were conducted between March and June 2024, following a pilot study in November 2023, at the Palaindoor facility in Padua. This indoor athletics venue is approved by the Italian Athletics Federation (FIDAL) and is one of only two such facilities in Italy, the other being in the city of Ancona. Unlike other indoor venues, Padua's Palaindoor has a 200-meter track surrounding the eight 60 m central lanes. The tests were conducted on a special ninth lane, designed and built specifically for the 60-meter straight, where all the equipment and instruments were set up.

Kinematic and kinetic quantities were recorded thanks to motion capture technologies and force platforms (also: force plates). Vicon Nexus was employed to track the data, and the resulting *.C3D* files were exported to Smart Track Analyzer BTS to extract the kinematic variables. Both the *.MDX* output file and the *.C3D* files were then imported into MATLAB to extract kinetic variables. In parallel, the author of this work developed the MATLAB script to replace the need of using BTS, as it proved too time consuming. Data from BTS and MATLAB was then compared to verify the correctness of the outputs. Such data was compiled into an *.csv* file, with each test represented by a row and the parameters by columns. This Excel file was subsequently analyzed. These results are shown in the final chapters of this thesis.

1.3.1 The study: trials

Each athlete was asked to participate in two sessions at the Palaindoor facility. One session was dedicated to Block Starts, the other to TSSR (also: Flying). The sessions took place in the morning and in the afternoon; each session saw between 1 and 5 athletes. Three athletes is the most balanced number, avoiding long sessions that are detrimental to the quality of the study. Three athletes participated in the start sessions but got injured before the flying sessions, and abandoned the study. Three athletes performed the starts and flying in the same session at the end of the study.

Three types of acquisition were performed:

- **Static Trial**: needed to check markers and to later reconstruct the dynamic trials.
- **Static Object Trial**: needed to acquire the starting blocks to later reconstruct the reference system.

- **Dynamic trial**: the actual running. It is either block start or flying.

The block start sessions required:

- 2 dynamic acquisitions of block start in the first configuration (A)
- 2 dynamic acquisitions of block start in the second configuration (B)

The flying sessions required:

- 2 dynamic acquisitions of sprinting in the first configuration (A)
- 2 dynamic acquisitions of sprinting in the second configuration (B)

Once the marker set is applied (see figure 1.6) to the athlete he will begin warm up. The warm up procedure was carried autonomously by athletes, with no intervention from operators. Once completed, the static trial is performed. Then, flying dynamic trials are performed with a rest of 6 minutes between trials, with 8 minutes between different conditions. Instead, Block starts are spaced by three minutes. Block starts were less physically demanding than flying trials.

Block start session

The athlete begins inside the acquisition volume, on the blocks. He must run for at least 20 meters in order to give a 100% effort. Based on pilot tests if the athlete is told to run ”until the end of the volume” it can happen that it slows down before reaching the end. By placing a couple cones further than the acquisition volume’s end we ensured no athlete slowed down prematurely. Once the operator gives the ”OK” signal, the athlete can go. The subject runs two tests with his normal blocks configuration (case A), and two tests with a modified configuration (case B). This is based on the suggestion of the coaches, to have the best position at the *Set* command. The reference degrees are: 120 degree between shank and thigh of back leg; 90 degrees between shank and thigh of the front leg; the shanks should be parallel. The modified configuration B is based on the following:

- Anterior block: constant 0,65 multiplied by the length of the leg (great throcanter to floor). $L_{ant} = 0{,}65 * L_{GT-Ground}$
- Posterior block: constant 0,97 multiplied by the length of the leg (great throcanter to floor). $L_{post} = 0{,}97 * L_{GT-Ground}$

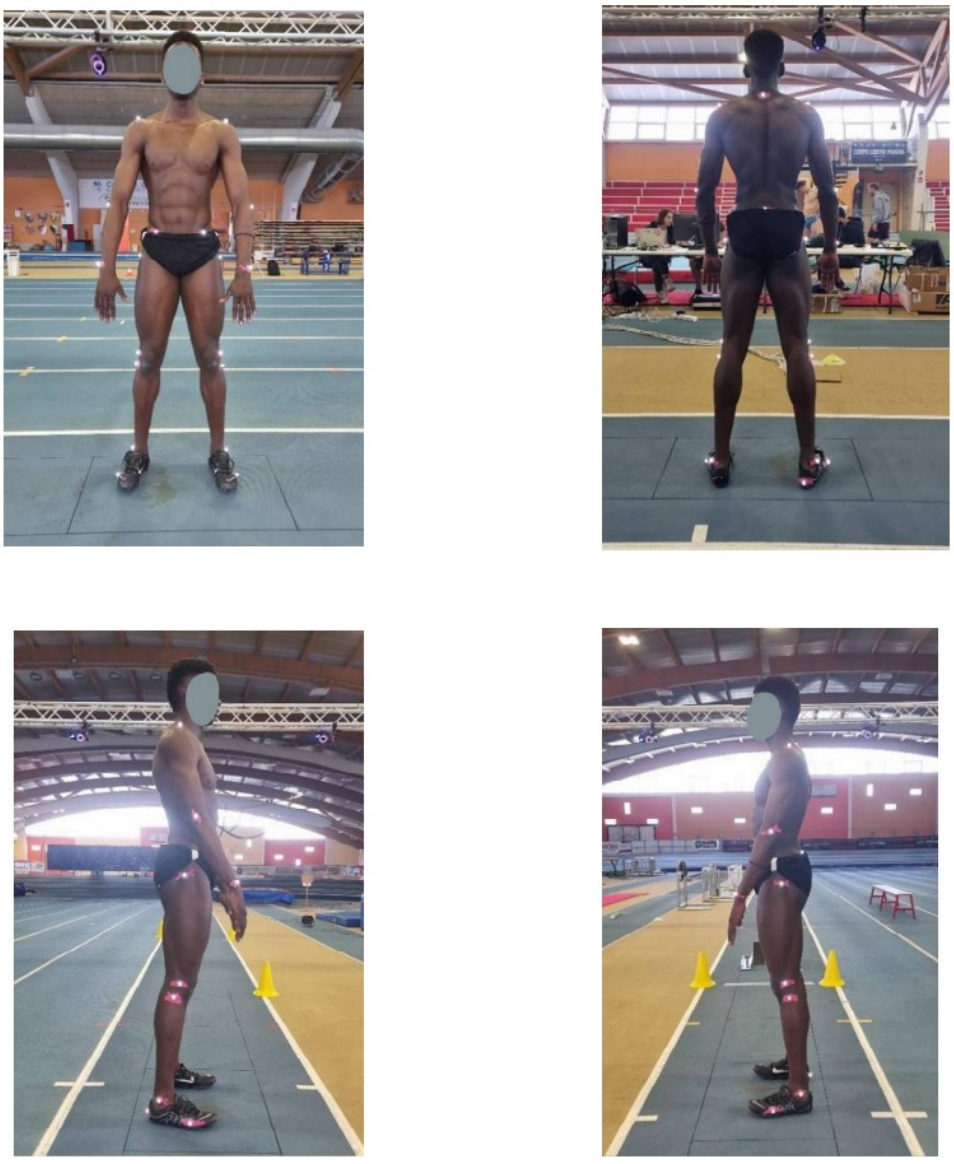

Figure 1.6: Marker set applied - 4 sides view

Flying session

The athlete begins at the 0 mark of the 60m race. He must run for the entire length at 100% effort. Once the operator gives the ”OK” signal, the athlete can go. The athlete runs two times in configuration A, that is how he would normally run, and two times in modified configuration B. In this case, the change is related to the step length. Plastic cones are placed on the ground, with their distance based on the following formula: constant 2,4 multiplied by the leg length (Great throcanter to ground).

$d = 2{,}4 * L_{GT-Ground}$.

Parameter	Optimal value	Reference
Distance between footplates	Longer Antero-Posterior distance	Nagahara and Oshima, 2019
	Longer Antero-Posterior distance (increase push phase, but no clear correlation)	Bezodis et al, 2019
	Elongated space between rear and front plates (increase impulse and velocity)	Majumdar and Robergs, 2011 Mero et al, 1992
	Based on anthropometry	Cavedon et al, 2019
Position on center of gravity of the body during 'Set'	High and near to the starting line	Mero et al, 1992
Horizontal position and velocity of CM during 'on your marks', 'set', 'block's clearance', 'foot strikes'	Great	Slawinski et al, 2010
	Horizontal position of hands during 'on your marks', 'set', 'block's clearance', 'foot strikes'	Great
Block velocity exit	-	Bezodis et al, 2010
Average horizontal block acceleration	-	Bezodis et al, 2010
Average horizontal external block power	-	Bezodis et al, 2010
Time and Velocity of sprint	-	Bezodis et al, 2010
Block's inclination	40 degrees	Majumdar and Robergs, 2011
Angles between thigh and shank during 'on your marks'	Front: 90 degrees	Mero et al, 1992
	Rear: 120 degrees	Mero et al, 1992
Location of COP on the starting blocks	Position correlated with the impulses exerted and so, with the velocity exit	Nagahara and Oshima, 2019
Flight durations	Shorter	Bezodis et al, 2019
	First stance duration longer	Bezodis et al, 2019
Time contact	Longer	Bezodis et al, 2019
Ankle joint	Stiffer	Bezodis et al, 2019
Knee joint	Extending during stance phase	Bezodis et al, 2019
Magnitude and propulsive GRFs at 'block clearance'	Correlated with the velocity	Nagahara and Oshima, 2019
	Greater force production at push on blocks	Bezodis et al, 2019
	Great force and power production	Mero et al, 1992

Table 1.1: Parameters and Values relevant for block start and acceleration in Literature

Parameter	Optimal value	Reference
Step length and step frequency Stride length and stride frequency	Longer and high values, increasing with acceleration	Nagahara et al, 2018
	High step frequency and step length	Majumdar and Robergs, 2011 Mero et al, 1992 Morin et al, 2012 [27] Yu et al, 2016
Contact Time	Shorter at max velocity	Mero et al, 1992 Morin et al, 2012 Alan Murdock
Flight Time	Kept constant during running	Mero et al, 1992
Center of gravity of the body	First step: ahead of contact point	Mero et al, 1992
	Third step: behind the contact point	Mero et al, 1992
TAV (thigh angular velocity)	High TAV, high peak of forces, high velocity	Ryan Grubbs Jonas Dodoo [28]
Hip displacement	-	Alan Murdock
Range between two thighs	-	Alan Murdock
Explosive force power	Increase	Mero et al, 1992
First steps vertical – horizontal forces	Predominant horizontal component	Mero et al, 1992
	Big propulsion and near to zero braking component	Mero et al, 1992
Acceleration and Maximal velocity phase vertical and horizontal	Maximize vertical force component	Nagahara et al, 2018
	Horizontal component predominant, with low vertical component	Mero et al, 1992 Yu et al, 2016
	Reduce braking component and increase propulsive component	Yu et al, 2016
Ratio of forces (RF = horizontal force/total force)	As high as possible	Morin et al, 2011, 2012
Angle of attack	Decreasing with increasing velocity	Kugler and Janshen, 2010
Angle of take-off	Increasing with increasing velocity	Kugler and Janshen, 2010

Table 1.2: Parameters and Values relevant for max velocity in Literature

Table 1.3: Participants Data

Subjects-Trial Name	Gender	Age	Weight (kg)	Leg (m)	Front foot	IAAF score (pt)
S1 - OSN38/45	M	30	82	0.92	R	1099
S2 - OSN30/42	M	21	72	0.875	L	843
S3 - OSN37/40	M	16	63	0.9	R	689
S4 - OSN31/40	M	21	90	1.05	R	910
S5 - OSN33/46	M	27	75.5	0.925	L	974
S6 - OSN37/46	M	22	73	0.88	L	1047
S7 - OSN29/40	M	22	64	0.84	L	857
S8 - OSN34/39	M	19	67	0.95	R	718
S9 - OSN32/43	M	24	76	0.91	L	860
S10 - OSN34/39	M	21	76	0.93	R	896
S11 - OSN38/47	M	23	73	0.92	R	1217
S12 - OSN30/40	M	23	68	0.93	L	933
S13 - OSN30/43	M	22	68	0.88	L	854
S14 - OSN30/44	M	27	71	0.87	L	875
S15 - OSN37/40	M	19	68	0.91	L	815
S16 - OSN33/41	M	17	67	0.825	L	797
S17 - OSN37/39	M	19	85	0.975	L	932
S18 - OSN33/41	M	19	68	0.88	R	916
S19 - OSN47/47	F	20	66	0.88	L	1172
S20 - OSN47/47	F	28	60	0.85	R	1120
S21 - OSN37/46	F	31	53	0.84	L	1040
S22 - OSN46/46	F	27	59	0.84	R	1129
Standard Deviation	/	4.3	9.08	0.06	/	161.2

Chapter 2

Instruments and acquisitions

In the previous chapter we discussed the current state of the literature, describing the current take on improving sprinting performance. We moved then to our study, reasoning on why and how we are conducting it. In this second chapter, we go over the instruments and materials that were used to capture the sprinting subjects. First, we start with location information that is relevant to the outcome of the trials. We delve then into Materials and instruments, to conclude with the actual process: using the described instruments to setup the system, capture and store the data for future analysis.

2.1 Location

The acquisitions were performed at the indoor ”Palaindoor” track facility in the city of Padova, Italy. This allowed continuity to the study as weather elements were mostly ruled out of the equation. No wind and no significant air movement and the temperature was between 25 and 30 degrees Celsius. The trials were performed between spring and summer, and care was taken to avoid the hottest hours of the day, as in the indoor facility may impact repeated trials performance.

2.2 Materials and Instruments

2.2.1 Applying markers

Watercolor pencil

A Watercolor pencil was used to pinpoint the exact locations on which the passive markers were to be applied. A dedicated person, expert in finding the relevant spots in the body, marked all of them. Then the passive markers could be easily applied of the marks.

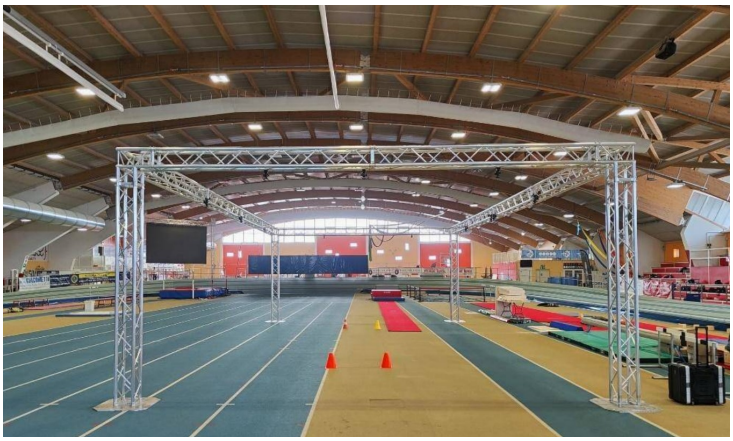

Figure 2.1: Aluminum portal inside Palaindoor

(a) Watercolor skin pencil

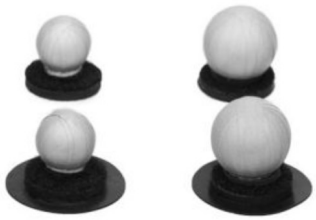

(b) Passive markers

Figure 2.2: Materials

Passive Markers

Passive markers are small, lightweight spheres used in motion capture systems. They're usually made of plastic and covered in a reflective material, which bounces back infrared light emitted by cameras around the setup. The cameras then capture this reflection to track the marker's movement in 3D space.

These markers don't have any electronics inside, which makes them simple and unobtrusive to use. They're great for tracking movements precisely, so they perfectly suit our sport analysis goal. They need good lighting and the right setup for the cameras to pick up the reflections consistently. A marker needs to be seen at any time by at least two cameras; if not, it won't be recorded. Such event can happen due to the nature of sprinting with moving limbs and peculiar body posture during block start.

(a) Pre-tape spray

(b) Kinesio tape

Figure 2.3: Materials

Pre-tape spray

Pre-tape spray is used before applying markers in motion capture to make sure they stick securely to the skin. It's an adhesive spray that creates a sticky layer on the skin, helping markers stay in place when the subjects are sweating. This is especially helpful when markers are placed on joints or areas with a lot of motion, like knees or shoulders, as it prevents them from shifting or falling off. Adhesive spray was crucial in areas like knees and lower back.

Double sided tape

Double sided tape was used to position markers on the skin above the watercolor marks covered in pre-tape spray.

Kinesio tape

Kinesio tape was used to further secure the markers to the skin. Two stripes of tape were placed over the plastic base of the marker without covering any reflective part. This helped in securing markers on particularly sweaty subjects or males with hair on their legs and arms.

2.2.2 Starting Blocks

The selected starting blocks are the Olympic-WA model competition starting blocks (Sportissimo srl, Bergamo,Italy), approved (WORLD ATHLETICS certificate nr. E-15-0833). We selected these blocks in order to be as close as possible to the race conditions. It should be noted that an athlete using a different block (for example not competition-approved) may hinder the performance. As we can see in the image, the block was cut in half, allowing us to place the

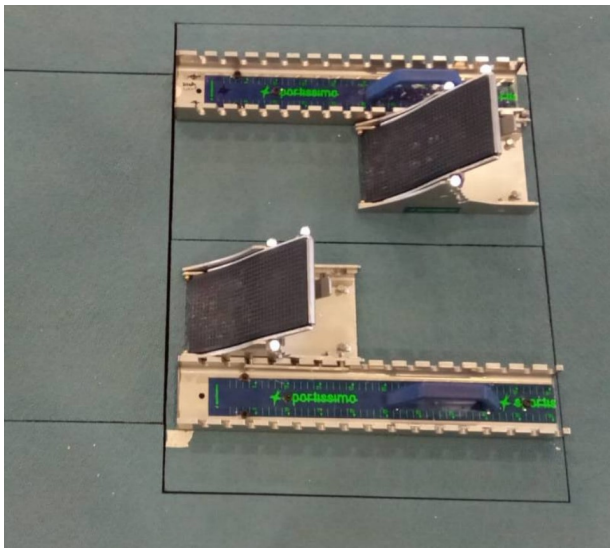

Figure 2.4: Starting blocks

pedals on two distinct force platforms. This way, we're able to record the single components of the initial push out of the blocks.

2.2.3 Speed and recording

Videos

All sessions were recorded from a sagittal point of view, with 4K resolution ad 60 FPS smartphone camera. This allowed to get both immediate visual feedback and later during the analysis phase.

Witty timing measurement

A photocell timing measurement system Witty (Microgate Srl. Bolzano, IT) was used to measure the time taken from 30 to 40 meters and 40 to 50 meters during the flying sessions.

Sacrum tracking

The starting sessions rely instead on the Sacrum marker (name: S), which is tracked in Vicon and used to determine the athlete's velocity.

2.2.4 Aluminum Portal

The system consists of a moving aluminium double portal structure (dimension: 13x7x3.5 m). The cameras are anchored on it, evenly spaced.

(a) Witty time measurement

(b) Aluminum portal detail with camera

Figure 2.5: Materials

2.2.5 Motion Capture System

A Motion Capture System (Mo-Cap) was used to capture the trials. The selected Mo-Cap System is Vicon Motion Systems, LA, USA. It is an optoelectrical system, composed of:

Vicon Valkyrie cameras

10 Valkyrie cameras were used. 2 were placed at the beginning of the acquisition volume. 2 were placed at the end of the acquisition volume. The remaining 6 were equally placed on the sides. Such cameras have a frequency of 250Hz and a resolution of 8 Megapixels.

FLIR BLACKFLY S video cameras

2 FLIR BLACKFLY S video cameras were used. One placed on the end of the acquisition volume and on the the right hand side with respect to the running direction. Such cameras ran at 125Hz with 2.3MP resolution.

2.2.6 Hardware

PoE+ switch

This unit provides the power source and connectivity for the Vicon Valkyrie system. Each infrared camera is connected to it through an Ethernet cable. This PoE+ switch is directly connected to the PC.

(a) Vicon Valkyrie cameras

(b) FLIR BLACKFLY S cameras

Figure 2.6: The Cameras

(a) PoE+ switch

(b) Back view of the system

Figure 2.7: The PoE+ and Lock system

Lock

The Lock is a unit that allows other elements (e.g. force plates and video cameras) to be synchronized with the Vicon system. The output cable of force platform amplifiers and the sync cable of FLIR video cameras are connected to it. It is connected to the PoE+ switch through which it communicates with the work station.

PC workstation

The PC workstation is made by a high-performance Vicon-supplied PC, enabling communications between the PoE+ switch and the installed Vicon application software. This is where it is possible to capture, view, and process the data from the Vantage system and any supported third-party devices integrated into it (AMTI Force Plates).

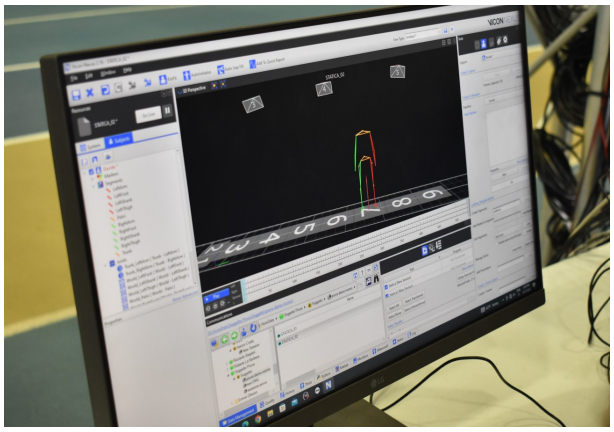

Figure 2.8: Vicon Nexus during calibration

2.2.7 Vicon Software

Vicon Nexus (© Vicon Motion Systems Ltd UK) was at the heart of the project. Without such proprietary software, no analysis can be carried. Nexus allows to calibrate the system with live information about the quality of calibration. Then it shows a live view of the capture volume. The software allows to record a trial and save it as a file for future review and analysis. It also allows immediate analysis and feedback to the athlete. The force plates and the cameras are shown in the 3D screen.

2.2.8 Speed and recording

2.2.9 Force plates

The force plates are instruments commonly used in gait analysis, because they allow the measurement of ground reaction forces, moments and the center of pressure. The force plate used in the present work is AMTI OR6 Series. Seven 60 x 90 cm force plates are placed in a row and two 40 x 60 cm force plates are placed side by side at the beginning of the force plate system. For this study, their acquisition frequency has been set to 1500Hz. Such frequency is a multiple integer of the frequency of acquisition of the Motion Capture system (250 Hz). The resolution of the force plates is six times greater than that of the markers. Each force plate has a local coordinate system and measures the following six load components:

- Fx: x component of the force applied to the force plate;
- Fy: y component of the force applied to the force plate;
- Fz: z component of the force applied to the force plate;
- Mx: torque applied to the force plate about x axis;

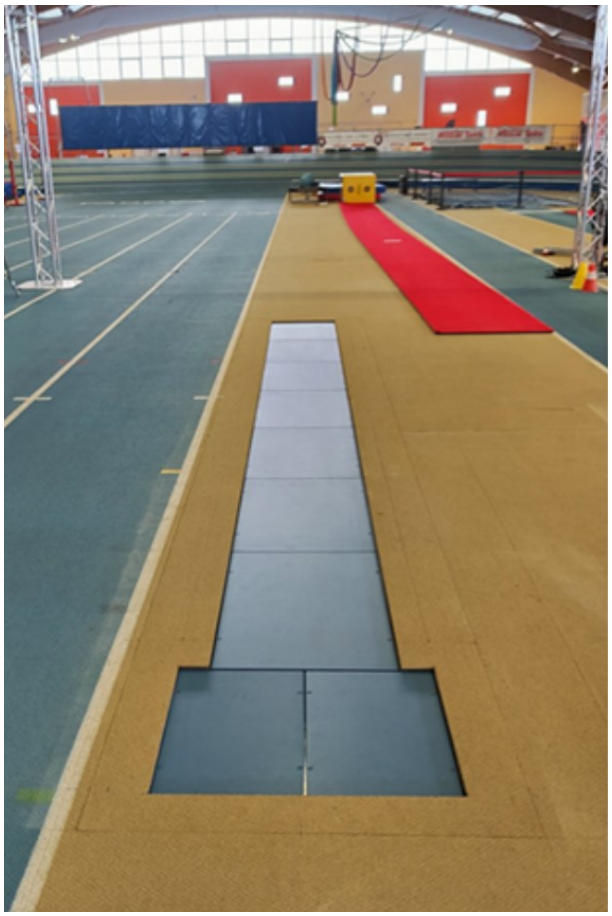

Figure 2.9: The force plates under the tartan

- My: torque applied to the force plate about y axis;

- Mz: torque applied to the force plate about z axis.

It's worth saying that the force platform gives as output the force and the moments that it receives. This, along with the orientation of local reference system of each force plate, must be taken into account when analyzing the trials. Track tartan slices has been cut and attached to the superior surface of each force platform. In that way, even if there is a strong tangential force to the surface like the anterior-posterior ground reaction force during sprinting, each force plate is not influenced by forces acting on adjacent force plates. Small effects were rarely found during the trials, but a simple threshold in the data analysis phase allowed to filter them out without impairing any data collection. Each force plate is connected to its amplifier that also works as signal conditioner. The signal conditioner and amplifiers are connected to the Lock, that allows the force plates system to be integrated and synchronized with the other systems in place.

Figure 2.10: Active wand

2.2.10 Wands

Active Wand

The active Wand is used in the Cameras Calibration procedure. As the Vicon Valkyrie calibrate, an operator walks in the volume moving the active wand facing the cameras. Then it can be placed in the desired origin of the global coordinate system of the laboratory to help calibrate the system. It is a crucial component used in setting up the system.

Passive Wand

The passive Wand (with three reflective markers aligned on it) is used in the Cameras Calibration procedure. An operator enters the volume of acquisition with the passive want. The three passive markers are selected and the operator asses that the makers trajectories are not lost in the calibrated volume. If their trajectories are continuous, the Calibration Procedure succeeded.

2.3 Sensors setup and calibration

In order to acquire data from athletes we need to set up and calibrate the system. The aluminum moving portal structure is placed in the correct position around the Force Platforms. Vicon Motion Capture cameras are mounted on the portal and their cables are connected to the PoE+ switch. The zoom, the aperture and the focus of each camera have been previously adjusted using some moving and fixed markers in the acquisition volume and checking the view of each camera from the Nexus software (each marker must be clearly visible, with a cross exactly in the centroid of the marker blob). This way, every time there is a need to acquire data, cameras need only to be anchored to the portal.

Force Platforms are connected to their amplifiers and then to the Lock connected to the PoE+ switch. In addition, the sync cables of FLIR video cameras are connected to the Lock and their power-data cable to the PC workstation. Finally, the PoE+ switch has been connected to the computer of the workstation. In order start the Setup of the system it is necessary to go in LIVE MODE pressing the button GO LIVE in Resources pane. In the Resources pane under Systems, it is possible to see all the systems connected to the workstation: the 10 Vicon Valkyrie Cameras; the 2 FLIR Video Cameras; the 9 AMTI Force Platforms.

All the cameras (Valkyrie and FLIR) are selected and pressing the Camera button in the view pane in is possible to check what the selected cameras see. There may be some light points that must be masked. After that, the Cameras Calibration begins. An operator with the active Wand that emits infrared light, passes through the acquisition volume and moves the wand in different directions so that it can be seen from all the Cameras. During calibration, the software creates a *.xcp* file containing the calibration parameters for each camera and the description of the capture volume necessary to produce accurate 3D data.

Once Cameras Calibration ended, the active Wand can be placed in the desired origin of the global coordinate system of the laboratory (midpoint between lower left corner of the force plate 1 and lower right corner of force plate 2) with the Y axis (wand's handle) pointing forward so the cameras are aligned with the floor plane. Once the origin of the global reference system is set, the floor plane must be adjusted. Three markers are placed in the acquisition volume (one in the lower right corner of force plate 1, one in the lower left corner of the force plate 2 and one in the middle of the upper side of the force plate 9). Using the Nexus software, the operator selects the three markers that defines the plane. After that, the global coordinate system is accurately aligned with the floor. Hence, under 3D Perspective in the View pane the three markers of passive wand moving through the acquisition volume are selected and the operator asses that the makers trajectories are not lost in the calibrated volume. If their trajectories are continuous, the Calibration Procedure went well.

Then, also the force platforms can be set. Firstly, while paying attention that all force plate are not loaded, the Zero Hardware button on the amplifier of each force plate is pressed. After that, the force plates are selected in System under Resources pane and after a right click, the Zero Level button can be pressed. At that point, a subject goes on each corner of each force plate and the workstation operator checks that the measured force is coherent with the subject's weight and the location of the reaction force is in the correct corner. An important check can be done by walking forward on force plate's side and assessing that the Ground Reaction Force lies near the edge of force plates. Now the system is ready to capture data and the Session folder can be created in Data Management pane. Inside the Session folder, the Athlete folder is created. In order to start an acquisition, in Capture pane the name of the trial can be added along with a

description of it. By pressing the button Start the acquisition begin. Finally, by pressing Stop button the acquisition ends and, it is saved in the Athlete folder. Each acquired trial belong to one of the following test categories:

- **Static Trial**: the athlete goes in the middle point of the acquisition volume and remains still while the operator captures for a few seconds. This trial is fundamental for the tracking procedure.
- **Block calibration**: three markers are placed on the block pedals to create two planes for later analysis. A quick capture is performed, with no other marker in the acquisition volume other than those on the blocks.
- **Dynamic Trial**: there are two variants of this trial. Block start and Track steady state running (TSSR). These are the actual ”performance” trials; this is what all the previous work has been done for.

2.4 Marking subjects

When the athletes arrive at Palaindoor, the operators must begin placing the markers in parallel with the calibration process. First, they locate the correct anatomical positions for the markers through palpation, feeling for the right points on the body. Any hair in these areas may be shaved to ensure a better grip, and pre-tape spray is applied to help the markers stick securely to the skin.

Using a watercolour pencil, the operator marks the identified points. The markers are then carefully placed on the prepped skin using double-sided tape. To reinforce them, kinesio-tape is applied over the markers, providing additional hold and reducing the risk of them falling off during movement.

After all the markers are in place, the length from the athlete’s greater trochanter to the ground is measured. The athlete will the begin the warm up. The marker set used in this study is a lightweight model, consisting of 22 markers in total. This setup is necessary for creating a 2D representation of the athlete during tracking.

The Vicon system’s color convention for markers is followed: green for the right side, red for the left side, yellow for the trunk, and blue for asymmetry markers, which are recommended to improve tracking accuracy. The details of each marker placement are shown in the table and figure below.

If any marker falls during the trials it will be replaced and a new static acquisition will be performed to ensure tracking correctness.

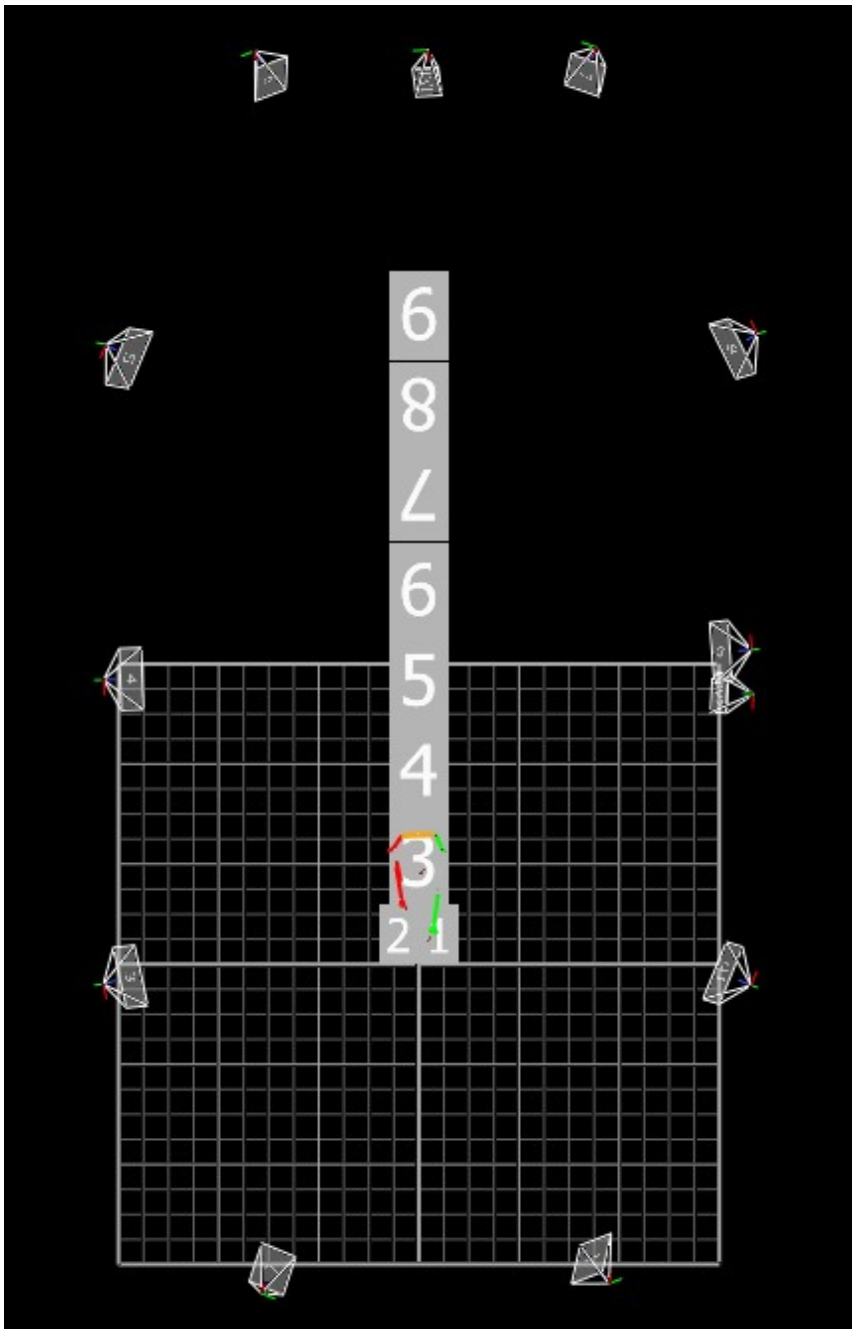

Figure 2.11: Top view of the system in Nexus

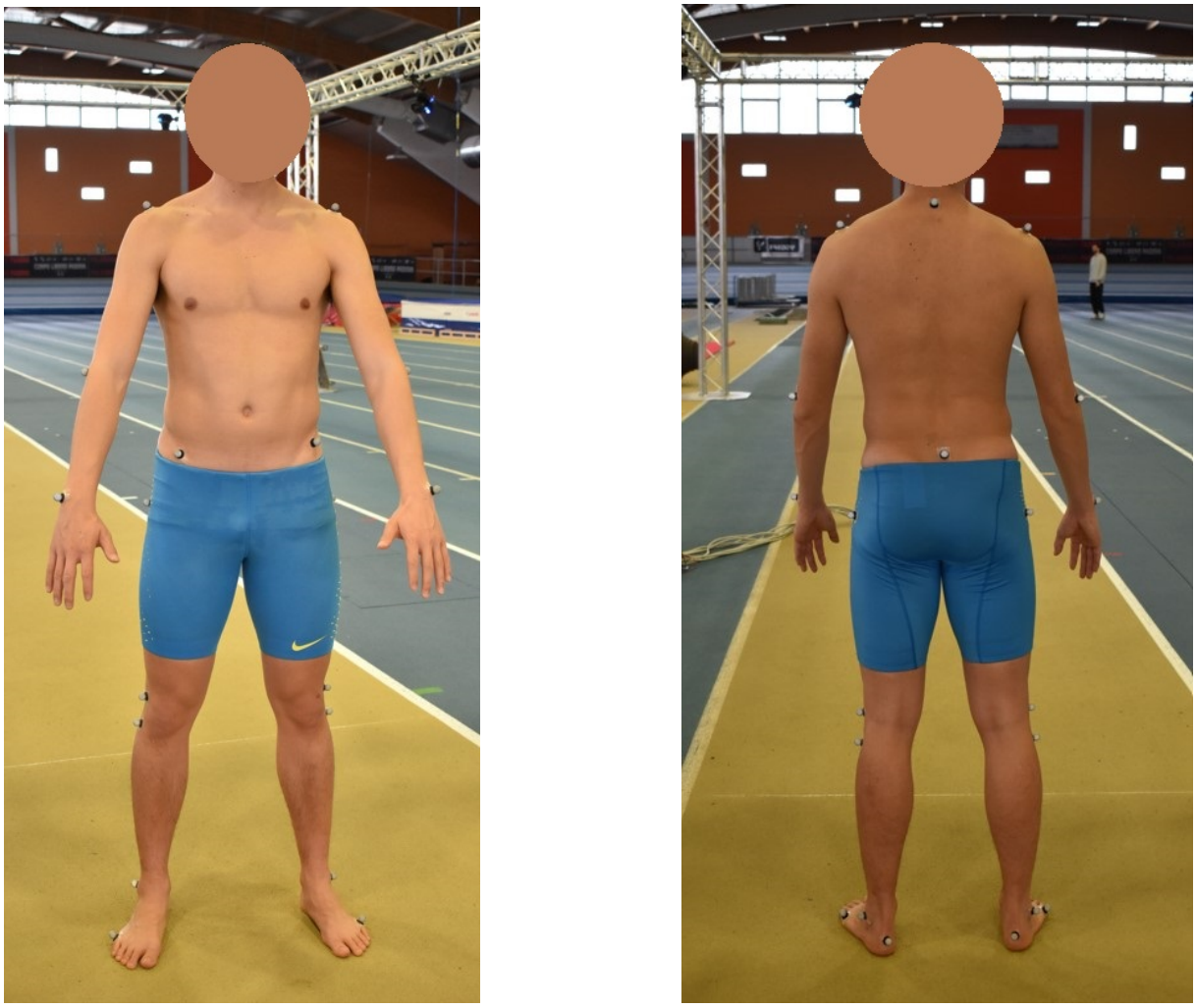

(a) Front view of marked athlete

(b) Rear view of marked athlete

Figure 2.12: A fully marked subject with 22 passive markers

2.5 Data acquisition

The acquisition phase can start once the system is calibrated and warmed up, and the athlete has completed the warm up and worn the spiked shoes (also known as ”*spikes*”). A named session folder is created - or the existing one is used if the athlete is performing a second session - and the trial name is created. There are three types of acquisition:

- **Static trial**: the athlete stands still; the operator checks if all the markers can be seen from the cameras and then *Start* the acquisition; this acquisition is fundamental to reconstruct the dynamic trial in the processing of data.
- **Static object trial**: in the starting block session, the starting blocks are placed on force platforms 1 and 2. The Zero Level of the Force Platforms Calibration is performed when the blocks are placed on them. The static acquisition of the starting blocks allows to reconstruct the reference system of each block in the processing phase to obtain the force exerted on the blocks.
- **Dynamic trial**:
  - block start session: the athlete starts inside the acquisition volume and must run around 20 meters at 100% effort. An agreement is reached in how to signal that the acquisition is ready to start. For example saying ”*on your marks*” allows the athlete to walk into the space and the operator to click on the Start button.
  - flying session: the athlete stands at the beginning of the 60 meters mark. He must run for 60 meters with a maximal effort. The Software operator will communicate once the system is ready - for example saying ”*ready*” - and the athlete will start sprinting.

Chapter 3

The Parameters

After the literature and context overview in chapter 1 and after the Description of Tools, Materials, and Sensors: Vicon Tracking, Kinematic and Kinetic Quantities in chapter 2, it is time to move on to a discussion on which parameters were covered in the study.

3.1 The choice of parameters

When choosing the parameters, we took into account multiple sources.

- We asked expert coaches, based on their experience, what they observe during training sessions and what they keep track of. Among these, an Italian coach of Olympic level, and another coach that led athletes to win Italian titles in the past.
- We explored the main parameters used by leading analysts in the field. [33]
- We researched the main parameters considered by literature.

This study considered both old parameters and new ones, in an attempt to both verify the value of acclaimed ones, and try to determine if new ones may be added to the list. It should be noted that expert coaches had both overlapping opinions and discordant ones on parameters. The starting point was therefore the sum of all the mentioned parameters.

3.1.1 Challenges

When talking about challenges related to parameters, the main issue is that most parameters were not identifiable as good or bad *a priori*. We found that, on one side, coaches observe recurring characteristics like contact time; on the other, some parameters are unique to the coaching style of individuals. While literature indicates that some parameters (e.g.: maximum ground reaction forces and impulses) should be more correlated with performance than other, we also wanted

to put to good use the hardware we had at out disposal. We believe it is a great opportunity to investigate less studied parameters and to pursue research thanks to the system described in chapter 2.

3.1.2 The list of parameters

Parameters can be grouped in three categories, valid for both sprinting and block start:

- **Spatial** parameters
- **Temporal** parameters
- **Angular** parameters

Each parameter will be dealt with in detail in the following section, explaining which category it belongs to, which limbs it affects, which markers are used and how it is computed.

The following is the list of parameters for the Max Velocity phase, also called Track Steady State Running (TSSR) or ”Flying” phase.

1. Contact Time
2. Flight Time
3. Step Length
4. Stride Length
5. HIP Horizontal Displacement
6. Pelvis COM* Max
7. Support Angle at Midstance
8. Push Angle at Foot Off
9. Thigh to Horizontal Angle at knee max height
10. Shank to vertical Angle at knee max height
11. Ankle Angle at knee max height
12. Thigh Range at Foot Off
13. Early Flexion Angle with Angular Velocity
14. Full Flexion Angle with Angular Velocity

15. Early Extension Angle with Angular Velocity

The following is the list of parameters for the block start phase.

1. Push angle
2. Thigh-Trunk Angle
3. Knee Angle
4. Shank to Vertical Angle
5. Thigh Angle
6. Trunk angle
7. Block to First Foot Strike

3.1.3 The marker set

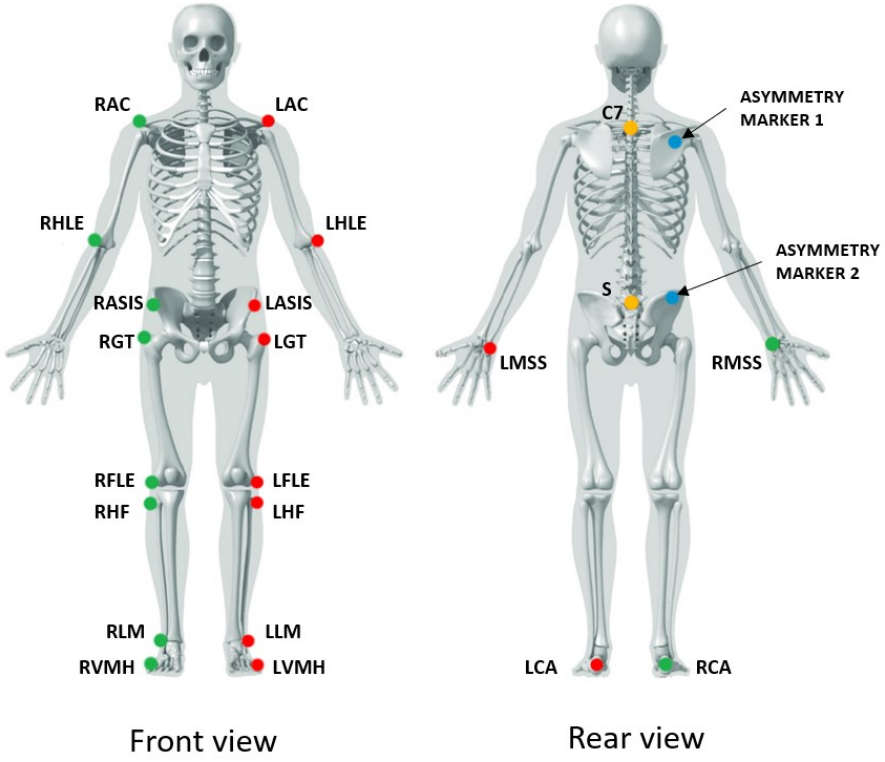

Figure 3.1: Marker set used in the study

As we can see from the image 3.1 the marker set used in this analysis counts 22 markers. The markers colour convention adopted is the following, and will be respected also when defining segments and angles:

- Right body side: Green
- Left body side: Red
- Trunk: Yellow
- Asymmetry markers: Blue

The use of asymmetry markers is recommended by Vicon specifications to help the tracking process; due to the symmetric nature of the human body, placing 22 markers will result in a symmetric marker set. Adding the blue markers to one side of the body allows software applications to better distinguish the two sides of the body, reducing human intervention during the tracking phase. Tracking will be discussed in chapter 4. The table 3.2 provides an overview of segments and their markers. Colors follow the above conventions.

SEGMENTS	MARKERS
LeftArm	LAC, LHLE, LMSS
LeftFoot	LLM, LCA, LVMH
LeftShank	LHF, LLM
LeftThigh	LGT, LFLE
Pelvis	S, RASIS, LASIS
RightArm	RAC, RHLE, RMSS
RightFoot	RLM, RCA, RVMH
RightShank	RHF, RLM
RightThigh	RGT, RFLE
Trunk	C7, S

Figure 3.2: Segments and relative markers

Lastly, as we will appreciate in the following images describing parameters, angles are also categorized based on their type. A different color corresponds to a different type of angle.

3.2 Kinematic Parameters: Track Steady State Running

When performing a sprinting action - also called ”max velocity” phase - the athlete executes a series of actions in a cyclic pattern. The athletes captured in our acquisition volume reached their top speed right before entering the 3D space. We picked four instants that we believe well-represent the gait cycle. Temporal, spatial and angular parameters are computed at - or between - the following four instants:

- **Foot Strike**: the instant in which a foot touches the ground.

ANGLE TYPE	DESCRIPTION	BETWEEN	INSTANT	SYMBOLS	COLOR
Absolute(V) segment angle	Single body segment	From Vertical to segment	Same instant Different instants	Theta: **θ** Delta Theta: **Δθ**	Gold
Absolute(H) segment angle	Complementary angle of Theta	From Horizontal to segment	Same instant	Theta capital: **Θ** (= 90 - **θ**)	Pink
Relative joint Flex/Ext angle	Same side body segments	Two body segments	Same instant	phi: **φ** (=Θ_2-Θ_1)	Silver
Relative joint Angle	Supplementary angle of Phi	Two body segments	Same instant	phi capital: **Φ** (=180-**φ**)	Brown
Contra-lateral angle	Different side body segments	Two contralateral body segments	Same instant	gamma: **γ**	Purple
Ideal Line Inclination (H)	Joining line (GT-ML)	From Horizontal to Line	Same instant	beta: **β**	Azure

Figure 3.3: Angle types: definitions and color scheme

- **Midstance**: The instant in which the great trochanter and malleolus of the supporting leg are vertically aligned.
- **Foot Off**: the instant in which a foot is no more in contact with the ground.
- **Knee Maximum Height**: The instant in which the knee of the leading leg is at its maximum height.

To better visualize the cyclic pattern of TSSR running, a grid was built. The images contained in the grid will be used in the current chapter to aid with the representation of each parameter.

As we can observe:

- **Foot Strike** occurs at instants t0 and t8 for right leg, t4 for left leg.
- **Midstance** occurs at instants t1 and t9 for right leg, t5 for left leg.
- **Foot Off** occurs at instants t2 and t10 for right leg, t11 for left leg.
- **Knee Max Height** occurs at instants t3 and t1 for right leg, t7 for left leg.

3.2.1 Temporal Parameters

1. Contact Time - $T_C(s)$

- **Instants of measuring**: From Foot_Strike to Foot_Off. Right leg: t0 to t2. Left leg: t4 to t6.

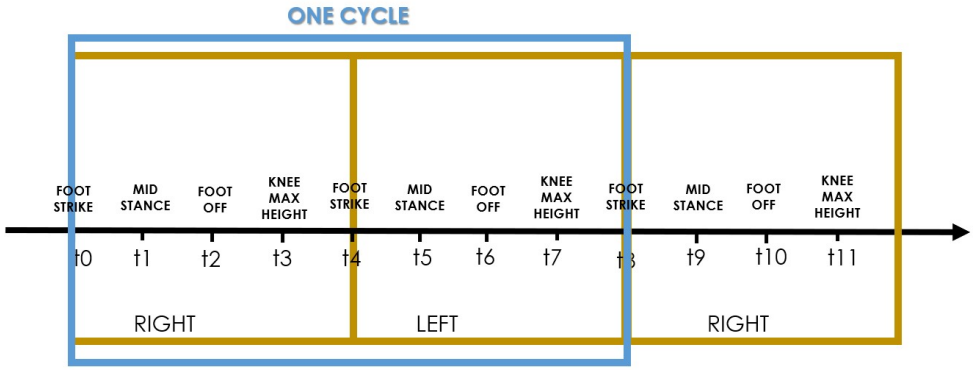

Figure 3.4: The cycle scheme

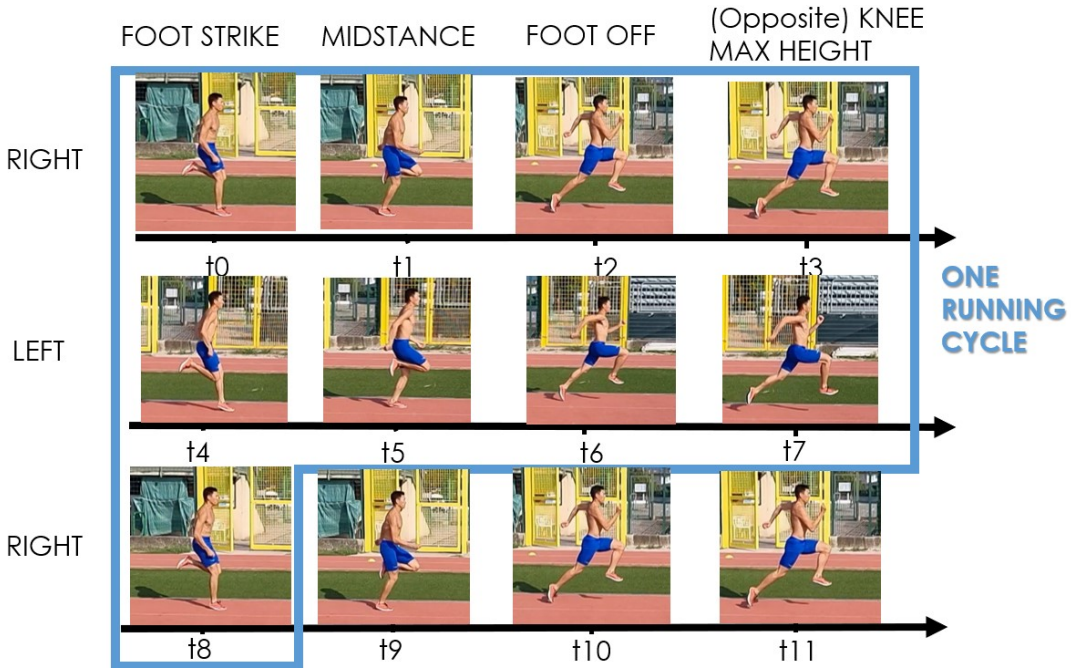

Figure 3.5: The cycle scheme visualized

- **Description**: The time occurred between Foot_Strike and Foot_Off, during which one foot touches the ground.
- **Markers used**: RVMH, LVMH
- **Segments identified**: None.
- **Formalization**:
  - $T_{C,R} = t2 - t0$
  - $T_{C,L} = t6 - t4$

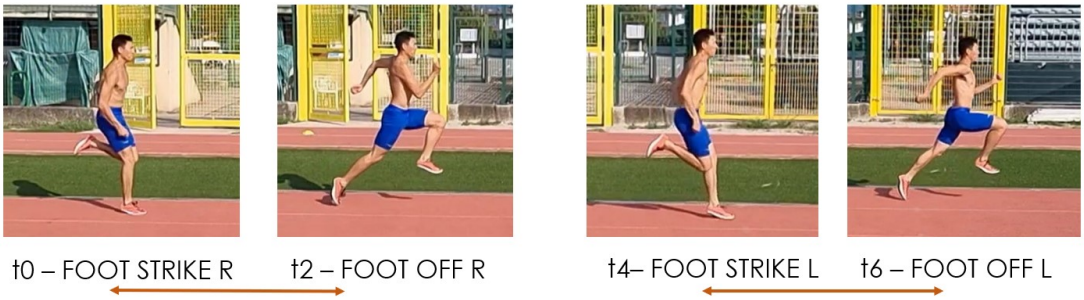

Figure 3.6: Contact time.

2. Flight Time - $T_{FL}(s)$

- **Instants of measuring**: From Foot_Off to Foot_Strike. Right leg: t2 to t4. Left leg: t6 to t8.
- **Description**: The time occurred between Foot_Off and Foot_Strike, during which neither foot touches the ground.
- **Markers used**: RVMH, LVMH
- **Segments identified**: None.
- **Formalization**:
  - $T_{FL,R} = t8 - t6$
  - $T_{FL,L} = t4 - t2$

Figure 3.7: Flight time

Figure 3.8: Step Length

3.2.2 Spatial Parameters

3. Step Length - $Len_{step}(m)$

- **Instants of measuring**: From Foot_Strike of one foot to Foot_Off of the other foot. Right leg: t0 to t4. Left leg: t4 to t8.
- **Description**: The horizontal distance between the contact point of a foot on the ground and the contact point on the ground of the subsequent foot.
- **Markers used**: RVMH, LVMH.
- **Segments identified**: None.
- **Formalization**:
  - $L_{step,R} = X_{RVMH}(t8) - X_{LVMH}(t4)$
  - $L_{step,L} = X_{LVMH}(t4) - X_{RVMH}(t0)$

4. Stride Length - $L_{stride}(m)$

- **Instants of measuring**: From Foot_Strike of one foot to Foot_Off of the same foot. Right leg: t0 to t4. Left leg: t4 to t8.

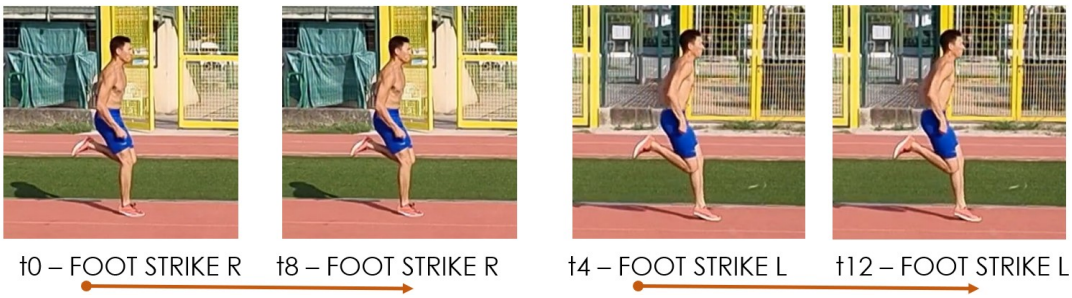

Figure 3.9: Stride Length

- **Description**: The horizontal distance between the contact point of a foot on the ground and the subsequent contact point on the ground of the same foot.
- **Markers used**: RVMH, LVMH
- **Segments identified**: None.
- **Formalization**:
  - $L_{stride,R} = X_{RVMH}(t8) - X_{RVMH}(t0)$
  - $L_{stride,L} = X_{LVMH}(t12) - X_{LVMH}(t4)$

5. Hip Horizontal Displacement - $D_h(m)$

- **Instants of measuring**: At Foot_Off. Right leg: t2. Left leg: t6.
- **Description**: The distance between the point in which foot touch the ground (RVMH, LVMH) and the projection of corresponding side GT (RGT or LGT) on the ground.
- **Markers used**: RGT, LGT, RVMH, LVMH.
- **Segments identified**: None.
- **Formalization**:
  - $D_{h,R} = XRG_{TV}(t2) - X_{RVMH}(t2)$
  - $D_{h,L} = X_{LGT}(t2) - XLV_{MH}(t2)$

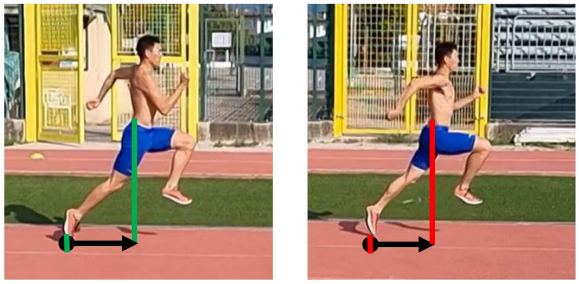

Figure 3.10: Hip Horizontal Displacement

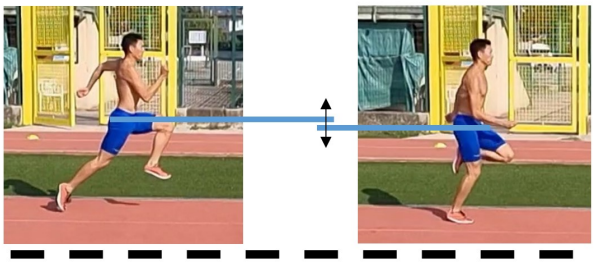

Figure 3.11: Pelvis COM* Excursion

6. Pelvis COM* Excursion - $\Delta Y(m)$

- **Instants of measuring**: Observe the position of COM* of ASIS (mean of LASIS and RASIS) for the whole duration of the test. COM* represents the Pelvis Midpoint.
- **Description**: The maximum variation of COM* during the sprint (difference between the max and min values).
- **Markers used**: RASIS, LASIS.
- **Segments identified**: None.
- **Formalization**:
  - $\Delta Y(m) = Y_{MAX} - Y_{MIN}$

3.2.3 Angular Parameters

7. Support Angle - $\Phi_{TH-SH}(^{\circ})$

- **Instants of measuring**: At Midstance. Right: t1. Left: t5.
- **Description**: (Relative) angle between the back of thigh and shank segments of supporting leg (leg in contact with ground) at Midstance (instant when GT is over the VMH)

- **Markers used**: RGT, LGT, RFLE, LFLE, RHF, LHF, RLM, LLM.
- **Segments identified**: RightThigh, LeftThigh, RightShank, LeftShank.
- **Formalization**:
  - $\Phi_{TH-SH,R}(^\circ)$
  - $\Phi_{TH-SH,L}(^\circ)$

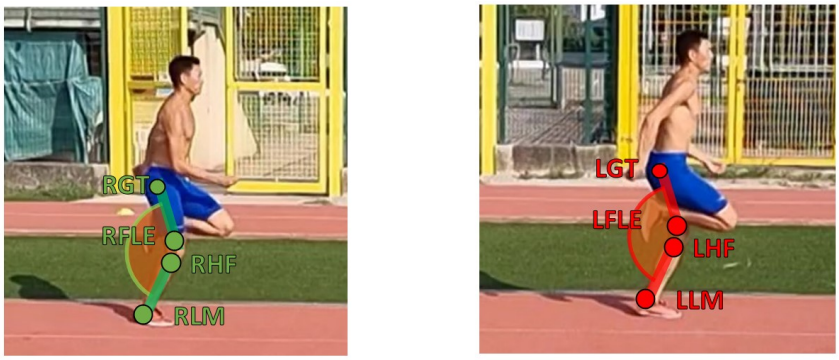

Figure 3.12: Support Angle

8. Push Angle - $\beta_{LEG}(^\circ)$

- **Instants of measuring**: At Foot_Off. Right: t2. Left: t6.
- **Description**: Angle between the Horizontal and the Ideal Line connecting GT and LM.
- **Markers used**: RGT, LGT, RLM, LLM.
- **Segments identified**: The line connecting RGT and RLM, and LGT and LLM.
- **Formalization**:
  - $\beta_{LEG,R}(^\circ)$
  - $\beta_{LEG,L}(^\circ))$

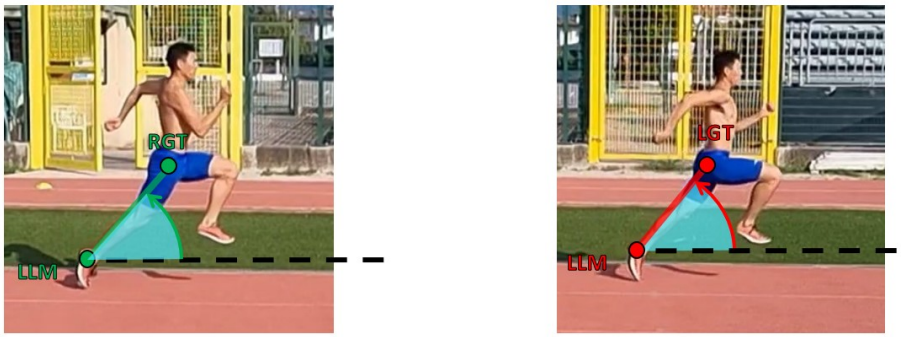

t2 – FOOT OFF R t6 – FOOT OFF L

Figure 3.13: Push Angle

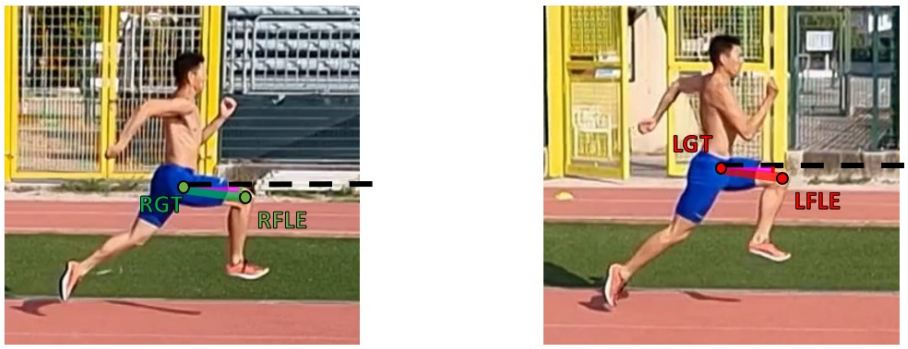

t7 –KNEE$_R$ MAXh t3 –KNEE$_L$ MAXh

Figure 3.14: Thigh To Horizontal Angle

9. Thigh To Horizontal Angle - $\Theta_{TH}(^\circ)$

- **Instants of measuring**: At Knee_Max_Height. Right: t3; Left: t7.
- **Description**: The angle between horizontal axis and the thigh axis of the leg in flight.
- **Markers used**: RGT, LGT, RFLE, LFLE.
- **Segments identified**: RightTigh, LeftThigh.
- **Formalization**:
  - $\Theta_{TH,R} = \theta_{TH,R}(^\circ) - 90^\circ$
  - $\Theta_{TH,L} = \theta_{TH,L}(^\circ) - 90^\circ$

10. Shank To Vertical Angle - $\theta_{SH}(^\circ)$

- **Instants of measuring**: At Knee_Max_Height. Right: t3; Left: t7.
- **Description**: the angle between the vertical and the shank of leg in flight

Figure 3.15: Shank To Vertical Angle

- **Markers used**: RGT, LGT, RLM, LLM.
- **Segments identified**: RightShank, LeftShank.
- **Formalization**:
  - $\theta_{SH_R}(^\circ)$
  - $\theta_{SH_L}(^\circ)$

11. Ankle Angle - $\Phi_{ankle}(^\circ)$

- **Instants of measuring**: At Knee_Max_Height. Right: t3; Left: t7.
- **Description**: The angle between the shank front face and the foot upper face of the leg in flight.
- **Markers used**: RHF, LHF, RLM, LLM, RCA, LCA, RVMH, LVMH.
- **Segments identified**: RightShank, LeftShank, RightFoot, LeftFoot.
- **Formalization**:
  - $\Phi_{ankle,R}(^\circ)$
  - $\Phi_{ankle,L}(^\circ)$

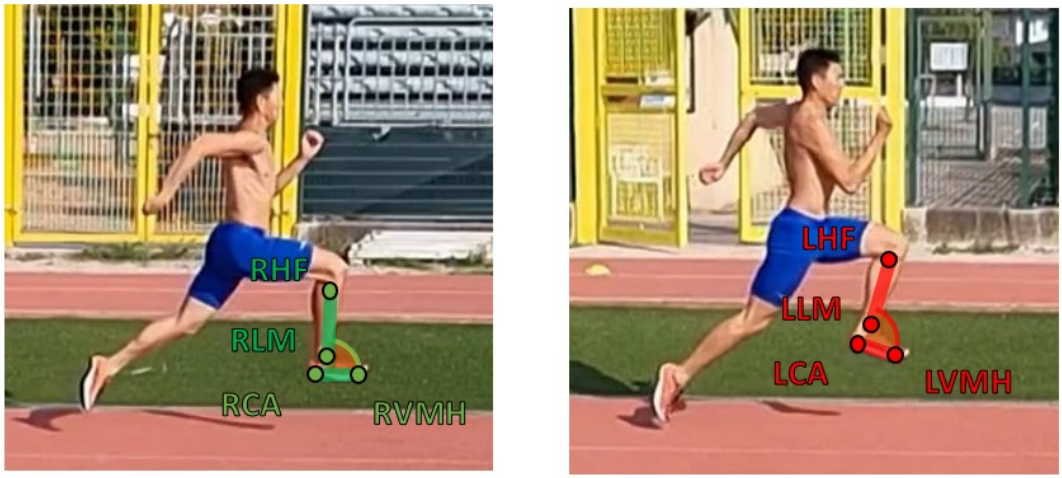

Figure 3.16: Angle Angle

12. Range At Foot Off - $\gamma_{TH}(^\circ)$

- **Instants of measuring**: At Foot_Off. Right: t6; Left: t2.
- **Description**: Relative contralateral angle between two thighs.
- **Markers used**: RGT, LGT, RFLE, LFLE.
- **Segments identified**: RightThigh, LeftThigh.
- **Formalization**:

$$\gamma_{TH,L}(t2) = \theta_{TH,L}(t2) - \theta_{TH,R}(t2)$$
$$\gamma_{TH,R}(t6) = \theta_{TH,R}(t6) - \theta_{TH.L}(t6)$$

3.2.4 Thigh Angular Velocity Parameters

13. Early Flexion - $\Delta\Theta_{EF}(^\circ), TAV_{EF}(^\circ/s)$

- **Instants of measuring**: From Foot_Off to contralateral Midstance. Right: t2 to t5; Left: t6 to t9.
- **Description**:
  - $\Delta\Theta_{EF}(^\circ)$ is the difference between two absolute angles: thigh absolute angle at contralateral Midstance and thigh absolute angle at Foot_Off.
  - $\Delta\Theta_{EF,R}(^\circ) = \Theta_{TH,R}(t5) - \Theta_{TH,R}(t2)(^\circ)$

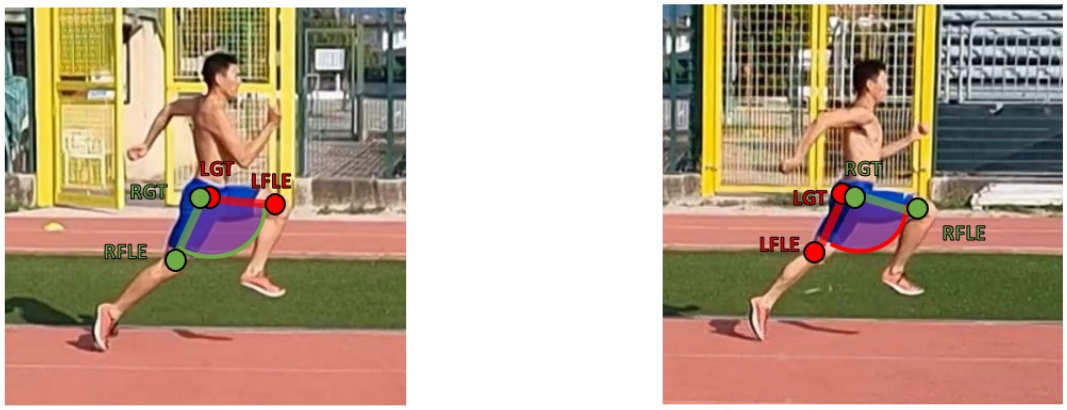

t2 – FOOT OFF L t6 – FOOT OFF R

Figure 3.17: Thigh Switch Range at Foot Off

- $\Delta\Theta_{EF,L}(^\circ) = \Theta_{TH,L}(t9) - \Theta_{TH,L}(t6)(^\circ)$
- $\Delta\Theta_{EF}(s)$: it's the time interval between two instants: contralateral midstance (t5, t9) and Foot_Off (t2,t6)
- $TAV_{EF}(^\circ/s)$: it's the angle covered by the thigh over the selected time interval of Early Flexion.

- **Markers used**: RGT, LGT, RFLE, LFLE.
- **Segments identified**: RightThigh, LeftThigh.
- **Formalization**:
  - Right leg at Foot_Off: $\theta_{TH,R}(t2)$
  - Right leg at Midstance_L: $\theta_{TH,R}(t5)$
  - Left leg at Foot_Off: $\theta_{TH,L}(t6)$
  - Left leg at Midstance_R: $\theta_{TH,R}(t9)$

$$TAV_{EF}(^\circ/s) = \omega_{EF,TH,R} = \frac{\Delta\theta_{EF,TH,R}}{\Delta t_{EF}} = \frac{\theta_{TH,R}(t5) - \theta_{TH,R}(t2)}{(t5 - t2)}$$

$$TAV_{EF}(^\circ/s) = \omega_{EF,TH,L} = \frac{\Delta\theta_{EF,TH,L}}{\Delta t_{EF}} = \frac{\theta_{TH,L}(t9) - \theta_{TH,R}(t6)}{(t9 - t6)}$$

14. Full Flexion - $\Delta\Theta_{FF}(^\circ), TAV_{FF}(^\circ/s)$

- **Instants of measuring**: From Foot_Off to contralateral Knee_Max_Height of same leg that was in contact with ground. . Right: t2 to t7; Left: t6 to t11.
- **Description**:

Figure 3.18: Early Flexion

  - $\Delta\Theta_{FF}(^\circ)$ is the difference between two absolute angles: thigh absolute angle at contralateral Knee_Max_Height and thigh absolute angle at Foot_Off.
  - $\Delta\Theta_{FF,R}(^\circ) = \Theta_{TH,R}(t7) - \Theta_{TH,R}(t2)(^\circ)$
  - $\Delta\Theta_{FF,L}(^\circ) = \Theta_{TH,L}(t11) - \Theta_{TH,L}(t6)(^\circ)$
  - $\Delta\Theta_{FF}(s)$: it's the time interval between two instants: contralateral midstance (t7, t11) and Foot_Off (t2,t6)
  - $TAV_{FF}(^\circ/s)$: it's the angle covered by the thigh over the selected time interval of Full Flexion.

- **Markers used**: RGT, LGT, RFLE, LFLE.
- **Segments identified**: RightThigh, LeftThigh.
- **Formalization**:
  - Right leg at Foot_Off: $\theta_{TH,R}(t2)$
  - Right leg at Knee_Max_Height_R: $\theta_{TH,R}(t7)$
  - Left leg at Foot_Off: $\theta_{TH,L}(t6)$
  - Left leg at Knee_Max_Height_L: $\theta_{TH,R}(t11)$

$$TAV_{FF}(^\circ/s) = \omega_{FF,TH,R} = \frac{\Delta\theta_{FF,TH,R}}{\Delta t_{FF}} = \frac{\theta_{TH,R}(t7) - \theta_{TH,R}(t2)}{(t7 - t2)}$$

$$TAV_{FF}(^\circ/s) = \omega_{FF,TH,L} = \frac{\Delta\theta_{FF,TH,L}}{\Delta t_{FF}} = \frac{\theta_{TH,L}(t11) - \theta_{TH,R}(t6)}{(t11 - t6)}$$

15. Early Extension - $\Delta\Theta_{EE}(^\circ), TAV_{EE}(^\circ/s)$

- **Instants of measuring**: From contralateral Knee_Max_Height to Foot_Strike. Right: t7 to t8; Left: t3 to t4.

Figure 3.19: Full Flexion

- **Description**:
  - $\Delta\Theta_{EE}(^\circ)$ is the difference between two absolute angles: thigh absolute angle at Foot_Strike and thigh absolute angle at contralateral Knee_Max_Height.
  - $\Delta\Theta_{EE,R}(^\circ) = \Theta_{TH,R}(t8) - \Theta_{TH,R}(t7)(^\circ)$
  - $\Delta\Theta_{EE,L}(^\circ) = \Theta_{TH,L}(t4) - \Theta_{TH,L}(t3)(^\circ)$
  - $\Delta\Theta_{EE}(s)$: it's the time interval between two instants: contralateral midstance (t8, t4) and Foot_Off (t7,t3)
  - $TAV_{EE}(^\circ/s)$: it's the angle covered by the thigh over the selected time interval of Early Extension.
- **Markers used**: RGT, LGT, RFLE, LFLE.
- **Segments identified**: RightThigh, LeftThigh.
- **Formalization**:
  - Right leg at Foot_Strike: $\theta_{TH,R}(t8)$
  - Right leg at Knee_Max_Height_R: $\theta_{TH,R}(t7)$
  - Left leg at Foot_Strike: $\theta_{TH,L}(t4)$
  - Left leg at Knee_Max_Height_L: $\theta_{TH,R}(t3)$

$$TAV_{EE}(^\circ/s) = \omega_{EE,TH,R} = \frac{|\Delta\theta_{EE,TH,R}|}{\Delta t_{EE}} = \frac{|\theta_{TH,R}(t8) - \theta_{TH,R}(t7)|}{(t8 - t7)}$$

$$TAV_{EE}(^\circ/s) = \omega_{EE,TH,L} = \frac{|\Delta\theta_{EE,TH,L}|}{\Delta t_{EE}} = \frac{|\theta_{TH,L}(t4) - \theta_{TH,R}(t3)|}{(t4 - t3)}$$

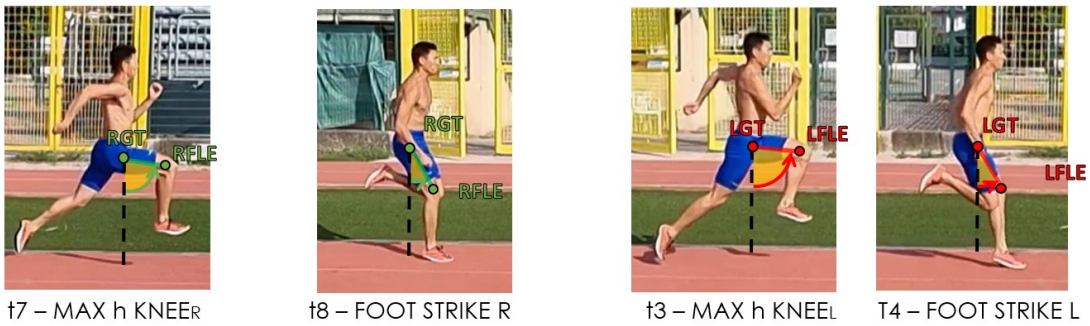

Figure 3.20: Early Extension

3.3 Kinematic Parameters: Block Start

When performing block starts - also known as the beginning of the acceleration phase - the athlete executes a series of actions in a moderately cyclic pattern. Due to the nature of the block start, an athlete will set the starting blocks with the preferred leg in front. Therefore, we have two possible start cases: left leg in front and right leg in front. The only difference is in the order of steps. If the left leg is in front, it will clear the block last, thus the right leg landing the first step out of the block. Similarly, if the right leg is in front, the left leg performs the first step. After this, the steps keep alternating similar to TSSR, although the athlete is accelerating and has not yet reached max velocity. We picked three instants that we believe well-represent the start cycle. Temporal, spatial and angular parameters are computed at - or between - the following four instants:

- **Gun**: The instant in which the start signal is given. In a competition, a gun is fired. The athlete is holding the position for a few seconds, waiting for the signal.
- **Block clearance**: The instant in which the front leg of the athlete clears the block: no part of the foot is touching the block anymore.
- **Foot Strike**: the instant in which the foot touches the ground.
- **Foot Off**: the instant in which the foot is no more in contact with the ground.

To better visualize the block start pattern, a grid was built. The images contained in the grid will be used in the current chapter to aid with the representation of each parameter.

As we can observe in 3.21:

- Gun occurs at instant t0, regardless of leg position.
- Block Clearance occurs at instant t1, regardless of leg position.
- Foot Strike occurs at instants t2, t6, t10 for rear foot, t4 and t8 for front foot.

- Foot Off occurs at instants t3, t7, t11 for rear foot, t5 and t9 for front foot.

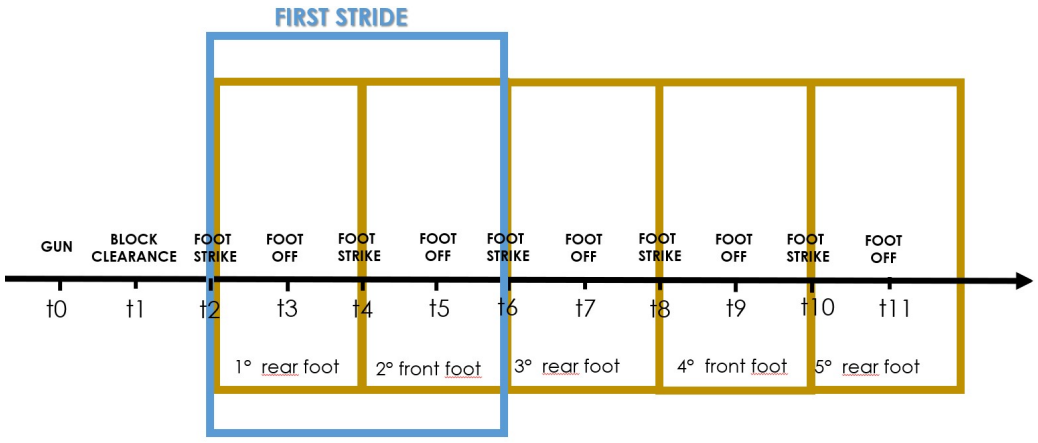

Figure 3.21: Start cycle scheme

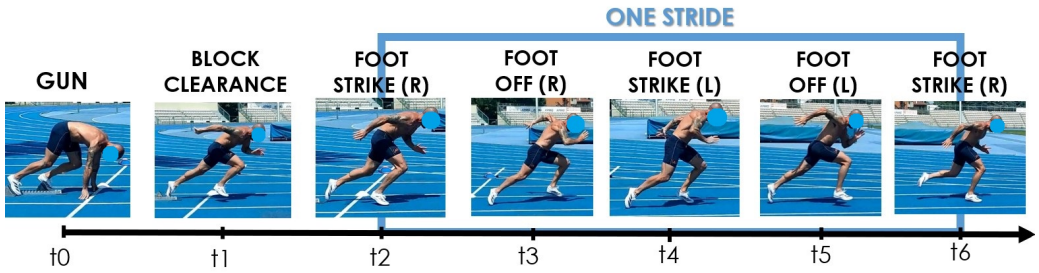

Figure 3.22: Start Cycles scheme visualized

3.3.1 Temporal Parameters

10. Contact time - $T_c(s)$

- **Instants of measuring**: From Foot_Strike to Foot_Off. Right leg: t2 to t3. Left leg: t4 to t6.
- **Description**: The time occurred between Foot_Strike and Foot_Off, during which one foot touches the ground.
- **Markers used**: RVMH, LVMH
- **Segments identified**: None.
- **Formalization**:

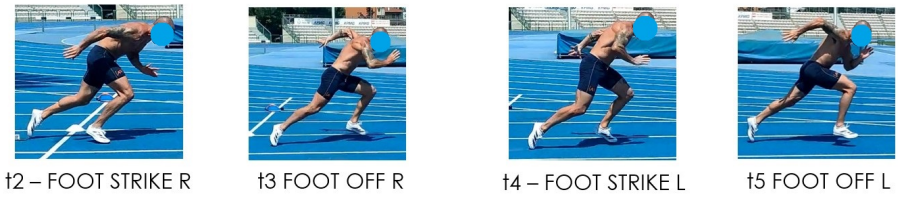

Figure 3.23: Contact Time

- $T_{C,R} = t3 - t2$
- $T_{C,L} = t5 - t4$

11. Flight Time - $T_{FL}(s)$

- **Instants of measuring**: From Foot_Off to Foot_Strike. Right leg: t5 to t6. Left leg: t3 to t4.
- **Description**: The time occurred between Foot_Off and Foot_Strike, during which neither foot touches the ground.
- **Markers used**: RVMH, LVMH
- **Segments identified**: None.
- **Formalization**:
  - $T_{FL,R} = t6 - t5$
  - $T_{FL,L} = t4 - t3$

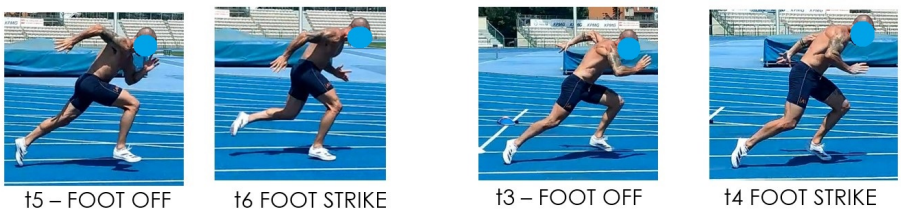

Figure 3.24: Flight Time

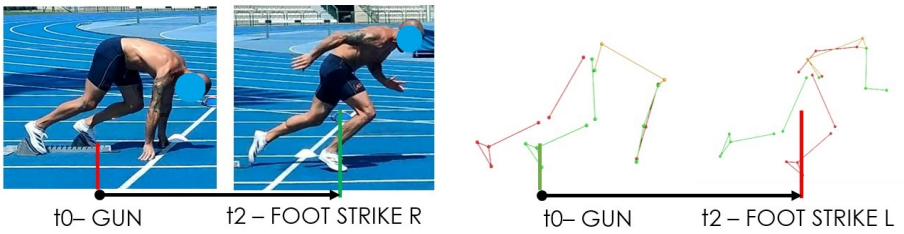

Figure 3.25: Block To First Foot Strike

3.3.2 Spatial Parameters

12. Block To First Foot Strike - $Len_{blockStep}(m)$

- **Instants of measuring**: From Foot_Off to Foot_Strike. Right leg: t2 to t4. Left leg: t4 to t6.
- **Description**: the distance measured from the contact of the front block foot in the block to the contact with the ground of the rear block foot.
- **Markers used**: RVMH, LVMH
- **Segments identified**: None.
- **Formalization**:
  - $Len_{blockStep,R}(m) = X_{RVMH}(t2) - X_{LVMH}(t0)$
  - $Len_{blockStep,L}(m) = X_{LVMH}(t2) - X_{RVMH}(t0)$

13. Step Length - $Len_{step}(m)$

- **Instants of measuring**: From Foot_Strike of one foot to Foot_Off of the other foot. Right leg: t2 to t4. Left leg: t4 to t6.
- **Description**: The horizontal distance between the contact point of a foot on the ground and the contact point on the ground of the subsequent foot.
- **Markers used**: RVMH, LVMH.
- **Segments identified**: None.
- **Formalization**:
  - $L_{step,R} = X_{RVMH}(t6) - X_{LVMH}(t4)$
  - $L_{step,L} = X_{LVMH}(t4) - X_{RVMH}(t2)$

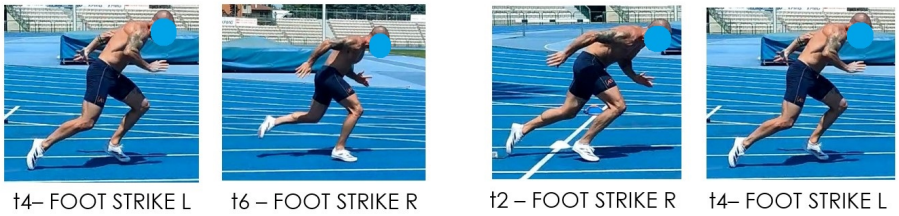

Figure 3.26: Step Length

Figure 3.27: Push Angle at Block Clearance

3.3.3 Angular Parameters

1. Push Angle at block clearance - $\beta_{push,LEG}$

- **Instants of measuring**: Block Clearance. Instant t1.
- **Description**: Ideal angle between horizontal and pushing leg GT-ML segment and horizontal.
- **Markers used**: RGT, LGT, RLM, LLM.
- **Segments identified**: Ideal lines between LGT and LLM, RGT and RLM.
- **Formalization**:
  - $\beta_{push,R}$
  - $\beta_{push,L}$

2. Thigh-trunk angle - Φ_h

- **Instants of measuring**: Block Clearance. Instant t1.
- **Description**: Relative angle between thigh and trunk posterior faces.

Figure 3.28: Thigh trunk angle at block clearance

- **Markers used**: RGT, LGT, RFLE, LFLE, C7.
- **Segments identified**: RightThigh, LeftThigh, Trunk.
- **Formalization**:
  - $\Phi_{h,R} = (180 + \phi_{h,R}(^\circ))$
  - $\Phi_{h,L} = (180 + \phi_{h,L}(^\circ))$

3. thigh-shank angle - Φ_k

- **Instants of measuring**: Block Clearance. Instant t1.
- **Description**: relative angle between thigh and shank posterior face.
- **Markers used**: RGT, LGT, RFLE, RFLE, RHF, LHF, RLM, LLM.
- **Segments identified**: RightThigh, LeftThigh, RightShank, LeftShank.
- **Formalization**:
  - $\Phi_{k,R} = (180 + \phi_{k,R}(^\circ))$
  - $\Phi_{k,L} = (180 + \phi_{k,L}(^\circ))$

Figure 3.29: Thigh-Shank angle at block clearance

Figure 3.30: Shank to vertical angle at block clearance

4. Shank to vertical angle - Θ_{SH}

- **Instants of measuring**: Block Clearance. Instant t1.
- **Description**: absolute angle between the vertical and shank anterior face.
- **Markers used**:RHF, LHF, RLM, LLM.
- **Segments identified**: RightShank, LeftShank.
- **Formalization**:
  - $\theta_{SH,R}$
  - $\theta_{SH,L}$

Figure 3.31: Thigh Angle at block clearance

5. **Thigh angle -** Θ_{TH}

   - **Instants of measuring**: Block Clearance. Instant t1.
   - **Description**: absolute angle between the vertical and shank anterior face.
   - **Markers used**:RHF, LHF, RLM, LLM.
   - **Segments identified**: RightShank, LeftShank.
   - **Formalization**:
     - $\Theta_{TH,R} - 90^{\circ}$
     - $\Theta_{TH,L} - 90^{\circ}$

6. **Push angle -** $\Theta_{push,SH}$

   - **Instants of measuring**: Foot Strike. Instant t2.
   - **Description**: absolute angle between horizontal and shank of pushing leg.
   - **Markers used**:RHF, LHF, RLM, LLM.
   - **Segments identified**: RightShank, LeftShank.
   - **Formalization**:
     - $\Theta_{push,SH,R} = 90^{\circ} - \theta_{SH,R}{}^{\circ}$
     - $\Theta_{push,SH,L} = 90^{\circ} - \theta_{SH,L}{}^{\circ}$

Figure 3.32: Push Angle at Foot Strike

Figure 3.33: Trunk angle at Foot Strike

7. **Trunk angle -** Θ_{TR}

- **Instants of measuring**: Foot Strike. Instant t2.
- **Description**: relative angle between horizontal and trunk.
- **Markers used**: S, C7.
- **Segments identified**: Trunk.
- **Formalization**:
  - $\Theta_{TR} = 90° - \theta_{TR}(°)$

(a) Right leg.

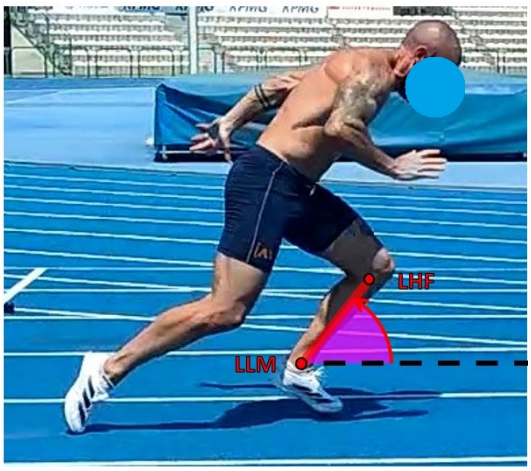

(b) Left leg.

Figure 3.34: Push Angle at Foot Off.

8. Push angle - $\beta_{push,LEG}$

- **Instants of measuring**: Foot Off. Instant t3.
- **Description**: Ideal angle between pushing leg GT-ML segment and horizontal.
- **Markers used**: RGT, LGT, RLM, LLM.
- **Segments identified**: Lines connecting RGT and RLM, LGT and LLM.
- **Formalization**:
  - $\beta_{push,R}$
  - $\beta_{push,L}$

9. Thigh-trunk Angle - Θ_h

- **Instants of measuring**: Foot Off. Instant t3.
- **Description**: relative angle between thigh and trunk.
- **Markers used**: RGT, LGT, RFLE, LFLE, S, C7.
- **Segments identified**: RightThigh, LeftThigh, Trunk.
- **Formalization**:
  - $\Theta_{h,R}(^\circ) = (180 + \theta_{h,R}(^\circ))$
  - $\Theta_{h,L}(^\circ) = (180 + \theta_{h,L}(^\circ))$

(a) Right leg.

(b) Left leg.

Figure 3.35: Thigh-trunk angle at Foot Off.

14. Range At Foot Off - $\gamma_{TH}(^\circ)$

- **Instants of measuring**: At Foot_Off. Right: t3; Left: t5.
- **Description**: Relative contralateral angle between two thighs.
- **Markers used**: RGT, LGT, RFLE, LFLE.
- **Segments identified**: RightThigh, LeftThigh.
- **Formalization**:
  - $\gamma_{TH,L}(t3) = \theta_{TH,L}(t3) - \theta_{TH,R}(t3)$
  - $\gamma_{TH,R}(t5) = \theta_{TH,R}(t5) - \theta_{TH.L}(t5)$

3.4 Kinetic parameters: TSSR and Block Start

The 9 AMTI OR6 series force plates allow the collection of precious data related to ground contact. Thanks to a frequency of 1500Hz, we are able to detect events with a granularity of less than 1 millisecond.

3.4.1 TSSR

For each leg we record maximum ground reaction force on mediolateral, vertical and horizontal axis, and the impulse in over the three axis. The measurement occurs between Foot Strike and

t3 – FOOT OFF R

(a) Right leg.

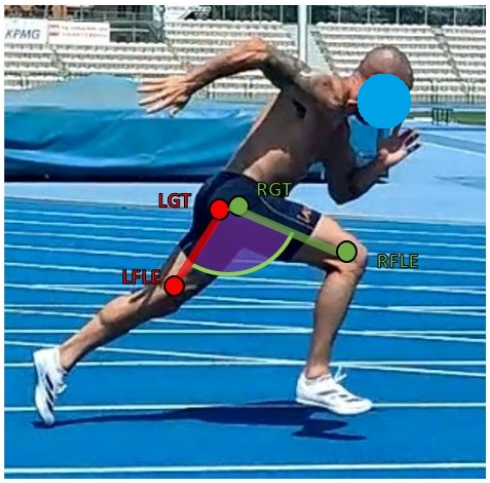

t5 – FOOT OFF L

(b) Left leg.

Figure 3.36: Thigh switch range at Foot Off.

Foot Off: from instant t0 to instant t2 for right leg; from instant t4 to instant t6 for left leg. (see 3.5)

- Left Impulse: vertical, horizontal, braking, net propulsive, mediolateral
- Left maxGRF: vertical, horizontal
- Right Impulse: vertical, horizontal, braking, net propulsive, mediolateral
- Right maxGRF: vertical, horizontal

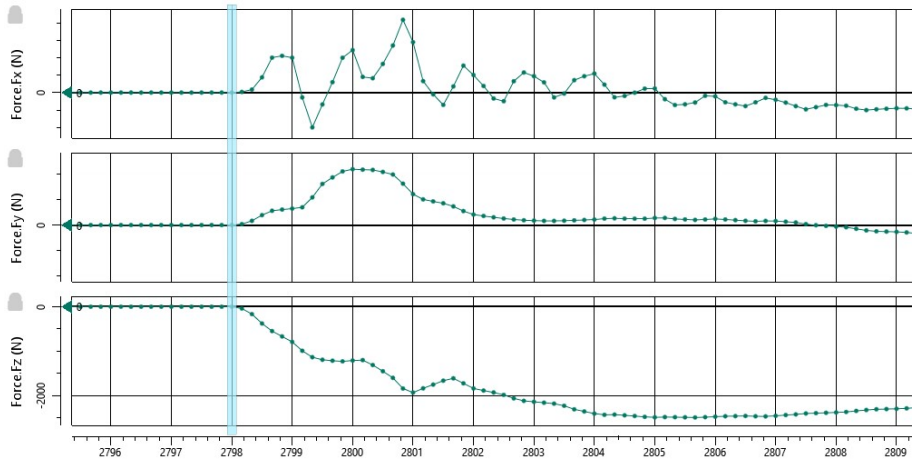

Figure 3.37: Ground Reaction forces (X mediolateral, Y anteroposterior, Z vertical) from Vicon Nexus

As we can notice, it is hard to understand this GRF data. Through the MATLAB script we are able to better visualize the steps and the GRF involved.

3.4.2 Block start

As mentioned in the previous chapter, 9 force plates are installed on the ground, below a layer of track compound. Two smaller force plates are placed under the starting block, allowing capturing each foot distinctly. These two plates will provide the meaningful output while the athlete performs the first push until block clearance. After a shot period of flight time, the back leg foot will step on the track, usually on the third plate. The front leg foot will follow and the pattern will continue. Due to the nature of the start, we record different data between block and subsequent steps. The details follow.

Block Clearance

For each leg we record maximum and mean ground reaction force and the impulse over the three axis. The measurement occurs between Gun instant to block clearance: t0 to t1. (see 3.22)

- Right Impulse: vertical, propulsive, braking, net horizontal, mediolateral
- Left impulse: vertical, propulsive, braking, net horizontal, mediolateral
- Right maxGRF: vertical, anteroposterior, mediolateral
- Left maxGRF: vertical, anteroposterior, mediolateral

Subsequent Steps

For each leg we record maximum ground reaction force on vertical and horizontal axis, and the impulse in over the three axis. The measurement occurs between Foot Strike and Foot Off: from instant t2 to instant t3 for rear foot; from instant t4 to instant t5 for front foot and so on. (see 3.22)

- Left Impulse: vertical, propulsive, braking, net horizontal, mediolateral
- Left maxGRF vertical, horizontal, mediolateral
- Right Impulse: vertical, propulsive, braking, net horizontal, mediolateral
- Right maxGRF vertical, horizontal, mediolateral

An in depth review of data and plots is conducted on chapter 6.

Chapter 4

From raw data to C3D files

4.1 The C3D file standard

C3D files [34] were created in 1987 by Andrew Dainis. The format was developed to address the need for a standardized file format capable of handling 3D motion data alongside analog data, such as force measurements or EMG, for biomechanics and motion analysis.

C3D files store 3D coordinate data, along with analog data such as force plates, electromyography (EMG), or other sensors. Developed to handle large datasets, C3D files are flexible and compatible with many motion capture and analysis systems. The format organizes data in a way that is easy to process and analyze, containing both raw and processed data, and can store metadata like event markers or frame rates.

C3D files are ideal for biomechanics analysis because they store complex datasets in a compact and organized format. They allow the integration of 3D motion data, ground reaction forces, and other sensor data, all within a single file. This makes it easy to synchronize multiple data streams, which is critical for accurate biomechanical analysis. The standardized format also ensures compatibility with most biomechanics software tools, enabling researchers to share and analyze data easily across different platforms.

4.2 Data pre-processing using Vicon Nexus

Any collected data from the trials at the Palaindoor facility were stored in a C3D file. This file, however, needs to be processed to ensure proper reading from MATLAB scripts. Vicon Nexus 2.15 has been used to perform such task. The main objective was to correctly label markers, remove noise, and fill broken trajectories. Reference manuals were used (see: [35]).

4.2.1 Creating a labeling skeleton template

In order to be efficient, we want to avoid the creation of a new template for every subject in the study. We need a base template that can be applied to each athlete. To do so, Vicon Nexus requires information such as a description of the generic relationship between segments and joints and the Vicon markers for the subject. This information, which identifies the markers that Nexus is to track and how these markers are connected to the underlying segments, is stored in the following file types:

- *VST*: labeling skeleton template (.vst file). It describes the generic relationship between physical markers attached to a subject and the skeletal structure to which the markers are attached for a certain type of subject, for example, a human being. It contains the names of the markers in the marker set (e.g. RASIS), the skeletal structure of the subject being tracked (e.g. the Femur connected to the Pelvis, the Tibia connected to the Femur), the relationship between the marker set and the skeletal structure (e.g. the RASIS marker is attached to the Pelvis segment), the type of joints that connect the segments to other segments (e.g. ball joint, free joint) and other properties, such as segment, marker and joint names and colors, and how the markers are displayed in the 3D Perspective view;

- *VSK*: labeling skeleton (.vsk file). Describes the relationship between physical markers and the skeletal structure to which the markers are attached for a specific subject of the type described in the associated VST. For example, if the VST represents a human being, the VSK contains the marker arrangement and skeletal structure calibrated for an individual person.

This way, two subjects with different anthropometries won't need different VSTs. We can use the same marker protocol and update the VST by calibrating of the specific subject. This information, like segments length, is stored in the labeling skeleton (VSK) for any subject. The skeleton template is created from the Static Trial, performed at the beginning of any session.

4.2.2 Static Trials

After opening the trial file, a new Blank-Subject is created from Resources − Subject pane toolbar as shown in 4.1.

We defined a model template called *NormoStatic*. This allowed us to calibrate to each subject. The segments and joints were defined, along with their respective markers. Joints are necessary to connect different segments; in the NormoStatic template were used:

- Ball Joint: joint with three rotational degrees of freedom; it's used to link two adjacent segments;

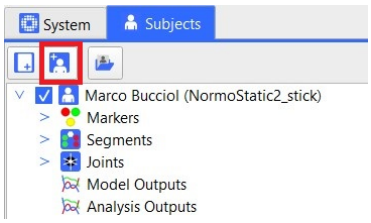

Figure 4.1: New Subject

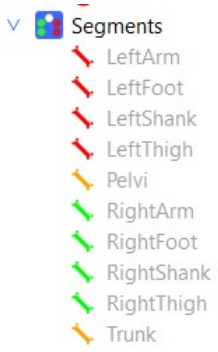

(a) Segments

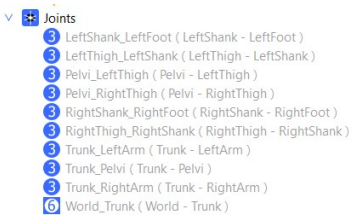

(b) Joints

SEGMENTS	MARKERS
LeftArm	LAC, LHLE, LMSS
LeftFoot	LLM, LCA, LVMH
LeftShank	LHF, LLM
LeftThigh	LGT, LFLE
Pelvis	S, RASIS, LASIS
RightArm	RAC, RHLE, RMSS
RightFoot	RLM, RCA, RVMH
RightShank	RHF, RLM
RightThigh	RGT, RFLE
Trunk	C7, S

(c) Segments and markers

Figure 4.2: Segments and Joints in Nexus

- Free Joint: joint with six degrees of freedom (rotational and translational); it's used for the root segment, in particular to link Pelvis with global origin.

It can be noted that segment names contain either "left" or "right" to automatically associate a color to the segment. The chosen standard is green for right side, red for left side. Orange for segments that don't belong to a side, like *Pelvis* or *Trunk*. Such colors will prove greatly helpful during the tracking procedure. To link two segments, the parent segment must be selected, that is the proximal segment of the joint, and the child segment that is the distal segment of the joint.

Once the .vst file NormoStatic is attached to the subject, we can reconstruct the markers in 3D space using the *Reconstruct* button as shown in figure 4.3.

Taking care to use the *Forward Labeling*, manual tracking of the markers is performed. Usually, Nexus will aid in this by tracking the name if there is absence of noise. Then, all frames are checked for errors. Once done, calibration is run through commands *Static Skeleton*

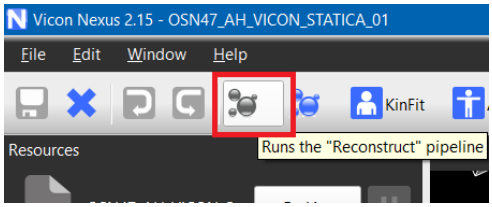

Figure 4.3: Reconstruct button

(a) Reconstructed Markers (b) Labeled Segments

Figure 4.4: Unlabeled and Labeled skeleton

Calibration and *Update Skeleton Parameters*. Lastly, export the C3D static file.

4.2.3 Dynamic Trials: TSSR

The tracking procedure will be described for the flying trials. In the subsequent section, about block starts, only the specific differences will be addressed to avoid repetitions.

First we open the trial file. We run *Reconstruct* from the pipeline in figure 4.6. This, similar to the static file, reconstructs the markers in 3D space. Then we run *Label*, to automatically assign labels and segments. Depending on the subject and the state of tracking, Nexus may be able to correctly categorize all the markers in every frame. More often than not, human intervention is needed. By selecting the time section of interest - sometimes the live operator starts recording too soon - we can get rid of empty data; we then move to the first frame and check the labeling, correcting if needed. Again, making sure that *Forward Labeling* is selected. The main task of the human operator is to make sure that markers are not flipped, as in right/left side and in the same limb. Sometimes this subtly happens and is hard to catch. A good way is to check the trajectories of the markers by selecting them a few at a time. Markers may be isolated at the beginning and at the end of the acquisition volume due to the nature of the camera setting, with more focus on the middle and fewer cameras on the start and end of acquisition volume.

Once all the markers are labeled, we move run *Fill gaps - woltring* and *Fill gaps - cyclic*. These scripts will fill most gaps in the data. It can happen that some gaps are not filled due to scarce marker data or noise. Human intervention is possible with 5 different options:

- Spline Fill: it performs a cubic spline interpolation operation to fill the gap, this is not the best way to interpolate marker trajectories but can be used to fill small frames gaps;
- Pattern Fill: it uses the shape of another trajectory without a gap to fill the selected gap.

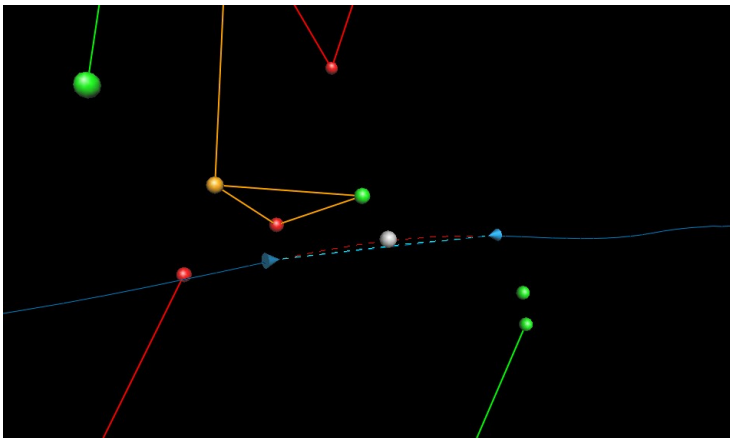

Figure 4.5: Fixing Trajectories

This way can be useful only if there is a suitable marker with a trajectory similar to the one whose gap need to be filled. This is typically the case when the trajectories originated from markers attached to the same segment

- Rigid Body Fill: it uses the shape of the trajectory of other three markers without a gap to fill the selected gap. Hence, that way is useful if there is a rigid or semi-rigid relationship exists between markers (e.g. LASIS, RASIS);

- Kinematic Fill: this option uses information about the connection of markers to segments in the labeling skeleton template (VST);

- Cyclic Fill: for trials that contain captured data that is cyclic in nature (e.g. running), this option uses patterns from a missing marker from earlier or later gait cycles to fill gaps

The two most used ways to fill gaps has been the Rigid Body and the Cyclic Fill. In some cases also Pattern and Spline Fill turned to be useful. After filling as many gaps as possible - it can happen that a few gaps can't be filled - we run *Functional Skeleton Calibration* if it's the first dynamic trial, and *Update Skeleton Calibration*. The Functional Skeleton Calibration operation can be run in order to update the labeling skeleton of the specific subject (VSK). As previously mentioned, to improve later labeling of other Dynamic Trials, also the labeling skeleton template (VST) must be updated to match the data that was calculated for this specific subject (VSK) during the Dynamic Trial. To do so, the Update Skeleton Parameters operation must be run. Lastly, "*Export .C3D*" is run. It's possible to move onto the next trial, repeating the pipeline.

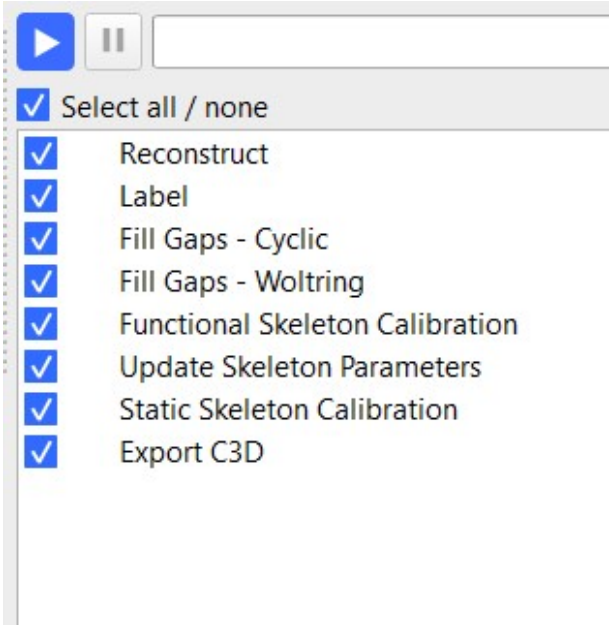

Figure 4.6: Vicon Nexus - Pipeline

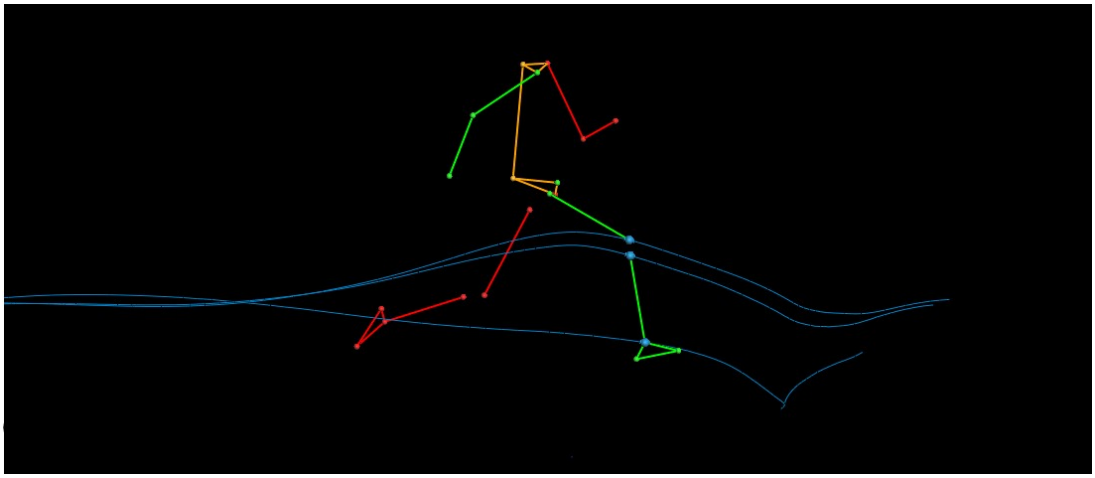

Figure 4.7: Checking Trajectories

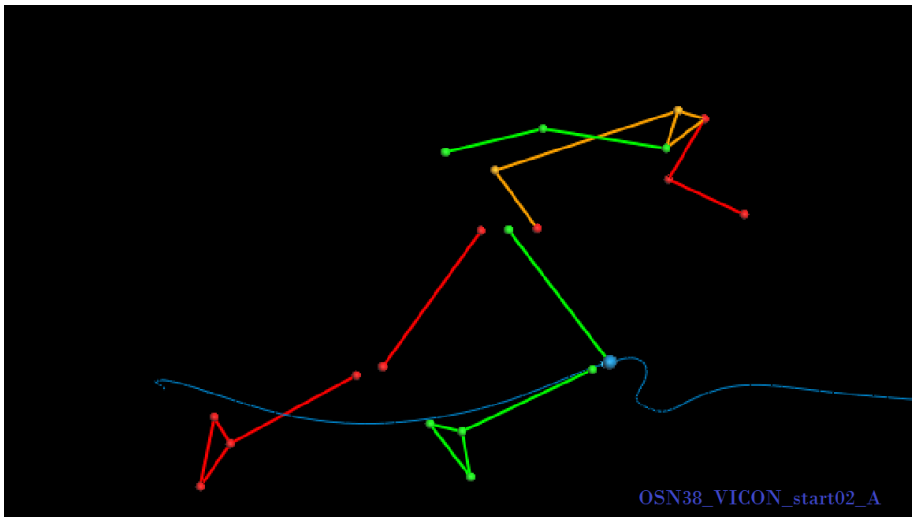

Figure 4.8: A tracked block start

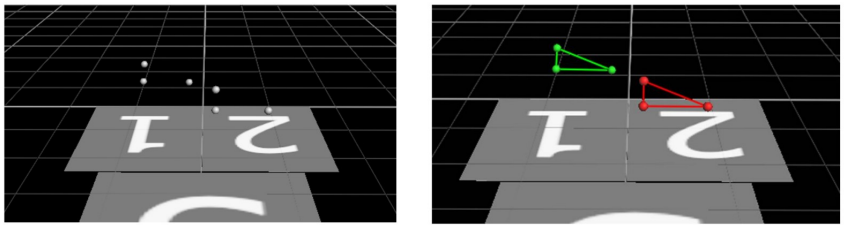

Figure 4.9: Labeling Blocks

4.2.4 Dynamic Trials: Block Start

Tracking Block starts is very similar to TSSR. The difference is that the athlete is already in the acquisition volume once the acquisition is in progress. The athlete is ready on the blocks, and it was decided to keep C3D data from the moment the athlete goes into ”Set” position to the instant after the last force plate is cleared.

Block pedals have to be tracked in order to create the two planes on which athletes push. To do so, 3 markers were placed on each pedal to define the plane. The same procedure of Static Tracking is followed for Block tracking. Dedicated names were given to such markers:

- Right pedal: Rside, Rdown, Rcenter.
- Left pedal: Lside, Ldown, Lcenter.

This Block Orientation C3D file will be given to MATLAB, that will be able to extract the pedal steepness and apply a rotation matrix to the forces exerted on the force plates 1 and 2.

Chapter 5

Programming for sprinting

5.1 Overview

In order to reduce the workload and speed up the production of results, it is necessary to make use of automated tools. These also guarantee accuracy and objectivity in the execution. The choice landed on MATLAB [36], a high-level programming language and environment used for numerical computing and data analysis. It is widely used in engineering, scientific research, and academia for its ability to handle complex mathematical operations, visualize data, and develop algorithms. MATLAB is particularly suited for applications like bio-mechanics, where data from sensors and tracking systems require detailed analysis. The second reason for this choice is that work has already been done on this subject by the laboratory of Sports Engineering for the PROLYMPIA project. Programming on MATLAB allows to leverage and expand the existing structure. MATLAB is well suited for Bio-mechanics due to the wide choice of libraries for data input-output operations, data visualization, analysis and reporting. While the application PRONORMO was in development, a parallel approach was followed to extract the data from dozens of trials in order to move straight to a data analysis phase. While this method - using the SMARTAnalyzer software to produce an .mdx file - enabled the data analysis to be performed while development of PRONORMO was in progress, it became clear that it was too time-consuming. Human intervention was needed for each trial, requiring at least 30 minutes for a complete analysis to be created. While the development of PRONORMO required months, at its current state it can output multiple reports in seconds, depending on the resources of the computer that runs it. The author's laptop is able to output a report in less than 10 seconds. In this chapter we overview the PRONORMO software, and consider:

- Code Logic
- Identification of Key Time Points

- Angle Calculations
- Force Calculations
- Validation of Outputs
- Challenges

It should be noted that the amount of code written during months of works exceeds six thousand lines. Considering an average of 7 words per line, it translates to more than 44 thousand words.

5.2 Code Logic

First let us introduce the diagram representing the logic of the application. The first action is the selection of the .c3d files to be analyzed. These are the output of Vicon Nexus software, and contain the markers and force plates data. For the specifics, refer to the chapter 4, where details about technologies and materials are discussed. The software will then classify the files based on their name. When a static file is found, body weight and leg length are extracted to be used later in the process. When a ”Block Configuration” file is found, the inclination of the block pedals (or block footplates) is extracted to allow exact computation of ground reaction forces lates in the process. When a TSSR file is found, cleans the raw data by removing unused and unlabeled markers. Applies a low pass filter to remove noise, and unifies the force plates into a single one. Then, detect the events we already introduced: foot strike, foot off, midstance and max knee height. Based on these, performs kinematic and kinetic analysis. When a Block start file is found, clean the raw data by removing unused and unlabeled markers. Apply a low pass filter to remove noise, and unify the force plates into a single one, excluding the plates 1 and 2 under the blocks. Then, detect the events we already introduced: gun, block clearance, foot strike, foot off. Based on these, perform kinematic and kinetic analysis. At last, results will be output as a PDF report, and stored in a CSV file for further analysis. The whole process requires no human input except at the beginning during the selection of the files. The report will be shown in the next chapters.

5.3 Identification of Key Time Points

The key time points for TSSR are - following gait order:

1. Foot strike

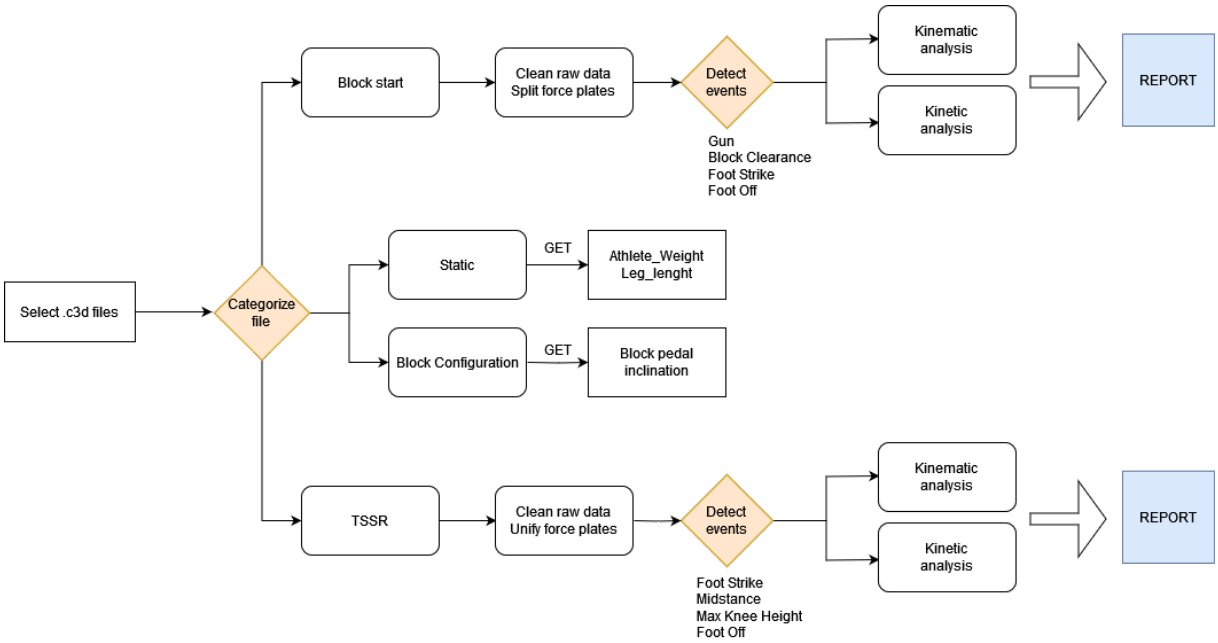

Figure 5.1: PRONORMO Diagram

2. Midstance
3. Knee max height
4. Foot off

The key time points for Block start are - following gait order:

1. Gun
2. Block Clearance
3. Foot strike
4. Foot off

Both need specific approaches to detect the exact instants. The script relies on both markers' coordinates and force plate data.

5.3.1 Track Steady State Running

When performing TSSR the gait cycle is repeated for a few steps. Our system at the Palaindoor Track in Padova allowed us to capture 3 or 4 steps of each athlete. This was based on gender, ability and distance of the first step from the beginning of the acquisition volume.

To determine **foot strike and foot off** instants we used force plate data. Markers data was not precise enough to ensure correctness and consistency of instant detection intra and inter trials. The script logic is the following: detect vertical force on Z axis; after a threshold is crossed - around 40 Newtons - mark a foot strike. Once the Z value falls under the threshold, mark a foot off. Between steps the reading should be zero due to the nature of the running cycle. A timed threshold system was added to filter out plate aftershocks or toe dragging. Once Z value reaches 40 N again, a new step is registered. Details on this will follow in the next sections.

To determine **Midstance** instants, we used markers RGT and RVMH 3.1 for right side and LGT and LVMH for left side. We defined midstance the instant when such markers are on the same vertical line, meaning they share the closest Y coordinate value recorded.

To determine **Knee max height** instants, we used markers RFLE for right side and LFLE for left side. We defined Knee max height the instant when such markers are on a local peak, meaning they have the highest local Z value. Due to the nature of sprinting, such peak is clearly identifiable by standard signal analysis functions as we can see from the image.

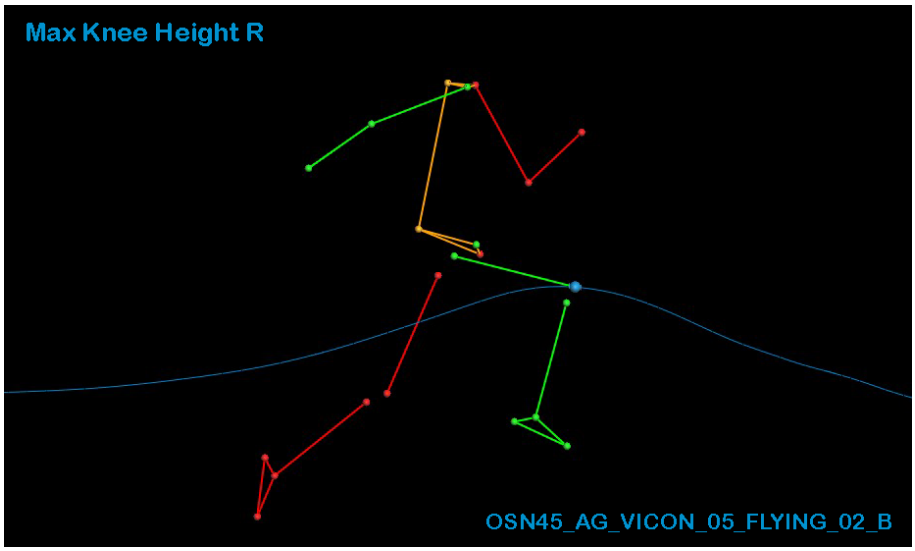

Figure 5.2: Max Knee height of right leg

Code Example: Finding Midstance

```
function [rightMaxHeight, leftMaxHeight] = find_KneeMaxHeight(markers, firstFrame)
  % Initialize output arrays
  rightMaxHeight = [];
  leftMaxHeight = [];

  % Get the vertical coordinates for each marker
```

```
    rgtZ = markers.RGT(:, 3);
    rfleZ = markers.RFLE(:, 3);
    lgtZ = markers.LGT(:, 3);
    lfleZ = markers.LFLE(:, 3);

    % Look at the vertical position of knee markers
    [~, rightPeaks] = findpeaks(rfleZ, 'MinPeakDistance', 10);
    [~, leftPeaks] = findpeaks(lfleZ, 'MinPeakDistance', 10);

    % Check if the appropriate knee is higher at each peak.
    % Condition: RLFE > LFLE for right leg. Vice versa for left leg.
    rightPeaks = rightPeaks(rfleZ(rightPeaks) > lfleZ(rightPeaks));
    leftPeaks = leftPeaks(lfleZ(leftPeaks) > rfleZ(leftPeaks));
    rightMaxHeight = rightPeaks + firstFrame - 1;
    leftMaxHeight = leftPeaks + firstFrame - 1;

    % Check if any max height instants were found
    if isempty(rightMaxHeight)
        warning('No instants found. Check RFLE marker.\n');
    end

    if isempty(leftMaxHeight)
        warning('No instants found. Check LFLE marker.\n');
    end
end
```

This function identifies the maximum height reached by the right and left knees during a movement. It analyzes vertical marker data (RFLE and LFLE), finds the peaks with a minimum distance of 10 frames, and determines whether the right or left knee is higher at each peak. The output is the frame numbers of these maximum heights, adjusted for the starting frame for synchronization purposes with Vicon Software. If no valid peaks are found, a warning is issued.

5.3.2 Block Start

When performing Block starts the gait cycle is repeated for a few steps, although it changes over time. There are two possible start sequences, based on whichever foot is in front on the block. The rear foot is consequently the first step on the ground. After the gun and block clearance

phase, the athlete performs a sequence of foot strike and foot off instants, alternating between legs. Our system at the Palaindoor Track in Padova allowed to capture 4 or 5 steps of each athlete. This was based on gender, ability and distance of the first step from the beginning of the acquisition volume.

To determine the **gun** instant, a force plate-based approach was used. As the athlete is on ”Set” position, the body is tense, waiting for the signal. No marker is moving, the force applied to the ground is stable. We can determine the gun instant by finding when the vertical force component of plates 1 and 2 spikes up, as pedals were placed on two different plates (plate 1 for right pedal, plate 2 for left pedal). Then, subtract an average of 150ms worth of time, as this is the average reaction time of a subject.

To determine the **block clearance** instant a force plate-based approach was used. After the gun instant the athlete is now pushing against the block. The rear foot comes off the block first, while the front foot keeps pushing. Once the front leg straightens up and the push is complete, the left foot leaves the front block, thus the vertical force rapidly drops to zero marking the block clearance instant.

To determine **foot strike and foot off** instants we used force plate data. Markers data was not precise enough to ensure correctness and consistency of instant detection intra and inter trials. The script logic is the following: unify force plates from 3 to 9. Detect vertical force on Z axis; after a threshold is crossed - around 40 Newtons - mark a foot strike. Once the Z value falls under the threshold, mark a foot off. Between steps the reading should be zero due to the nature of the running cycle. A timed threshold system was added to filter out plate aftershocks or toe dragging. Once Z value reaches 40 N again, a new step is registered. To avoid false positives, a time threshold was added to the function with respect to the TSSR case. By finding the **block clearance** frame we are able to discard the data recorder before such event; as mentioned, the third force plate experiences the pressure from the hands, and occasional toe drags right after the block clearance. By making sure data is captured after **block clearance**, we are able to correctly categorize the subsequent steps.

A different approach was needed for the push out of the blocks, as pedals were placed on two different plates (plate 1 for right pedal, plate 2 for left pedal). The first two plates were segmented from the rest to be able to correctly detect the ground reaction forces of each foot. Moreover, given the varying steepness of each pedal, a rotation matrix was applied to correctly compute the force expressed by the athletes. The output of the rest of the plates, unified from 3 to 9, is suppressed during this phase, as the hands of the athlete are providing support on the ground. Details on this will follow in the next sections.

Code Example: Finding Block Clearance

```
function [bc_frame, bc_viconFrame, bc_analog] = find_block_clearance
  (markers, plate1_fz, plate2_fz, firstFrame)
  % Determine which plate forces to use based on the initial marker positions
  rvmhPos = markers.RVMH;
  lvmhPos = markers.LVMH;

  % Use plate1_fz if RVMH is higher on the Y axis than LVMH,
  % otherwise use plate2_fz
  if rvmhPos(1, 2) > lvmhPos(1, 2)
      fprintf("Right leg on front block\n")
      fz = plate1_fz;
  else
      fprintf("Left leg on front block\n")
      fz = plate2_fz;
  end

  % Find the maximum absolute value in the fz data
  [~, minIdx_fz] = min(fz);

  % Initialize block_clearance variable
  block_clearance_frame = [];

  % Iterate over the subsequent values after the maximum in the fz vector
  for i = minIdx_fz:length(fz)
      % Check if force falls below the threshold of 20 N
      if (fz(i)) > -20
          block_clearance_frame = i;  % Found the instant
          break;
      end
  end

  % If no block clearance is found (i.e., force never drops below 20 N)
  if isempty(block_clearance_frame)
      warning('No block clearance found; forces did not drop below 20 N.');
      block_clearance_frame = NaN;  % Return NaN to indicate no clearance found
```

```
    else
        % Convert the block clearance force plate index to marker frame index
        block_clearance_analog = block_clearance_frame;
        block_clearance_frame = block_clearance_frame / 1500;
        block_clearance_frame = round(block_clearance_frame * 250);
        block_clearance_viconFrame = block_clearance_frame + firstFrame;
    end
end
```

This function determines the moment an athlete's foot clears the starting block by analyzing force data from two plates. Based on initial leg positions, it selects which plate to analyze, finds when the force falls below 20 N, and calculates the corresponding frame. It returns the block clearance time in different formats, with warnings if no clearance is detected. Different formats are needed to aid in the following analysis of angles and forces. As we mentioned in previous chapters, the markers data was set at 250Hz and the force plates at 1500Hz.

5.4 Angle Calculations

Angle calculation is performed through specific functions. Dedicated scripts were written to handle the different nature and requirements of the parameters. Most of these functions are based on the events {Foot strike, Midstance, Foot off, Max knee height} for TSSR and {Gun, Block clearance, foot strike, foot off} for block start. Other functions, instead, work over the entirety of the data frames. Refer to chapter 3 for the details on which parameters belong to TSSR and block starts.

```
function [outR, outL] =
get_parameterX(markers, instantsR, instantsL, firstFrame)
```

This is the standard structure of a function header. In input we have:

- the *marker* structure, containing a time series of XYZ coordinates of 22 markers.
- *instantsR*, the relevant frames to be used for extracting the parameters from the right leg.
- *instantsL*, the relevant frames to be used for extracting the parameters from the left leg.
- *firstFrame*, to keep synchronization with Vicon Nexus

Code Example

```
  % Function to compute the angle between thighs
  %
  % Inputs:
  % markers - A structure with marker data.
  % rightMaxHeight - instants of right knee max height
  % leftMaxHeight - instants of left knee max height
  % firstFrame - first frame to adjust the instants
  %
  % Output:
  % thighAnglesR - An array of computed angles in degrees.
  % thighAnglesL - An array of computed angles in degrees.

function [thighAnglesR, thighAnglesL] =
  get_thighSwitchRange(markers, rightMaxHeight, leftMaxHeight, firstFrame)
  % Initialize output arrays
  thighAnglesR = zeros(length(rightMaxHeight), 1);
  thighAnglesL = zeros(length(leftMaxHeight), 1);

  try
      % Extract marker positions
      rgtPos = markers.RGT;
      rflePos = markers.RFLE;
      lgtPos = markers.LGT;
      lflePos = markers.LFLE;

      % Compute relative contralateral angles using cross product
      for i = 1:length(rightMaxHeight)
          % Adjust frame index relative to the first frame
          frameRight = rightMaxHeight(i) - firstFrame;

          %fprintf("FrameRightLeg: %d \n", frameRight)
          % Vector for right thigh segment (RGT to RFLE)
          rightThighVector = rflePos(frameRight, :) - rgtPos(frameRight, :);
          %fprintf('RightThigh vector: :%d \n ',rightThighVector);
```

```
    % Vector for left thigh segment (LGT to LFLE) at the same frameRight
    leftThighVector = lflePos(frameRight, :) - lgtPos(frameRight, :);
    %fprintf('leftThigh vector: :%d \n ',leftThighVector);

    % Calculate the cross product of the two thigh vectors
    crossProd = cross(rightThighVector, leftThighVector);
    %fprintf('crossprod vector: :%d \n ',crossProd);

    % Calculate the angle
    angle = rad2deg(atan2(norm(crossProd),
        dot(rightThighVector, leftThighVector)));

    % Store the computed angle for the right leg event
    thighAnglesR(i) = angle;
end

% Compute relative contralateral angles using cross product
for i = 1:length(leftMaxHeight)
    % Adjust frame index relative to the first frame
    frameLeft = leftMaxHeight(i) - firstFrame;
    %fprintf("FrameLeftLeg: %d \n", frameLeft)

    % Vector for right thigh segment (RGT to RFLE) at the same frameLeft
    rightThighVector = rflePos(frameLeft, :) - rgtPos(frameLeft, :);

    % Vector for left thigh segment (LGT to LFLE)
    leftThighVector = lflePos(frameLeft, :) - lgtPos(frameLeft, :);

    % Calculate the cross product of the two thigh vectors
    crossProd = cross(leftThighVector, rightThighVector);

    % Calculate the angle
    angle = rad2deg(atan2(norm(crossProd),
        dot(leftThighVector, rightThighVector)));

    % Store the computed angle for the left leg event
```

```
            thighAnglesL(i) = angle;
        end
    catch ME
        % Error handling
        disp(['Error message: ' ME.message]);
        disp(['Error identifier: ' ME.identifier]);
        disp('Stack trace:');
        %disp(ME.stack);
        thighAnglesR = NaN;
        thighAnglesL = NaN;
    end
d
```

This function computes the thigh switch range 3.17 at foot off. It initializes the the output arrays to zero, and then extracts the markers positions. It computes the relative contralateral angle using cross products on the two vectors defined by the markers. From MATLAB: *"Find the cross product of A and B. The result, C, is a vector that is perpendicular to both A and B."* Then, *rad2deg()* converts the angle units from radians to degrees for each element. This logic applies to the whole script.

5.5 Force Calculations

Force calculation is performed through specific functions. Dedicated scripts were written to handle the different nature of block start. These functions are based on the events {Foot strike, Foot off} for both TSSR and block start.

The process is the following, written in high level language:

```
% Compute the forces from the analog data.
  forces = forcePlatformType2(c3d_file_trial);
% Remove crosstalk and noise
  forces=forces.cleanSignal("MaxRadius",size(forces.GRF,1)-2);
% Combine the forceplates to create a unique plate
  forces_combined = forces.combineFP();
% Force analysis
  [forceAnalysis] = force_analysis(forces_combined.GRF, athlete_weight);
% Force averaging
  [finalForcesAVG] = average_forces(forceAnalysis, firstStepLeg);
```

An integration must be made for block starts. The above process remains valid for the steps that are performed after block clearance, but a dedicated section must be written for the blocks that lay on plate 1 and plate 2. The dedicated section is the following, written in high level language:

```
Compute forces
  forces=forcePlatformType2(startFilePath);
emove crosstalk and noise
  forces=forces.cleanSignal("MaxRadius",size(forces.GRF,1)-2);
Extract the first two plates
  fp_2left=forces.GRF(:,:,2);
  fp_1right=forces.GRF(:,:,1);
Rotate forces based on block pedal angles.
  [fp2_left_rotated] = rotateForces_blocchi(fp_2left, pedalAngles(2));
  [fp1_right_rotated] = rotateForces_blocchi(fp_1right, pedalAngles(1));
Combine the forceplates to create a unique plate
  forces_steps = forces.combineFP();
Remove blocks, keep data of plates 3 to 9.
  forces_steps.GRF = forces_steps.GRF(bc_analogInstant+1:end, :);
```

Code Example

We now see a code section showing the application of a rotation matrix around the mediolateral axis. This is to ensure correct computation of forces given the inclination of the block pedals. The resulting force will be strongly vertical due to the rotation. In fact, the athlete is pushing out of the blocks in a forward fashion due to the steepness of the pedals.

```
function [F_pedal] = adjustForces_blocchi (myForces, pedal_angle)
% Given angle of inclination (in degrees) and force plate data
  theta_deg = abs(pedal_angle); % Inclination angle in degrees
  theta_rad = deg2rad(theta_deg); % Convert to radians

  % Rotation matrix for rotation around the X-axis
  R_x = [1, 0, 0;
         0, cos(theta_rad), -sin(theta_rad);
         0, sin(theta_rad), cos(theta_rad)];

  % Loop through each frame (row) and apply the rotation matrix
  for i = 1:numFrames
```

```
        % Extract the current force vector (1x3)
        currentForce = myForces(i, :)';

        % Apply the rotation matrix to the current force vector
        F_pedal(i, :) = (R_x * currentForce)';
    end
end
```

5.6 Validation of Outputs

Multiple checks were performed to validate this MATLAB script. First, after building the core functions to get a bare bone working script, their results were compared with those from Analyzer. Given a same trial and the same *.c3d* file, temporal, spatial and angular parameters were compared. This is also referred as ”Kinematic” data. Force readings from the 9 plates were also compared. This is also referred as ”Kinetic” data. Since the force readings were performed using the same MATLAB script - just without any graphic interface - the results were consistent. On the other side, the above mentioned parameters were found to be in a $\pm 2\%$ range which was deemed acceptable. Such checks were performed across dozens of trials, both from start and from TSSR.

Additionally, constant comparisons were run against Vicon Nexus data, both visually and numerically. Software like Kinovea was used to measure angles of athletes in orthographic projections, to ensure correctness and consistency of such angles with the standards defined in chapter 3. Force readings, their peaks and timestamps were verified using Vicon Nexus built-in graphical representation of forces over time. Force plate data processed by MATLAB has 1500Hz resolution, six times higher than markers. It was noted that Vicon Nexus trims force data to match the markers instants when visualizing, thus some peaks were incorrectly reported as lower. This is fortunately not a problem in this script.

The last step was to verify consistency between trials of the same athlete and between different athletes. This was done by having the MATLAB script write all the results into four distinct tables, split between Block starts and TSSR. Two tables contained kinematic data. The other two only kinetic data. Each table ended up with more than 50 rows of data, each representing a trial. Such data was used to determine if the outputs were consistent and to detect any bugs in the program. These tables, in their final version, represented the foundation for the data analysis process that will be described in the next chapters.

5.7 Challenges

Developing a piece of software from scratch implies facing unexpected difficulties on the path to completion. First of all, it was challenging to program an analysis software about gait analysis without a visual aid, as the .c3d files only contained raw data from Vicon. Developing a system for gait visualization would have been time consuming and beyond the scope of the project; thankfully, free instruments as MOKKA (Motion Kinematic and Kinetic Analyzer) allowed to visualize the time series of events and provided means for live checking. A more complete instrument is Vicon Nexus, although it requires a licence. Vicon Nexus was used for this project to ensure continuity from the capture at Palaindoor to the programming of the app. As a key takeaway, it would have been exceptionally hard to develop this software without such visual aids.

There were some asymmetries between developing this program and creating the blueprint from analysis in SMARTAnalyzer. At first we set up recurrent meetings to update each other on the work and check reciprocal progress, but it was time consuming. We soon realized that writing every detail about parameters and instants of measurement was the correct approach to this project: such work is shown in chapter 3. After this, the majority of the work was conducted following shared guidelines.

From a programmer perspective it was hard to determine which variables or parameters were inherently better. There was an expectation to see some patterns emerging from the data during the development and progressive extraction of data. However, even though running is a cyclic motion, it is not simply described by single variables. More on this on chapter 7. Therefore, the programming side was first devoted to extract as much data as possible from the raw data in *.c3d* files.

Building the application required substantial knowledge of athletics, fortunately possessed by the author as both athlete and assistant coach. This work was aimed at extracting and processing data from the trials; it should also be noted that, as processed data was increasing, it became easier to develop the rest of the application thanks to the growing insights from the data itself.

Lastly, the section on Block Starts proved to be challenging due to the unique nature of the physical effort. A specific script was written to handle the starting block behavior, and changes were made to existing functions handling force plate data.

Chapter 6

The report

Motivations

The main goal of this work was to produce a report capable of showing consistent and objective data to coaches and athletes. It was crucial to provide tangible data as early as possible after performing a test. Before this work, the trial could be visualized in Vicon Nexus software: the 3-D reconstructed acquisition volume shows markers and segments, GRF direction and intensity, speed and location of each marker. The problem is that such information is scattered, and cannot be observed at the same time. For example, to obtain GRF data and Sacrum marker velocity, first force plates must be accessed, data stored somewhere else, and then click on the marker to retrieve the velocity. What if, during a block start, a foot strike happens over two force plates and the other one is dragged over another one? This situation happened in the trials. Vicon software is unable to properly filter out the data. The MATLAB script allows to properly account for these events, and many others. As mentioned previously, the time it takes now to output the results is less than 30 minutes, most of which are taken by the tracking procedure performed on the software Vicon Nexus. The MATLAB script itself requires far less than a minute to provide the *.pdf* output. One of the crucial aspects we immediately noticed was the lack of results we could show to athletes and most importantly coaches. While Vicon Nexus makes for a good visual representation, objective data takes a lot of time to be extracted manually. Scaling up to many trials, it becomes impossible to keep up with them.

Talking to coaches and athletes made clear that being able to visualize how the subject runs plays a role in their willingness to repeat the trials. This allows for repeated tests over time: simply opening two *.pdf* reports allows to immediately compare result. Another option is to use the csv tables that allow for inter and intra athlete comparison. We considered how different coaches and athletes may require different levels of depth in the analysis of the running data. The report was created and evolved over multiple iterations thanks to feedback from coaches and researchers.

6.1 The report structure

The report is a multi-page document in *.pdf* format. This was the chosen output as MATLAB provides tools for reporting, and the average user will be able to effortlessly open such file on any of his devices. The report is organized in chapters, each one discussed in the following sections. The logic of the report is to provide the most important information immediately, both as numerical data and plots. Secondary information follows, with full parameter tables at the end of the report.

As standard, any data related to body left side is red-colored, and data related to body right side is green colored.

This is the structure overview:

- Main parameters
- Speed
- GRF and Impulses
- Center of Pressure (CoP) plots
- Full kinematic parameters

What follows is extracted from a report generated over a TSSR trial performed by the author of this thesis.

6.1.1 Chapter 1: Main parameters

The first chapter of the report is dedicated to the most important tables. The first table 6.1 contains the most relevant parameters of the trial, chosen among the full set. The full set can be found at the end of the report. We intend the main parameters as those that can convey most information about the trial. Some of them give information about performance, others about the state of fitness of the athlete and repeatability of trials. These parameters were selected as a combination of the most relevant - statistically speaking - and those that coaches want to immediately see.

- Speed (m/s): the most important result, as we want athletes to achieve higher velocities.
- Step Frequency (Hz): to monitor frequency.
- Contact Time (ms): has to be reasonably low (i.e.: less than 100ms).
- Flight Time (ms): has to be low: high air time is less time spent pushing on the ground.

- Step Length (m): higher is better. However, overstriding causes excessive braking.
- Stride Length (m): to compare different trials.
- Hip displacement (cm): the distance between foot off position and hip.
- Support angle (deg): how much the support leg bends during midstance.
- Pelvis Excursion (cm): Pelvis movement up and down. Less is better.
- Leg angular velocity (deg/s): how quickly the thigh is moved.

Main kinematic parameters

Variable Name	Left leg	Right leg	Difference (%)
Speed (m/s)	9.82	9.82	
Step Frequency (Hz)	4.42	4.42	
Contact time (ms)	92	88	4.4
Flight time (ms)	140	132	5.9
Step length (m)	2.25	2.19	2.7
Stride length (m)	NaN	4.44	NaN
Hip displacement (cm)	53.59	50.39	6.2
Support angle (°)	149.5	154.54	3.3
Pelvis excursion (cm)	6.59	6.59	
Leg angular velocity (°/s)	NaN	367.11	NaN

Figure 6.1: Main Kinematic Parameters

This Ground Reaction table 6.2 shows the GRF peaks for each step, in order. Mediolateral, Anteroposterior and Vertical components are shown. All GRF are expressed in Newton (N).

Steps: GRF (N)

Leg	Mediolateral (N)	Anteroposterior (N)	Vertical (N)
Right	-403.70	611.60	3088.70
Left	414.10	568.30	2927.70
Right	-401.00	623.00	2974.20

Figure 6.2: GRF data for each step.

The second table 6.3 shows the impulses for each step, in order: Mediolateral, Anteroposterior and Vertical components are shown. The Anteroposterior component is split in 3: propulsive, braking, resulting. All Impulses are expressed in Newton-Seconds (Ns).

Steps: Impulses (Ns)

Leg	Mediolateral (Ns)	Propulsive (Ns)	Braking (Ns)	Resulting (Ns)	Vertical (Ns)
Right	-8.40	19.70	-12.00	7.60	160.40
Left	4.70	19.40	-14.20	5.20	157.20
Right	-9.30	19.60	-11.80	7.80	149.90

Figure 6.3: Impulse data for each step.

6.1.2 Chapter 2: Speed

This chapter is dedicated to speed related to the steps on the ground.

This 6.4 plot shows the speed curve. Foot strike (continuous line) and Foot Off (dashed line) instants are added to the plot to better visualize the running cycle. A shade is added between the lines to represent the time during which the foot is in contact with the ground. Green color is used for right foot, while red for left leg. Note: Spikes in the speed curve may be issue-related to the tracking of Sacrum Marker.

6.1.3 Chapter 3: GRF and Impulses

Below, the plots 6.5 show the GRF (N) components for the steps after block clearance. Note: maximum GRF alone is not enough to analyze the steps: the following graph about impulses considers the whole force applied over the contact time.

Then, the second plot 6.6 shows the Impulse (Ns) for the steps of the TSSR. Two trend lines are drawn to show the trend regarding Impulses generated at each step, both in Vertical and Net Forward direction.

6.1.4 Chapter 4: Center of Pressure (CoP) movements

This Plot 6.7 shows a vertical view of the CoP for each of the steps after block clearance. Right steps start on the right side of the plot, in the black circle. Left steps start on the left side of the plot, in the black circle. This graph can be used to compare the center of pressure between steps, especially if anomalies are found between steps or impulses. It was noted, for example, that rearward-heavy Center of pressure is often visualized in conjunction with high braking impulses. While this alone proves little, it shows how data visualization can help interpret running performance.

The below table 6.8 contains the averaged Kinetic parameters. These is the same data that was plotted in chapter 3 (GRF and Impulses), just shown as table. It should be noted that the last row is ”Propulsive Ratio”. This metric is the ratio between horizontal net impulse over vertical impulse. This metric is important, as discussed in literature in previous chapters, as it

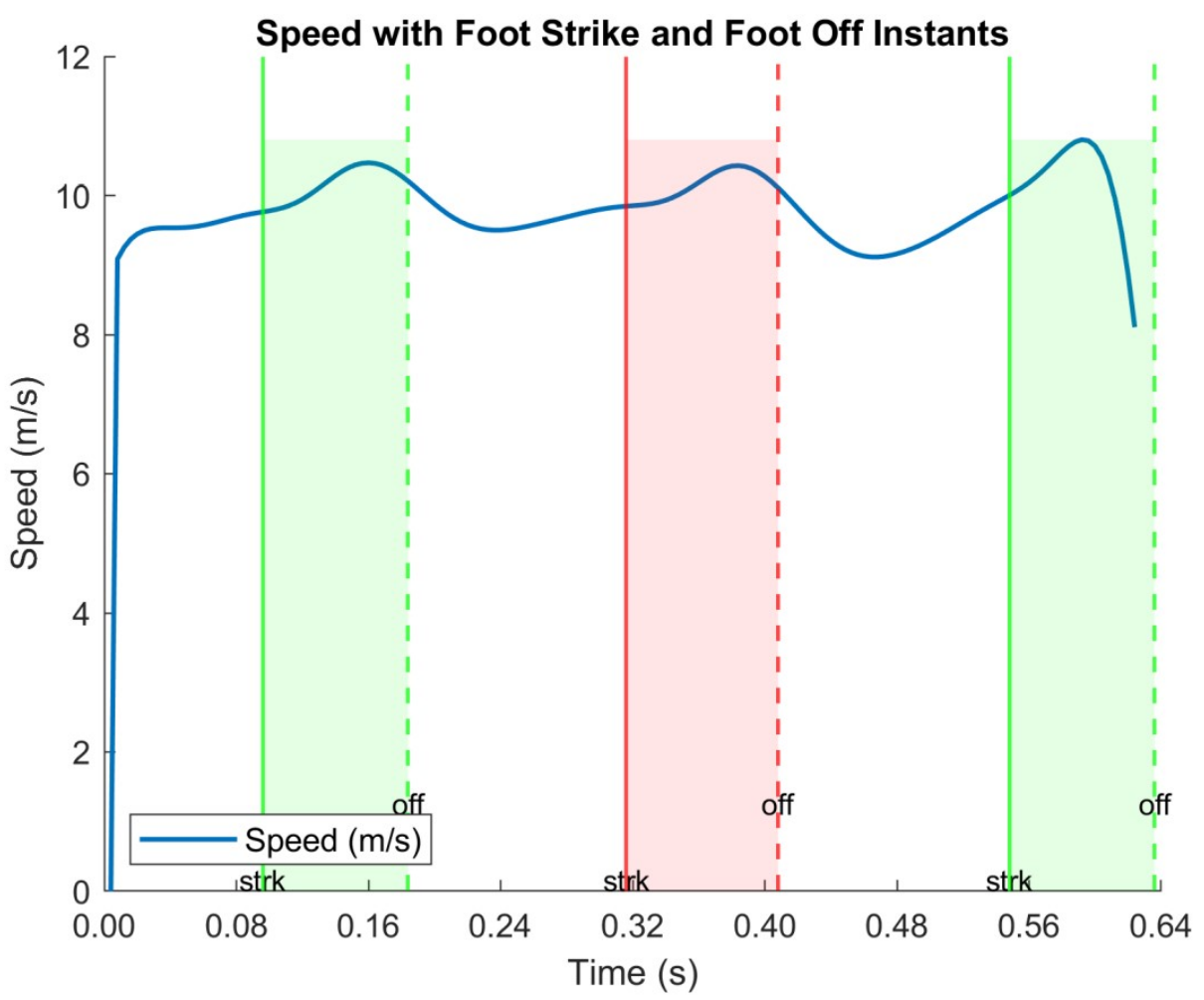

Figure 6.4: Speed data with Foot Strike, Foot Off.

distinguishes elite and non-elite sprinters.

6.1.5 Chapter 5: Full kinematic parameters

The following 3 tables contain the Spatial 6.9, Temporal 6.10, and Angular 6.11 parameters divided by leg, with the absolute distance shown as percentage (%) on the last column. By absolute distance we refer to the statistical measure used to quantify the difference between two values as a percentage of their average. It is commonly used to assess the relative difference between observed values, without directional bias. Note: ”NaN” is shown when not enough steps were captured to compute the data.

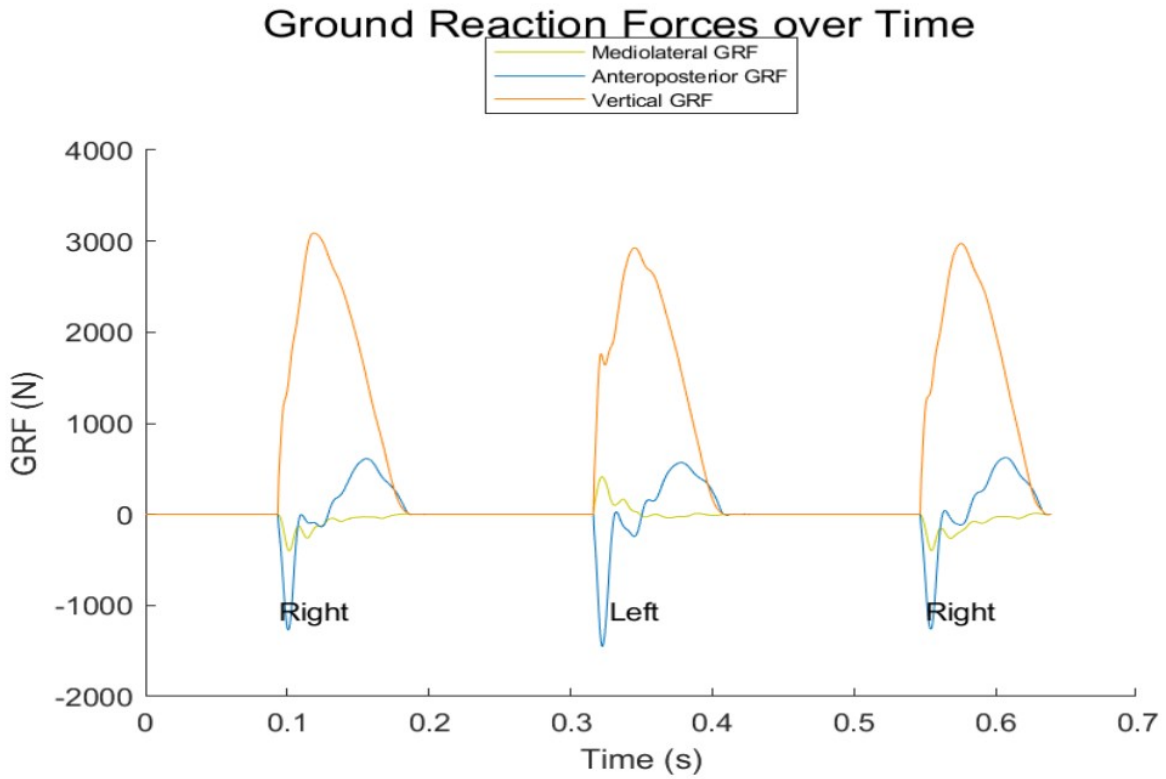

Figure 6.5: GRF components for each step.

Spatial parameters

The table 6.9 exclusively contains Spatial parameters. These are all extracted using markers positions in the acquisition volume, both continuously during the trial and at the specific gait cycle instants.

Temporal parameters

The table 6.10 exclusively contains Temporal parameters. These are extracted using markers positions and force plate data in the acquisition volume, both continuously during the trial and at the specific gait cycle instants. For example, to extract contact times a mix of force plates signals and feet markers were used to determine the position.

Angular parameters

The table 6.11 exclusively contains Angular parameters. These are all extracted using markers positions in the acquisition volume, both continuously during the trial and at the specific gait cycle instants. These parameters are less immediate, and prove more valuable when compared in big datasets against other subjects. Still, they are included in the report to facilitate their

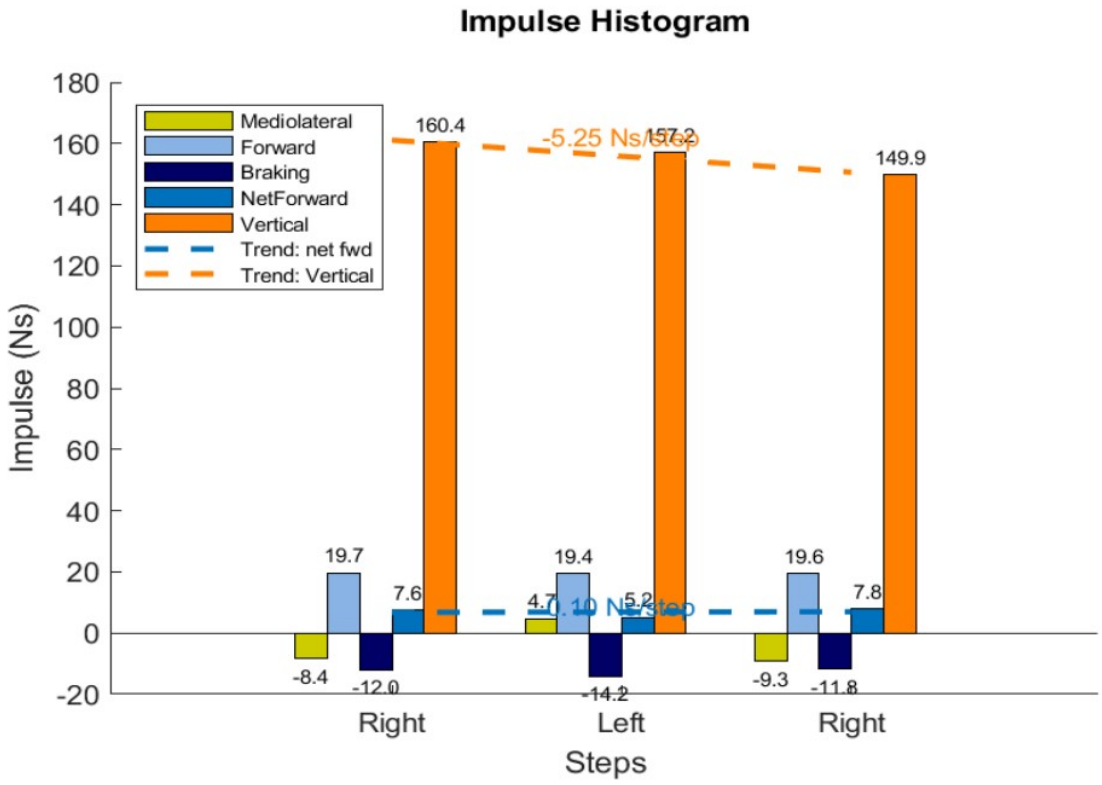

Figure 6.6: Impulse components for each step.

reading.

6.2 Block start: Additions

The block start is - bio-mechanically speaking - very different from the ”Flying” phase of a sprint. While most of the report structure is consistent with the TSSR case, a few additions are made to the Block start report. The main differences are that while on the TSSR we expect the steps to be consistent, every step of the start is different because the body is moving into an upright position. Moreover, there is the block footplates data to be considered separately from the steps data. Speed data, when plotted, also shows the ”block clearance” instant, as it is an important metric to determine performance. Lastly, the ratios between impulses are different among the steps.

6.2.1 Speed plot

This plot 6.12 shows the speed curve of the block start. Foot strike (continuous line) and Foot Off (dashed line) instants are added to the plot to better visualize the running cycle. A shade is added between the lines to represent the time during which the foot is in contact with the ground.

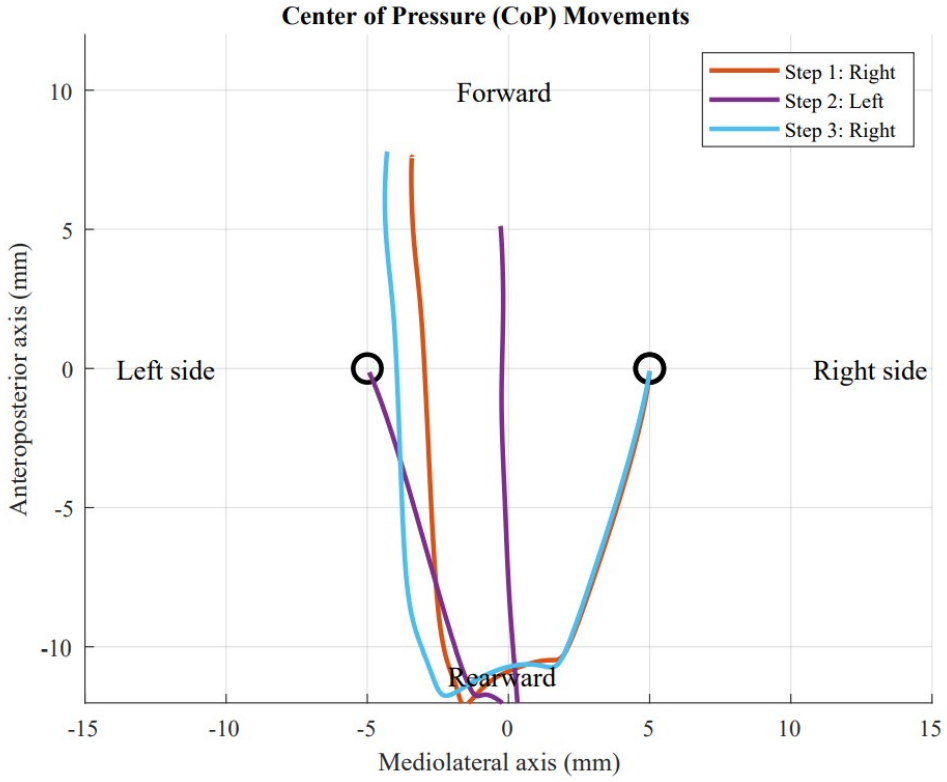

Figure 6.7: Center of Pressure, vertical view.

Green color is used for right foot, while red for left leg. Block clearance instant is added with a dashed purple line. Note: Spikes in the speed curve may be issue-related to the tracking of Sacrum Marker.

6.2.2 Block-specific data

The table 6.13 includes kinematic data exclusively related to block clearance. Data is shown on the column of the front leg, meaning the last leg to leave the block footplates. The other legonly shows data about the distance covered with the other leg

Kinetic Parameters - Averaged

Kinetic Variables	Left Leg	Right Leg	Difference (%)
Peak Propulsive GRF (N)	568.3	617.3	8.3
Peak Vertical GRF (N)	2927.7	3031.45	3.5
Peak lateral GRF (N)	414.1	-402.35	13897
Vertical Impulse (Ns)	157.2	155.15	1.3
Propulsive Impulse (Ns)	19.4	19.65	1.3
Braking Impulse (Ns)	-14.2	-11.9	17.6
Net Forward Impulse (Ns)	5.2	7.7	38.8
Lateral Impulse (Ns)	4.7	-8.85	653
Propulsive ratio (Horiz/vert)	0.03	0.05	50

Figure 6.8: Kinetic parameters averaged

Spatial Parameters

Variable Name	Left leg	Right leg	Difference (%)
Hip Displacement Normalized (cm/leg)	0.62	0.58	6.7
Hip Displacement (cm)	53.59	50.39	6.1
Maximum Sacrum Position (cm)	100.41	100.41	
Minimum Sacrum Position (cm)	93.82	93.82	
Range of Sacrum Motion (cm)	6.59	6.59	
Step Length (m)	2.25	2.19	2.7
Step Length Normalized (m/leg)	2.61	2.54	2.7
Stride Length (m)	NaN	4.44	NaN
Stride Length Normalized (m/leg)	NaN	5.15	NaN

Figure 6.9: Spatial parameters table.

Temporal Parameters

Variable Name	Left leg	Right leg	Difference (%)
Average Speed (m/s)	9.82	9.82	
Contact Time (ms)	92	88	4.40%
Fly Time (ms)	140	132	5.90%
Step Frequency (Hz)	4.42	4.42	

Figure 6.10: Temporal parameters table.

Angular parameters

Variable Name	Left leg	Right leg	Difference (%)
Ankle Angle (°)	89.63	85.34	4.9
Early Extension Angle (°)	-39.86	-47.64	17.8
Early Extension TAV (°/s)	-332.18	-384.18	14.5
Early Flexion Angle (°)	66.77	47.82	33.1
Early Flexion TAV (°/s)	439.29	323.11	30.5
Full Flexion Angle (°)	NaN	88.11	NaN
Full Flexion TAV (°/s)	NaN	367.11	NaN
Push Angle (°)	50.79	52.67	3.6
Shank Angle (°)	-6.01	-12	66.5
Support Angle (°)	149.5	154.54	3.3
Thigh Switch Range (°)	92.96	89.91	3.3
Thigh to Horizontal Angle (°)	-27.3	-21.78	22.5
Thigh to Vertical Angle (°)	25.09	19.9	23.1

Figure 6.11: Angular parameters table.

This plot 6.14 of Ground Reaction Force (GRF) show the force exerted on the Right (green) and Left (red) footplates of the block. The front foot is fixed in place for a longer period than the back foot, and it can be seen from this plot.

This plot 6.15 shows: on the left, the vertical Ground Reaction Force (GRF) components for

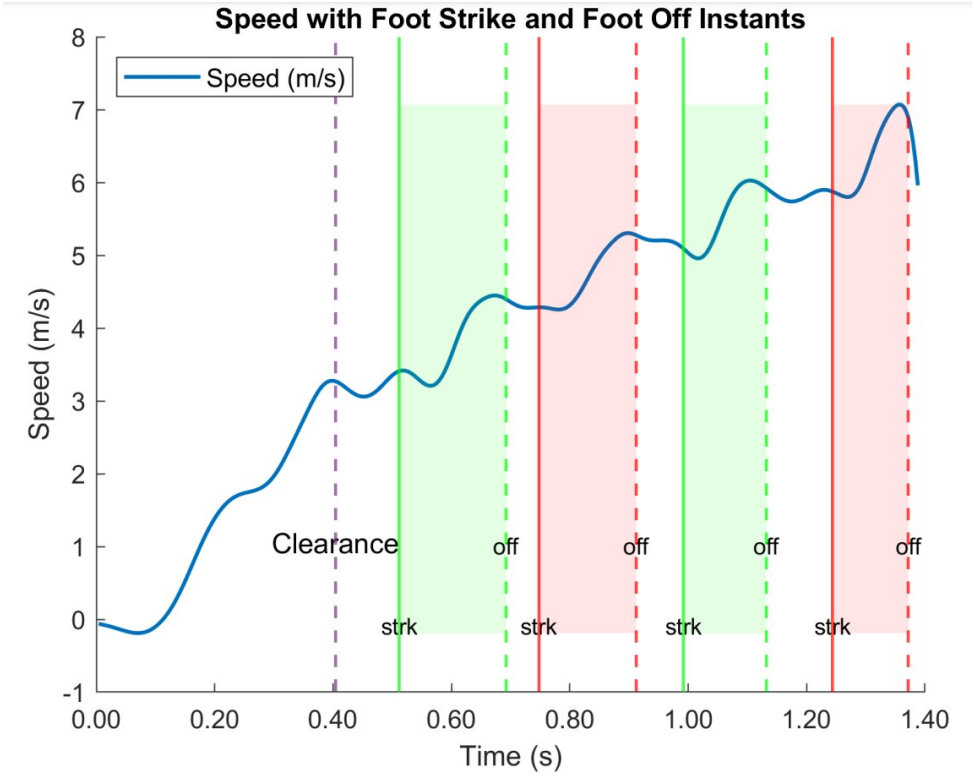

Figure 6.12: Speed plot for Block Start.

Table of Kinematic Parameters - Block Only

Variable Name	Left Leg	Right Leg	Difference (%)
Speed at Block Clearance (m/s)	3.27	-	
Distance: block to first FootStrike (cm)	-	66.58	
Distance: block to first FS norm (cm/leg)	-	79.06	
Push angle at block clearance (°)	35.82	-	
Thigh-Shank Angle at Block Clearance (°)	88.76	-	
Thigh-Trunk Angle at Block Clearance (°)	197.47	-	
Thigh to Horizontal Angle at BC (°)	-142.16	-	
Shank to Vertical Angle at BC (°)	-53.55	-	

Figure 6.13: Block Kinematic parameters table.

both legs on the block. On the right, the impulse generated by both legs on the block.

6.2.3 Kinematics variables

The table 6.16 contains the averaged kinematic parameters of first two steps of the trial. First are shown the most common parameters like contact time and flight time, step frequency and step length. Then, we add some normalized data - useful to compare different athletes - and angular data. This data reflects how the athlete is moving into an increasingly upright position after each step.

The same identical table is created for the last two steps of the trial, with the aim of showing

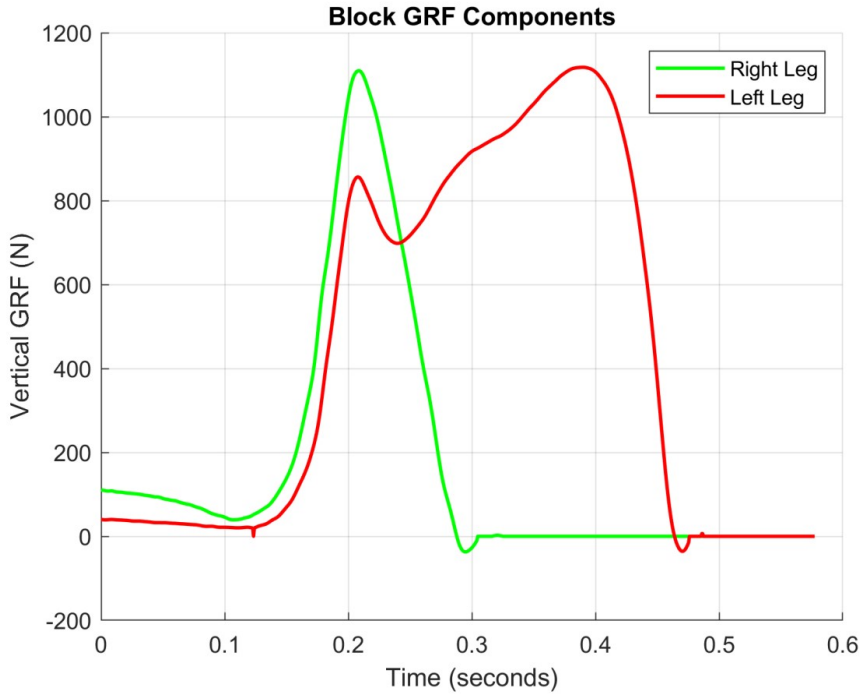

Figure 6.14: Block GRF Components over time.

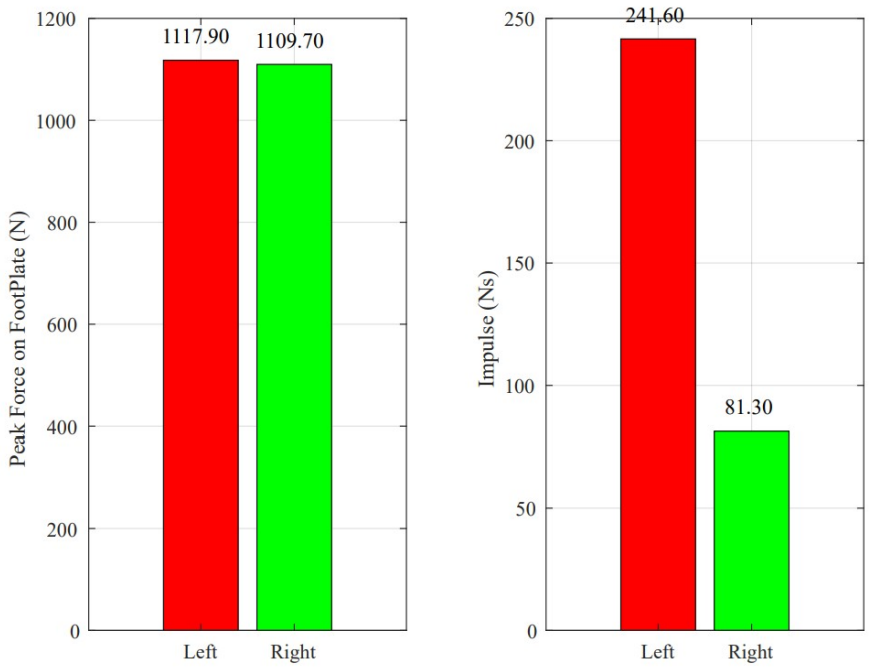

Figure 6.15: Block Histograms: GRF (Left) and Impulse (Right).

the differences between first and last step of each leg, and between both last steps.

Kinematic parameters: first step of each leg.

Variable Name	Left Leg	Right Leg	Difference (%)
Step Frequency (Hz)	4.1	4.1	0
Speed at Foot Strike (m/s)	4.29	3.41	22.9
Contact Time (ms)	164	180	9.3
Flight Time (ms)	80	56	35.3
Step Length (cm)	1.22	1.03	16.9
Step Length Normalized	1.45	1.22	17.2
Shank angle at Foot Strike (°)	50.23	39.19	24.7
Stride Length (cm)	2.65	2.26	15.9
Stride Length Normalized	3.15	2.68	16.1
Trunk Angle at Foot Strike (°)	43.11	33.68	24.6
Push Angle at Foot Off (°)	41.1	41	0.2
Thigh-Trunk Angle at Foot Off (°)	202.52	200.27	1.1

Figure 6.16: Kinematic parameters table.

6.2.4 Kinetic: impulses trend

This plot 6.17, similar in nature to the one of TSSR shows the Impulse (Ns) for the steps after block clearance. Two trend lines are drawn to show the trend regarding Impulses generated at each step, both in Vertical and Net Forward direction. In this case the trend lines are more inclined, as a greater loss of net forward impulse is expected after each step.

6.2.5 Ratios

Ratios for block start are considered for every step. Literature has shown how after each step the ratio becomes smaller. In this table 6.18 are shown the ratios between horizontal net impulse and vertical impulse. It is expected to see a decrease in the ratio as the steps follow one another: the athlete moves from the block position into a more vertical, upright position after each step.

6.3 Summary

The report described above is a comprehensive tool designed to bring advanced biomechanical analysis to coaches and athletes. By wrapping kinematic and kinetic data into a single, easy-to-read document, it overcomes the fragmentation of information inherent in software like Vicon Nexus. The report allows users to quickly access key metrics while also offering deeper insights through detailed tables and plots.

The key feature is the ability to provide tangible feedback in under 30 minutes, enabling real-time performance assessment and potential live improvements during training sessions if the tracking procedure is greatly improved. This rapid output facilitates comparisons between trials, whether intra-athlete for progress tracking or inter-athlete for benchmarking.

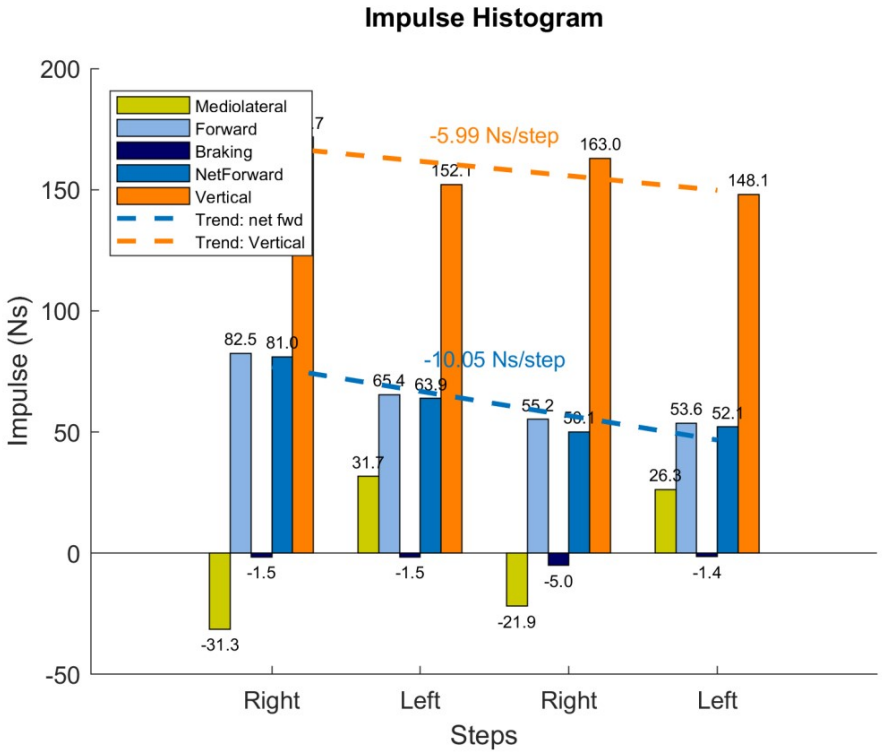

Figure 6.17: Impulses for steps after block clearance.

Ratios: horizontal impulse with respect to vertical impulse.

Leg	Ratio between horizontal and vertical impulse at subsequent steps.
Right	0.47
Left	0.42
Right	0.31
Left	0.35

Figure 6.18: Ratio: propulsive/vertical impulses of consecutive steps.

Feedback from coaches and researchers played a pivotal role in shaping the report. Its adaptability ensures that both high-level summaries and granular analyses are available to cater to varying expertise levels. By providing both *.pdf* and CSV formats, the report is versatile, offering immediate insights and long-term data aggregation for trend analysis. The addition of block-start-specific metrics further showcases the report's flexibility, accommodating the biomechanical nuances of different running phases. Metrics like propulsive-to-vertical impulse ratios and block footplate dynamics provide critical information for optimizing starts— an area of great importance in sprint performance.

This report serves as a practical and reliable tool for transforming complex motion capture data into valuable insights. By enabling quick and thorough analysis, the report promotes a more scientific and systematic way to enhance performance compared to other instruments, like 2-D video analysis.

Chapter 7

Results and discussion

7.1 Statistical findings

Prior to comparing the reports and the following insights it's crucial to go over the most important results from the statistical analysis of the data. This analysis was conducted by Emma Ghezzo (*Investigation of correlation between elite sprinter ranking and kinematic and kinetic iomechanical parameters during starting and sprinting, 2024* [37]) and Ling Wei Lei (*Analisi cinematica e dinamica della partenza dai blocchi e della corsa nella fase lanciata in velocisti dell'atletica leggera, 2024*) [38]. The main points are reported in this work in order to help understand how the report was structured, and why certain data is given wide attention with respect to other parameters; all the details can be found in the above mentioned theses.

About Block Start

A multiple linear regression approach showed that neither kinetic nor kinematic parameters alone explain the variability of the velocity. The best result comes from a set of parameters defined for the block exit with mixed parameters. It seems that the most important parameters to observe are the velocity at block clearance and push angle out of the blocks. The athlete should be as tilted as possible in a forward fashion, as if falling, to maximize horizontal propulsive component. As mentioned in TSSR, improving a multitude of parameters is the key to better performance. Knee angle and shank angle at block clearance also seem to play an important role during block clearance.

Based on the above findings, the athlete should improve the block position to maximize the impulses, thus achieving greater end velocity. It is critical to express as much horizontal forces as possible instead of vertical ones. From another perspective, vertical forces should be just enough to prevent the athlete from falling: the rest should be devoted to moving forward as fast as possible.

Mixed Linear Regression

Model Summary - VEL S 4° foot off (front)

Model	R	R^2	Adjusted R^2	RMSE
M_0	0.000	0.000	0.000	0.359
M_1	0.827	0.683	0.511	0.251

Note. M_1 includes Push Angle Clearance (front), Thigh to horizontal Angle Clearance (back), Lenght block-FirstStep, MEAN VERTICAL, MEAN BRAKING, MEAN PROPULSIVE

ANOVA

Model		Sum of Squares	df	Mean Square	F	p
M_1	Regression	1.494	6	0.249	3.956	0.023
	Residual	0.693	11	0.063		
	Total	2.187	17			

Note. M_1 includes Push Angle Clearance (front), Thigh to horizontal Angle Clearance (back), Lenght block-FirstStep, MEAN VERTICAL, MEAN BRAKING, MEAN PROPULSIVE
Note. The intercept model is omitted, as no meaningful information can be shown.

Coefficients

Model		Unstandardized	Standard Error	Standardized	t	p
M_0	(Intercept)	6.673	0.085		78.940	< .001
M_1	(Intercept)	9.439	1.822		5.182	< .001
	Push Angle Clearance (front)	−0.082	0.029	−0.595	−2.790	0.018
	Thigh to horizontal Angle Clearance (back)	0.011	0.015	0.183	0.749	0.470
	Lenght block-FirstStep	−0.710	0.537	−0.279	−1.323	0.213
	MEAN VERTICAL	−4.096	6.227	−0.117	−0.658	0.524
	MEAN BRAKING	−33.698	42.227	−0.159	−0.798	0.442
	MEAN PROPULSIVE	11.791	9.886	0.271	1.193	0.258

Figure 7.1: Regression analysis on Block parameters

The mixed parameters suggested by literature and coaches explain the 68.3 % of the variability of the Sacrum velocity at fourth step, with a statistical significance, p-value is equal to 0.023, in particular the Push Angle at clearance is statistical significative with p-value of 0.018

About TSSR

A multiple linear regression approach showed that kinetic parameters better explain the variability of the 20 m time performance with respect to the kinematic ones. A specific composition of parameters, composed by some kinematic and some kinetics parameters decided to best represent the sprinting, was particularly effective in explaining the variability of performance. The results, even if conducted on a limited sample, suggest that running technique is not the biggest determinant of performance in high-level and medium-level athletes. More important are impulses and ground reaction forces, especially braking and propulsive anteroposterior impulses. It seems that focusing on maximizing propulsive force generation may prove more effective in increasing the speed of an athlete. Moreover, improving a single parameter, based on the

Linear Regression_mixed parameters

Model Summary - Time_flying_20mt

Model	R	R^2	Adjusted R^2	RMSE
H_0	0.000	0.000	0.000	0.077
H_1	0.910	0.829	0.676	0.044

ANOVA

Model		Sum of Squares	df	Mean Square	F	p
H_1	Regression	0.084	8	0.011	5.438	0.010
	Residual	0.017	9	0.002		
	Total	0.102	17			

Note. The intercept model is omitted, as no meaningful information can be shown.

Coefficients

Model		Unstandardized	Standard Error	Standardized	t	p	95% CI Lower	95% CI Upper
H_0	(Intercept)	2.024	0.018		111.059	< .001	1.985	2.062
H_1	(Intercept)	1.875	0.429		4.370	0.002	0.904	2.845
	Impulse_vertical_mean	0.582	0.553	0.177	1.052	0.320	−0.669	1.834
	Impulse_horizontal_mean	−47.048	19.867	−1.168	−2.368	0.042	−91.990	−2.106
	Impulse_braking_mean	54.205	20.662	1.387	2.623	0.028	7.463	100.946
	Impulse_propulsive_mean	52.942	20.202	1.577	2.621	0.028	7.243	98.642
	HIP_Displacement_Mean	−3.438	0.944	−1.839	−3.642	0.005	−5.574	−1.303
	Contact_Time_Mean	16.167	4.369	1.503	3.700	0.005	6.284	26.050
	Flight_Time_Mean	2.518	1.083	0.583	2.324	0.045	0.067	4.969
	AngoloDiSpintaToeOff_medio	−0.007	0.007	−0.212	−0.981	0.352	−0.022	0.009

Figure 7.2: Regression analysis on TSSR parameters

regression analysis, may prove to be inefficient; it's better to improve a set of parameters, for example those that best justify the variability in performance (see fig. 7.2). The parameters that we found best explain performance are the following: vertical impulse, horizontal net impulse, braking impulse, propulsive impulse, Hip displacement, Contact time, Flight time, Push angle. These explain a variability of 82.9% of the 20 m time with a p-value of 0.010, so the result is statistical significant.

Literature: Confirmations and Contrasts

Referring to block start we found confirmation to what claimed by (Nagahara and Oshima, 2019) that Magnitude and propulsive GRFs at block clearance are correlated with velocity. This is also in line with "Greater force production at push on blocks" from (Bezodis et al, 2019) and (Mero et al, 1992). Moreover, some studies underline the importance of decreasing the braking components in the acceleration phase, maximizing the propulsive a minimizing the vertical. Also, the ratio between vertical and horizontal grows as more steps are made, which confirms reports from (Yu et al., 2016), (Kugler et Janshen, 2010).

Referring to TSSR, we found confirmation that a performance factor is reducing braking component and increasing propulsive component (Yu et al, 2016); we are in contrast with a finding from (Nagahara et al., 2018) that reports how the vertical component is more important than the horizontal one. A last point worth mentioning is that the ratio of forces was found coherent with what (Morin et al, 2011, 2012) claim, where having a horizontal component as high as possible differentiated faster subjects.

Discussing findings with coaches

As the last part of this section is included the outcome of a discussion with the athletic coaches mentioned in the early chapters of this work. Given the complete list of parameters we asked to point out which parameters, based on how much they expected them to play a role in explaining variation of performance, would be more relevant. We then showed our findings.

Coaches underlined parameters like horizontal GRF in block start, impulses, support angle, hip displacement and push angle that were also found to be relevant in our analysis. They also put great importance on the quickness of contact time, while some parameters like ankle angle or shin angle at maximum knee height we deemed less relevant. Coaches were surprised at how little kinematic parameters alone explained performance variability; they expected more distance between elite and average sprinters. On the other side, they expected kinetic parameters to better explain the performance of an athlete. They agreed that a mix of parameters both from kinematic and kinetic fields may be the most accurate solution to map performance with our system. In light of the results of this study, even if not final and with many limitations discussed in the next chapter, they suggested an approach that monitors the same group of athletes over a longer period of time, to determine whether different training programs may help improve performance based on the findings of this study.

7.2 TSSR: a comparison between able bodied athletes

In this section we compare two able bodied athletes. The first (subject A) is a male Olympian who participated in the Paris 2024 Games. This athlete corresponds to ’S_11’ in table 1.3. The second (subject B) is the author of this work, as he both participated as subject and student, given his athletic experience. This athlete corresponds to ’S_14’. The aim of this chapter is to show how data can be compared and what insights can be taken from it. Not every parameter will be shown, as some are deemed of less relevance to this 1 on 1 comparison. Many of them, in fact, belong to model computations and big datasets. As mentioned, this work explored the possibility of the system but many more tests and data are needed to obtain a solid classification of performance based on parameters. Below will be shown tables that compare each param-

eter among the two athletes and the difference between them. Then, a written comment will summarize the comparison. It should be noted that this is a step that, as mentioned in the future developments section can be integrated with appropriate effort and time in the program, to allow 1 on 1 or 1 to many comparisons automatically. Such improvement could plot data from two or more subjects on the same graph, improving comparison.

The considered trials were taken in the same month window. Data is normalized to leg length (for example: step length is meters/cm) and body weight in kg at the time of the trial (e.g.: forward impulse normalized is Ns/kg).

	Level	Age (y)	Height (cm)	Weight (kg)	100 m best (s)
Subject A	Olympian	23	171	73.2	9.97
Subject B	High-level	27	176	71.5	10.76

Table 7.1: Physical characteristics and 100 m performance.

Table of data

What follows is the table containing data about the two fastest trials performed by the Olympic sprinter and the author (high-level athlete). First, kinematic data is compared between corresponding legs. Then, kinetic data is compared in the lower section of the table. A difference is computed as percentage between these legs, defining how the high-level athlete performs compared to the Olympic level athlete. The average of this difference is then used to comment on how different the two subjects are in their running performance.

Table 7.2: Comparison of parameters: Olympian and High-level athlete on TSSR.

Parameter	Olympian (A)		High-level (B)		Difference between legs		Diff with Oly
	Left leg	Right leg	Left leg	Right leg	Left	Right	
Speed (m/s)	10.95	10.95	9.82	9.82	10.32	10.32	10.3
Step Frequency (Hz)	4.63	4.63	4.42	4.42	4.54	4.54	4.5
Contact time (ms)	86	84	92	88	-6.98	-4.76	-5.9
Fly time (ms)	128	132	140	132	-9.38	0.00	-4.7
Step length norm.	2.67	2.77	2.61	2.54	2.25	8.30	5.3
Hip Displacement norm.	0.6	0.63	0.62	0.58	-3.33	7.94	2.3
Support Angle (deg.)	154.18	145.33	149.5	154.5	3.04	-6.31	-1.6
Sacrum vert Excursion (cm)	5.78	5.78	6.59	6.59	-14.01	-14.01	-14.0
Leg angular Vel (deg/s)	439.27	/	367.11	/	16.43	16.43	16.4
Thigh to horizontal (deg)	-22.26	-23.71	-27.3	-21.78	-22.64	8.14	-7.3
Peak propulsive GRF norm.	6.6	7.28	7.94	8.62	-20.30	-18.41	-19.4
Peak vertical GRF norm.	51.7	47.27	40.89	42.3	20.91	10.51	15.7
Braking impulse norm.	-0.13	-0.14	-0.2	-0.17	-53.85	-21.43	-37.6
Net fwd impulse norm.	0.09	0.12	0.07	0.11	22.22	8.33	15.3
Vertical impulse norm.	2.11	2.08	2.16	2.2	-2.37	-5.77	-4.17
Propulsive ratio	4.30%	5.90%	3.30%	5%	23.26	15.25	19.3

The differences

In the selected trials, the Olympic-level athlete was 10.3% faster than the high-level one. Talking about kinematic parameters, the Olympic athlete had 4.5% higher step frequency. Step length was 5.3% longer, and contact times were 5.8% quicker. Hip displacement was only 2.8% greater, and the support angle at midstance only 1.8% smaller. A bigger difference in the vertical Sacrum movement: 14% less on the Olympic athlete. Leg angular velocity during flexion was higher by 16.4% on the Olympic subject.

About kinetic parameters: anteroposterior GRF peak was lower by 19.3% on the Olympic side, but the vertical GRF peak was 15.7% higher. The braking impulse was 37.7% less in Olympic subject, and net propulsive impulse also 15.3% greater. Vertical impulse only 4% smaller, and the propulsive ratio was 19.3% higher.

7.2.1 Visualizing through graphs

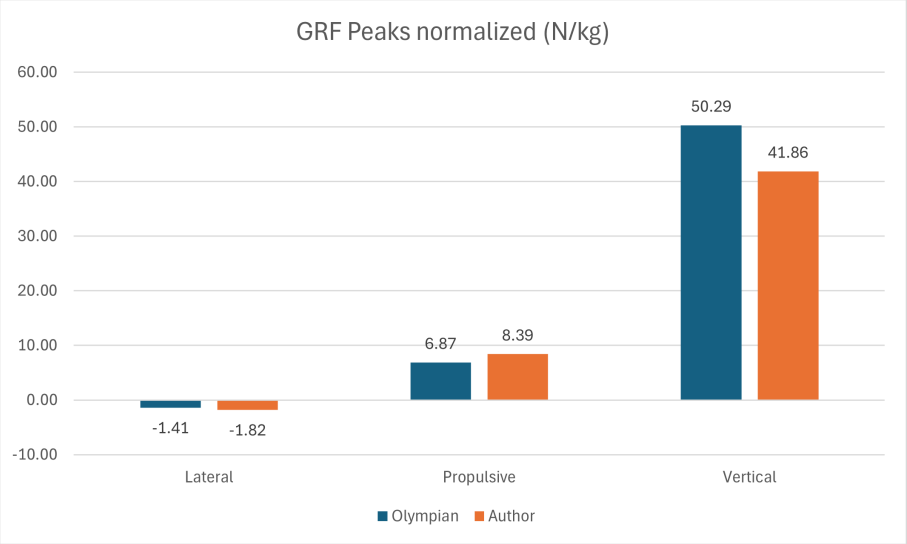

Figure 7.3: Ground Reaction Force peaks - average

7.2.2 Insights

We can notice how the main differences in kinematic parameters lie in step frequency and step length, that are the main requirements of achieving speed in sprinting. Without high leg turnover and without covering enough space with each step, Olympic level performance (i.e.: sub 10-s) is not achievable. Also contact time is reduced, while still being able to produce comparable or higher impulses. Notably, a big difference is found in the braking impulse, confirming what other researchers have found: higher level athletes are able to brake less compared to other.

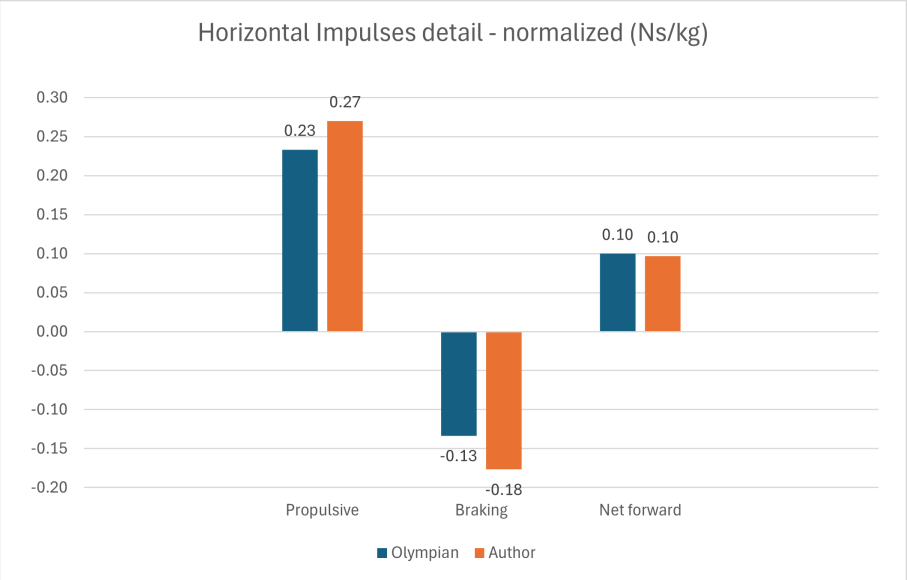

Figure 7.4: Anteroposterior impulses - average

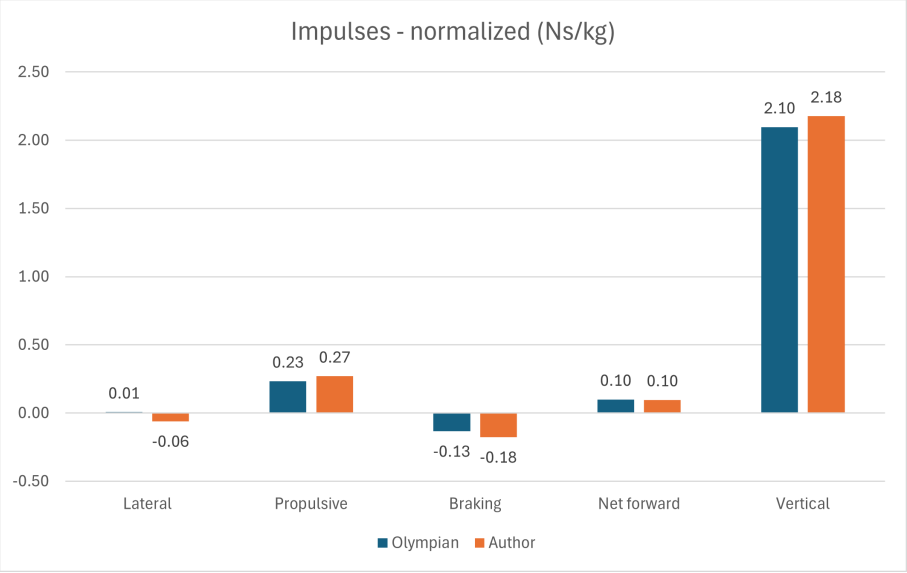

Figure 7.5: Impulses - average

Another crucial component is the propulsive ratio: 19.3% higher on Olympic data. This means that, even if the normalized vertical impulse on subject B is greater, subject A is pushing forward more efficiently. This may indicate that subject B is wasting too much energy in the vertical axis. As a final remark, while some parameters seem to be close between the two subjects - hip displacement, thigh to horizontal, support angle - there is a clear deficit in subject B on many areas. Most notably: Sacrum vertical excursion, leg angular velocity, braking impulse, and propulsive ratio.

The author believes that a sum of many elements, both biomechanical and biological, determines the final performance of the athlete. Singular parameters are insufficient to classify an athlete - excluding speed, as that is the final result of the effort - but they may give insights on the athletes' class, especially if a big dataset about such parameters is available. If, for example, a thousand data points about leg angular velocity were available instead of 22 from this research alone, better classification would be possible.

7.3 Block Start: a comparison between able bodied athletes

We now move on to the comparison of Block start between the same two subjects. It should be noted that data is normalized where possible, that both athletes have the left foot in front on the block and their first step is therefore right. On this section, more space will be given to data about block GRF and impulses, as the author believes it clearly shows the difference between the subjects' level.

Table of data

Table 7.3: Comparison of parameters: Olympian and High-level athletes on Block start.

Parameter	Olympian (A)		High-level (B)		Difference between legs		Diff with Oly
	Left leg	Right leg	Left leg	Right leg	Left	Right	
Speed at Block Clear. (m/s)	3.2	3.2	3.27	3.27	-2.19	-2.19	-2.2
Block to first strike (cm)	107.18	107.18	79.06	79.06	26.24	26.24	26.2
Push angle at BC (deg.)	38.57	38.57	35.82	35.82	7.13	7.13	7.1
Step Frequency (Hz)	4.59	4.59	4.1	4.1	10.68	10.68	10.7
Speed at 4th step (m/s)	6.03	6.03	5.87	5.87	2.65	2.65	2.7
Shank angle at fs_1 (deg.)	/	40.7	/	39.19	/	3.71	3.7
Push angle at fo_1 (deg.)	/	41.5	/	41	/	1.20	1.2
Shank angle at fs_4 (deg.)	56.99	/	66.08	/	-15.95	/	-16.0
Push angle at fo_4 (deg.)	45.79	/	41.34	/	9.72	16.43	13.1
Block: Peak GRF norm.	18.11	16.08	15.88	15.76	12.31	1.99	7.2
Block: Peak Impulse norm.	3.09	1.26	3.43	1.16	-11.00	7.94	-1.5

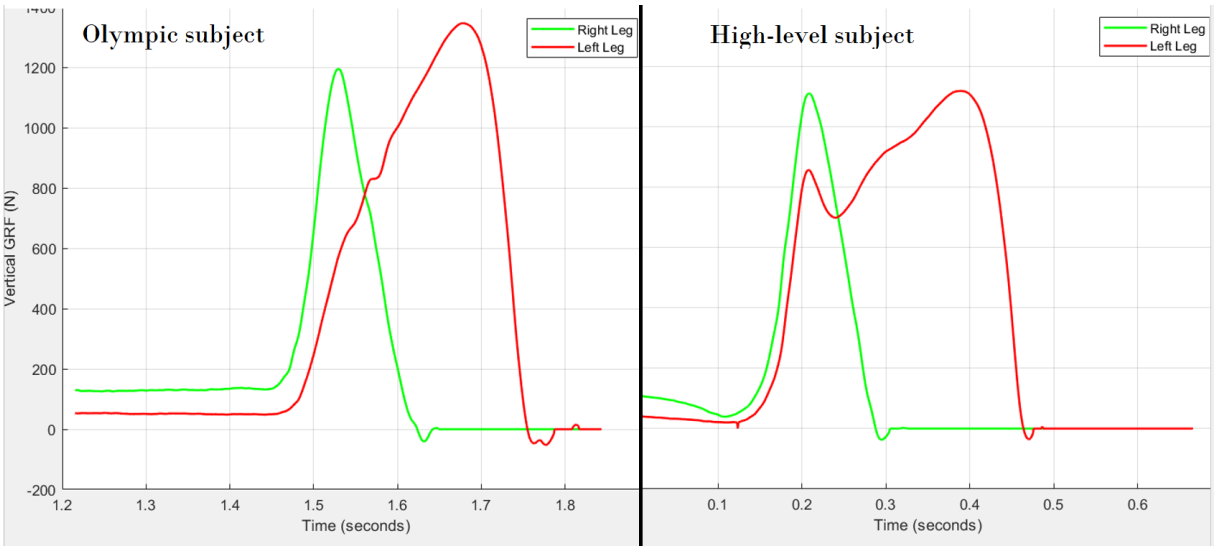

Figure 7.6: Block GRF plotted comparison.

The differences

Speed at block clearance (the instant in which the subject is not touching the block plates anymore) is 2.2% lower on the Olympic subject, but the distance covered with the first step is 26.2% greater. The push angle at block clearance is 7.1% greater on the Olympian, who also has 10.7% higher frequency in the steps happening after block clearance. Speed at 4th step is now higher by 2.7% for the Olympian, indicating a reverse in trend. The shank angle at foot strike 1 refers to how inclined the shank is when landing. Subject A is 3.7% more vertical - this angle should be as low as possible to favor forward propulsion. This changes however at step 4: the Olympian is 16% more horizontal than Subject B. This implies that he is more able to maintain his body tilted forward. This will be confirmed later by the kinetic comparison. Push angle at foot off, both at steps 1 and 4, is higher on Subject A. Lastly, the peak GRF on the block is 7.2% higher on the Olympic subject, while the peak impulse is 1.5% lower. It must be noted that this difference is due to the time spent on the block, much lower by subject A.

7.3.1 Visualizing through graphs

All the following data is normalized using the weight of the athletes.

7.3.2 Insights

First, let's consider the table about kinematic and kinetic data. Here we find less difference in speed as it's built up during the start. The speed at block clearance appears to be very similar, although at the fourth step we start seeing a difference between Subject A and B favoring the

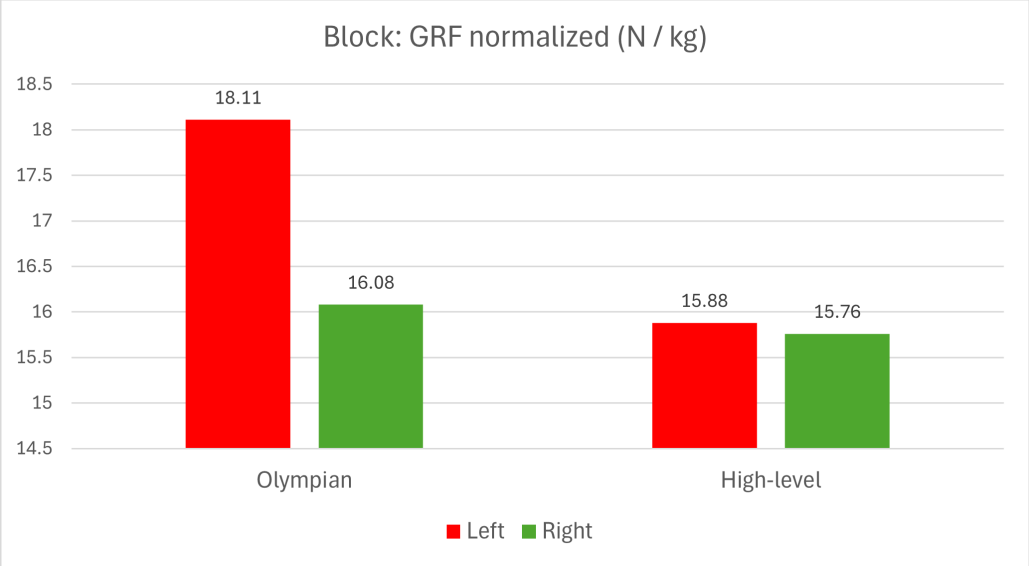

Figure 7.7: Block: peak GRF.

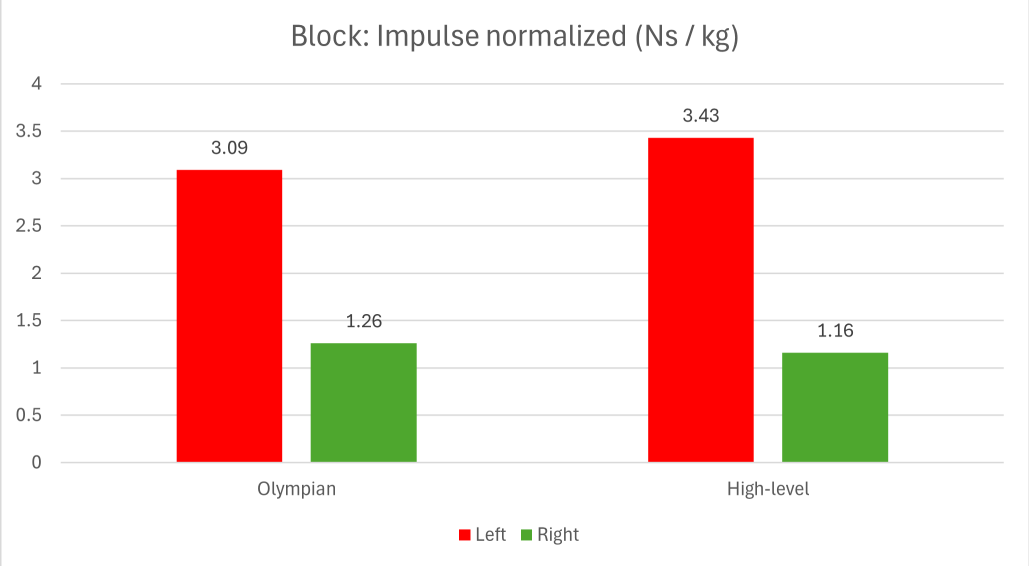

Figure 7.8: Block: impulses.

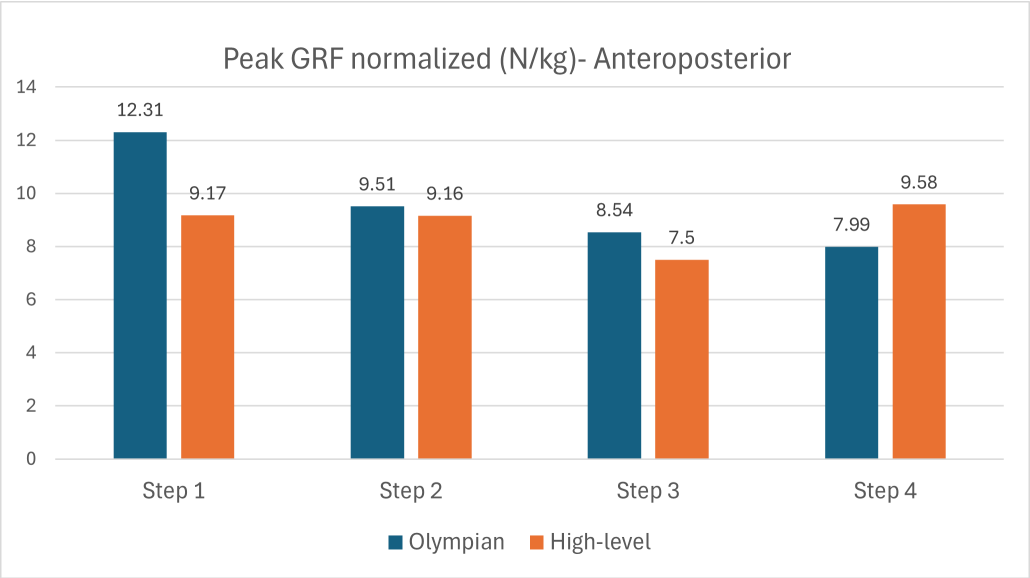

Figure 7.9: Peak steps GRF - anteroposterior

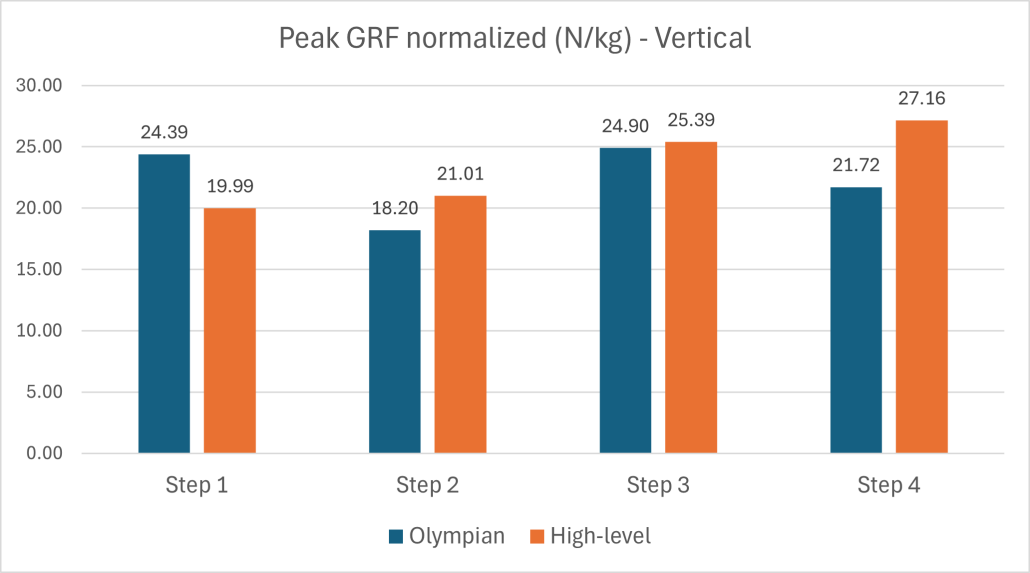

Figure 7.10: Peak steps GRF - vertical

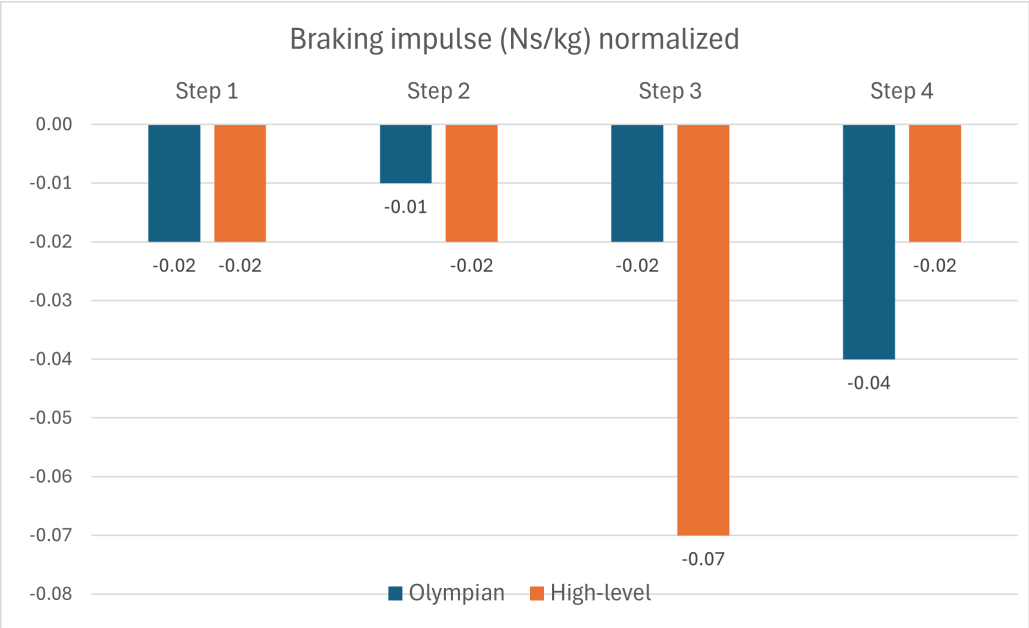

Figure 7.11: Braking impulse.

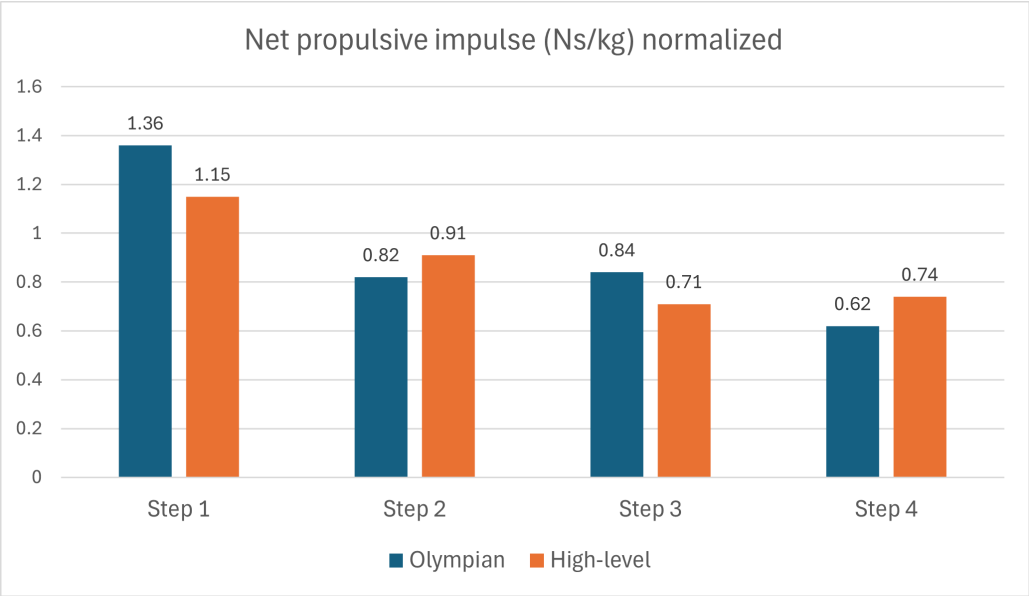

Figure 7.12: Net propulsive impulse.

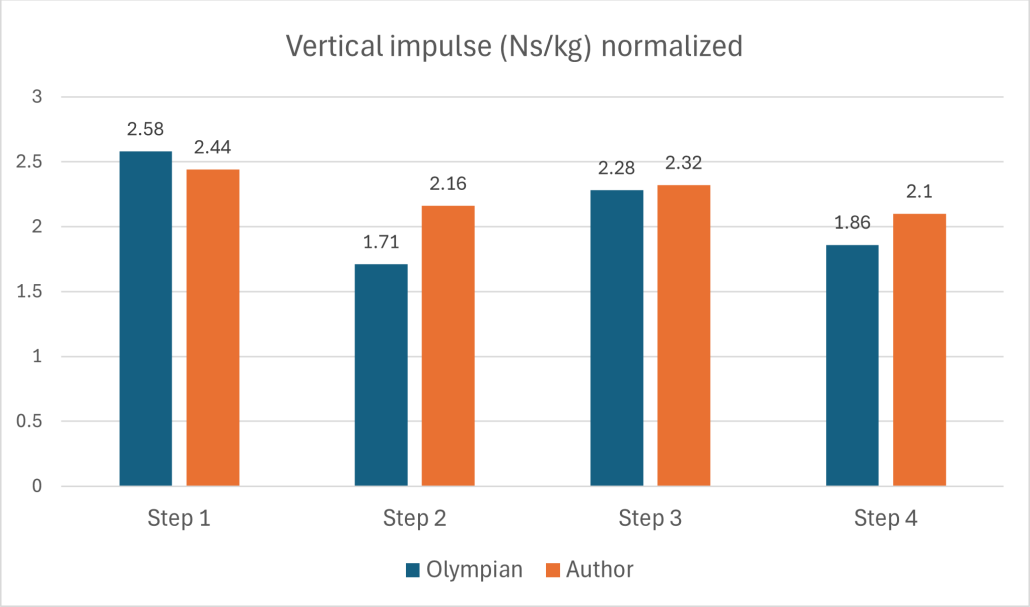

Figure 7.13: Vertical impulse.

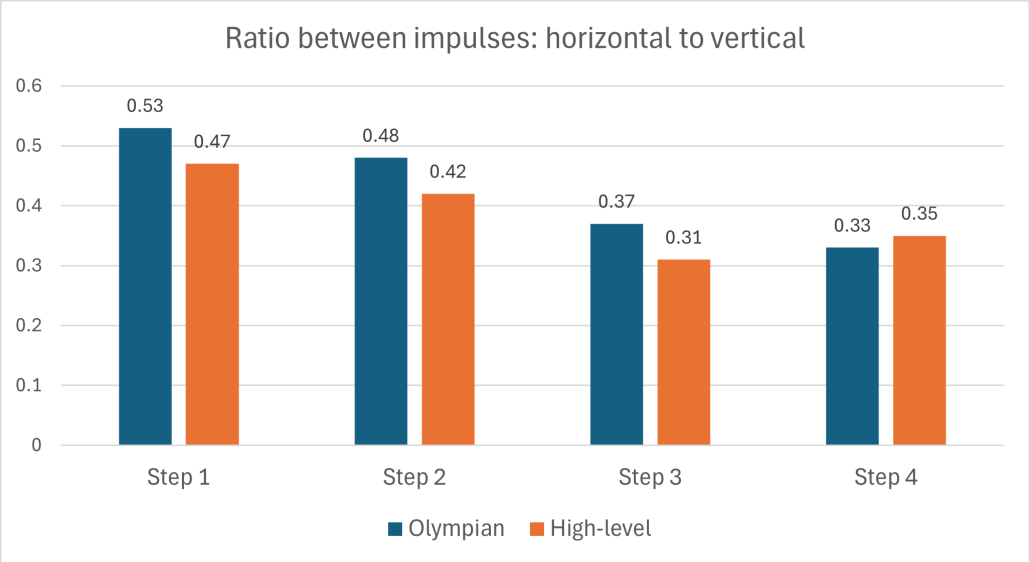

Figure 7.14: Ratio of impulses. Horizontal over vertical.

first. The most distant metric is the Block to first foot strike, showing an impressive 26% more in the Olympic subject. The push angles at foot strike and foot off don't seem too different, with the exception of the shank angle at foot strike on the fourth step. This may indicate a better capability of the subject A to remain tilted forward longer, increasing the forward propulsion before growing erect. Peak GRF on the block also favors subject A by 7.2%, while the impulse is similar.

Let us consider the graphs. As a reminder, subject A is the Olympic sprinter, and Subject B - High-level - is the author of this work. Figure 7.6 shows the plot of the GRF exerted on the blocks. On the left, subject A. On the right, subject B. We can immediately notice two elements. First, A is able to push better with the left leg, which is not impaired by the right leg leaving the block. Subject B has a sharp drop in left GRF when the right leg begins leaving the block. Only after is able to recover and increase the GRF applied, losing power output in the process. Second, A roughly spends at least 50 milliseconds less than B on the block, while being able to produce higher GRF and impulses. Another, less evident aspect, is that B is not perfectly synchronized at the beginning of the push: the left leg is slightly late. Moreover, the Olympian is much more stable before the "gun" signal - which happens right before the curve starts growing. Subject B is nowhere as stable, with a decrease in GRF applied before the "gun" signal.

Next, considering 7.7, we see how the Olympian has higher GRF peaks in both legs. Considering 7.8 the impulses on the block, left side is greater on subject B due to the greater time spent pushing on the block, while right side is greater on the Olympian.

Moving on to the steps after the block phase, we see in 7.9 that the peak anteroposterior GRF is generally higher on subject A, with the step 4 being the only exception. Figure 7.10 shows the vertical GRF component, showing the opposite trend: subject B shows higher peaks. This is not necessarily better, as during block start and acceleration phase we want to maximize horizontal drive, and reduce the vertical one to just enough to prevent the athlete from falling.

Figure 7.11 shows the braking impulse normalized. This is interesting as it shows how the Olympian brakes less overall. This data is consistent with what found in TSSR, even though there's less difference in this data.

Figure 7.12 shows the net forward impulse obtained subtracting braking impulse to propulsive impulse. In this case, subject A clearly performs better on the first and third step, while subject B is interestingly better on steps 2 and 4. Recalling what was mentioned above, figure 7.13 shows the vertical impulse: the high-level athlete does in fact produce greater vertical impulse except the first step.

Lastly, figure 7.14 shows the ratio between forward and vertical impulse for each step. Literature suggests that this value decreases with each subsequent step, and we find good confirma-

tion in the data. Apart for step 4, every step sees subject A perform better, with more propulsive ratio. The best step is the first, with 0.56. In other terms, if someone would push 100 Ns vertical, the net forward push would be 56 Ns. This is much higher than what we find in TSSR, where the ratio was not higher than 6%.

7.4 TSSR: applicability on Para athletes

This section aims to show the applicability of the report to Paralympic athletes. The report-making tool was initially developed for normo analysis using a 22-element marker set. Being this marker set a subset of the full one used in Paralympic trials, it is possible to analyze trials taken before the program was created. In this section, we show first some plot and data from reports of both Trans-tibial (TT) and Trans-femoral (TF) prostheses, and them compare them with the Olympic Subject. TT has a prosthesis in the right leg, while TF has a prosthesis on the left leg. Both athletes performed 3 steps in the acquisition. Data is not normalized as there was no weight recording on the day of the trial.

A comparison of plots

First, let us plot some GRF data about TF and TT. We can see in figure 7.15 how the second step of both athletes has a marked braking impulse. Both athletes perform the second step with the sane leg.

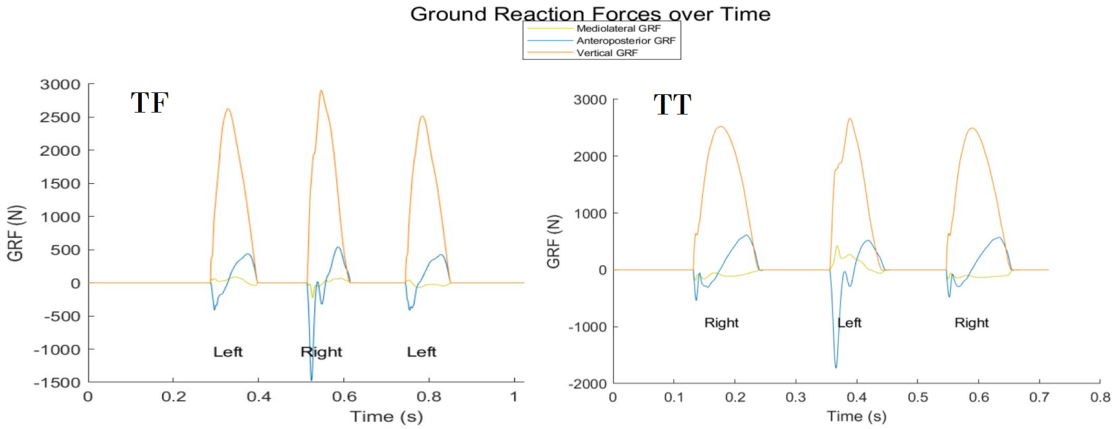

Figure 7.15: GRF visual comparison

An interesting comparison can be made between the CoP of both Paralympic athletes. We can notice in figure 7.16 how both subjects show a second step with a back-side CoP. This may be considered together with the GRF plot seen above: the sane leg is braking a lot more than the prosthesis.

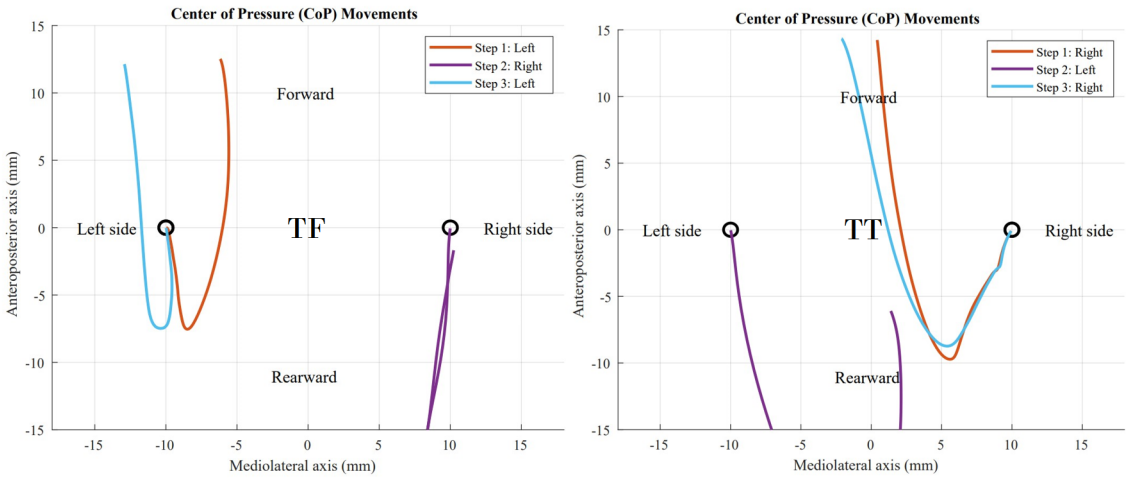

Figure 7.16: CoP comparison

A comparison of data: TT vs TF

Table 7.4: Comparison of parameters: TT and TF athletes on TSSR.

Parameter	TT		TF		Difference between legs (%)		Average
	Left leg	Right (prosthesis)	Left (prosthesis)	Right leg	Prosthesis legs	Sane legs	
Speed (m/s)	9.43	/	8.74	/	7.32	7.32	7.32
Step Frequency (Hz)	4.81	/	4.35	/	9.56	9.56	9.56
Contact time (ms)	88	108	106	100	1.85	-13.64	-5.89
Fly time (ms)	104	116	120	132	-3.45	-26.92	-15.19
Step length (m)	1.92	2	1.93	2.02	3.50	-5.21	-0.85
Hip Displacement (cm)	46.79	47.37	44.39	45.58	6.29	2.59	4.44
Support Angle (deg)	153.22	/	/	138.05	/	9.90	9.90
Sacrum vert Excursion (cm)	9.27	/	35.13	/	-278.96	-278.96	-278.96
Leg angular Vel (deg/s)	436.54	488.04	350.02	402.92	28.28	7.70	17.99
Peak Propulsive GRF (N)	518	593.75	435.15	541.7	26.71	-4.58	11.07
Peak Vertical GRF (N)	2665.6	2510.15	2575.25	2909.8	-2.59	-9.16	-5.88
Braking impulse (Ns)	-22.1	-9.2	-7.5	-19.3	18.48	12.67	15.57
Net forward impulse (Ns)	-6.1	14.35	12.3	-1.7	14.29	-72.13	-28.92
Vertical impulse (Ns)	130.4	168.35	166.15	166.9	1.31	-27.99	-13.34
Propulsive ratio (%)	-4.70	8.50	7.40	-0.10	12.94	97.87	55.41

Lets us comment this data table obtained from the two reports of TT and TF subjects. We notice how TT is faster by 7.3%, with a step frequency almost 10% greater. Contact time is also quicker on TT side, especially on the sane leg; same goes for fly time, with 15% lower time spent in the air. Step length does not differ between the subjects, while hip displacement (4%) and support angle of the sane leg (10%) are different, especially the latter suggesting either a partial collapse of the support leg or some binding caused by the bulkier TF prosthesis compared to the TT one. Sacrum vertical excursion as well is greatly different: TT athlete moves vertically almost 4 times less than TF. Leg angular velocity during flexion is quicker again in TT, in both legs, with average 18% more.

In terms of Kinetics, peak propulsive force is greater by 11% on TT, while peak vertical

GRF is greater by 6% on TF. TT does however break more: 15.5%. The forward impulse is greater in TF with 29% more. The sane leg of TT, in fact, carries a negative forward impulse, effectively braking. The vertical impulse is almost identical for the prostheses legs, while very different (28%) between the sane legs, favoring TF. Lastly, the propulsive ratio is 13% better for TT in the prosthesis leg, but 98% better in TF on the sane leg due to the extreme braking manifested by TT's sane leg.

A comparison of data: TT vs OLY

Table 7.5: Comparison of parameters: TT and Olympian athletes on TSSR.

Parameter	TT		Olympian (OLY)		Difference between legs (%)		Average diff
	Left leg	Right (prosthesis)	Left leg	Right leg	Left legs	Right legs (P)	
Speed (m/s)	9.43	9.43	10.95	10.95	-16.12	-16.12	-16.12
Step Frequency (Hz)	4.81	4.81	4.63	4.63	3.74	3.74	3.74
Contact time (ms)	88	108	86	84	2.27	22.22	12.25
Fly time (ms)	104	116	128	132	-23.08	-13.79	-18.44
Step length (m)	1.92	2	2.25	2.34	-17.19	-17.00	-17.09
Hip Displacement (cm)	46.79	47.37	50.42	53.38	-7.76	-12.69	-10.22
Support Angle (deg)	153.22	/	154.18	/	-0.63	/	-0.63
Sacrum vert Excursion (cm)	9.27	9.27	5.78	5.78	37.65	37.65	37.65
Leg angular Vel (deg/s)	436.54	488.04	439.27	439.27	-0.63	9.99	4.68
Peak Propulsive GRF (N)	518	593.75	491.55	537.3	5.11	9.51	7.31
Peak Vertical GRF (N)	2665.6	2510.15	3823.7	3490	-43.45	-39.04	-41.24
Braking impulse (Ns)	-22.1	-9.2	-9.55	-10.4	56.79	-13.04	21.87
Net forward impulse (Ns)	-6.1	14.35	6.6	9	208.20	37.28	122.74
Vertical impulse (Ns)	130.4	168.35	155.2	153.4	-19.02	8.88	-5.07
Propulsive ratio (%)	-4.70	8.50	4.30	5.90	191.49	30.59	111.04

7.4.1 Insights

TT is 16.3% slower than OLY, even with a 3.7% higher step frequency. He lags behind in step length, being 17% shorter. Fly time is lower on OLY with 12% less. TT also has less hip displacement at foot off, with 10% less. Interestingly, the support angle of the sane leg is almost identical, varying by 1 degree. Sacrum vertical excursion, however, differs by 37.6% and favors the OLY. Leg angular velocity is similar on the sane leg, but higher on the prosthesis leg in TT by 10%.

In terms of kinetic data, peak propulsive GRF is 7% higher on TT, but peak vertical GRF is 41% lower on TT. Braking impulse is lower on the prosthesis side with 13% less, but much higher on the left side with almost 57% more braking by TT. The same pattern applies to net forward impulse, with 37% better impulse on TT's right leg, but 208% less impulse on the right leg. Vertical impulse is overall 5% lower on TT, but again the prosthesis side shows a 9% higher than OLY. Lastly, the propulsive ratio follows the pattern: the prosthesis side has a 30% higher

ratio, but the sane leg (left) lags behind with 190% less, implying a negative ratio on the TT athlete.

7.5 Parameters and prostheses

When analyzing Paralympic athletes, adjustments to parameters are essential to account for prostheses, with their specific marker sets. For example, joint centers may need to be estimated differently due to altered biomechanics. Parameters such as joint angles and forces must account for the rigidity or compliance of the prosthesis. Comparing data across athletes requires normalization techniques, ensuring insights are meaningful while reflecting the unique dynamics of each prosthesis-limb system. Considering this, we show an example of how to modify the computation of the ”Support Angle” parameter for the case of TT and TF subjects. As mentioned in the concluding chapter, this work can be improved with the adaptation of all the prostheses related parameters to create a full-capability analysis program able to autonomously determine the type of prosthesis (if present) based on markers positions, and to adapt the analysis accordingly. What follows is an example of possible parameter adaptation to a TF athlete.

Original parameter

This is the original parameter ”Support angle 7.17” as described in chapter 3. It can be applied to any sane leg. For example, if a TF athlete has a left leg prosthesis, the original support angle will be computed on the right leg at midstance.

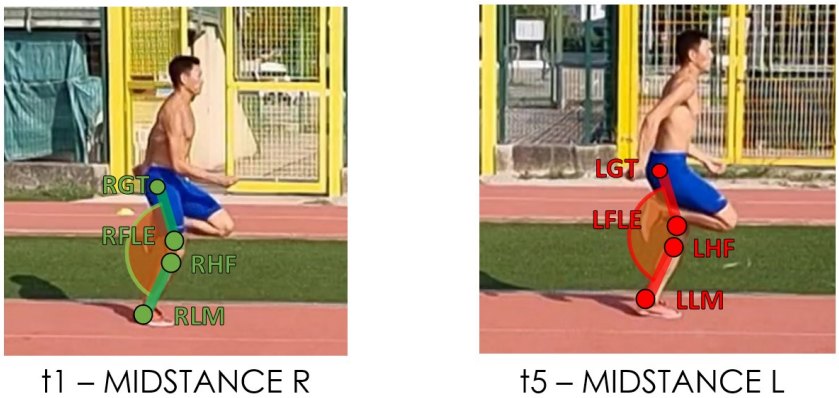

Figure 7.17: Support Angle

Adapted version

In order to produce meaningful results for the other leg, it is necessary to adapt the landmarks and chosen markers. As we can see from the picture, the marker set for TF is bigger, with new

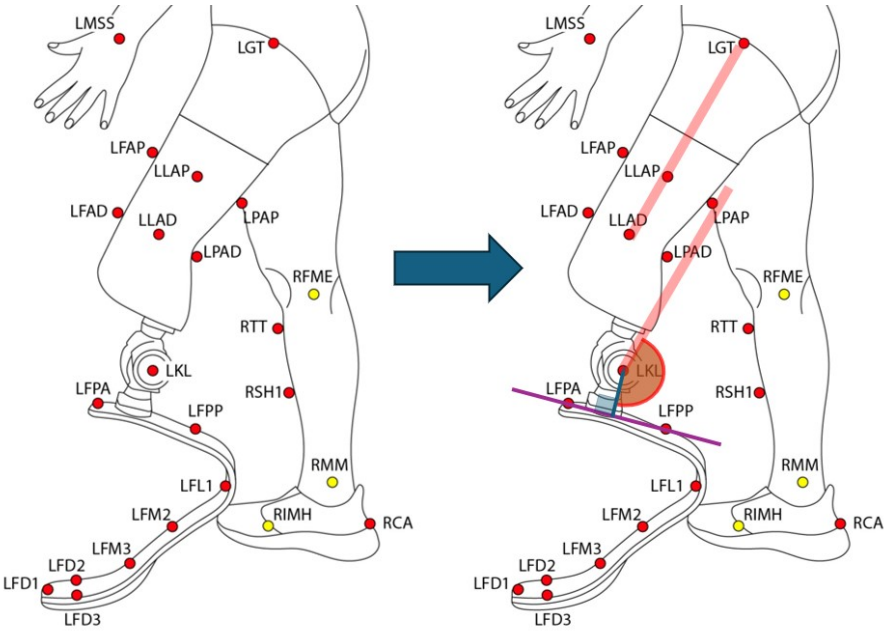

Figure 7.18: Adapting the parameter

markers placed on the prosthesis. The original parameter was based on two body segments: thigh and shank. While we still are able to compute the thigh, here there is obviously no shank. What we can do is project the thigh segment to align it with the marker ”LKL” (or ”RKL” for right side) and draw the line connecting LFPA and LFPP, finding the vertical line connecting LKL to it. We can compute this component’s angle as shown in the picture. As we consider each parameter we should ask whether it’s possible to map it, reconstruct it for the prosthesis, or if we should aim for different data. One last example as an open question. In chapter 3, one parameter is ”Ankle angle” 3.16. How are we supposed to compute such angle when there is no ankle, but a J-shaped or C-shaped prosthesis? Do we have to find the equivalent of the ankle angle or it’s better to analyze other aspects, like how much the prosthesis bends under load? The future development of this work will consider this kind of interrogatives, carefully evaluating each case on its own.

Chapter 8

Further developments

8.0.1 Limitations of the study

Subjects

The number of subjects was limited. We are aware that the number of samples needed to carry out a statistical analysis with significant results must be greater than our case.

We can also discuss about the level of the participants. Due to the small number, most of the athletes were considered of medium level, with few low level subjects and few high-level. 2 male athletes were Olympic-level. The number of subjects was too small to achieve a real distribution of athletes' performances. Therefore, there is a problem in the search for parameters that maximize performance, as the study is affected by the low number of faster and slower athletes; consequently, the angles and various parameters of the athletes being concentrated mainly on the medium level range may not give significant results on the most important parameters.

Instruments

During the acquisition phase two main issues were found. The presence of cones forced athletes to run a certain step length as intended; however, we did not consider that many athletes were unexperienced with such training method. The cones modified their gesture, as it became less natural due to their focus shifting to not hitting the cones instead of maximizing performance.

On the block start sessions we found that the force plates under the block were too small, as there is not enough room for the block. The block was cut in half, effectively split on two adjacent force plates. Subjects, however, start with either right or left foot in front, making two small adjacent force plates inadequate. These also forced athletes into a specific block width, while this parameter may also change among athletes. Another problem concerned the anchoring of blocks to the ground: having split the block in two halves, the forces exerted on the pedals lifted or moved the pedal from its starting position. In these cases, the test had to be

performed again. Strong tape was used to further secure the block to the ground, as the blocks' nails were not enough, especially for stronger athletes.

Software

Tracking of trials must be performed on Vicon Nexus software. Some versions of the software were incompatible with the computers used by researchers and the software seldom crashed. Tracking is a long and tedious process, especially if a lot of markers are applied on the subject. If reflections are captured in the volume due to clothing or light bouncing on surfaces, the process grows more complicated as Nexus is unable to determine which markers are which. The researcher must manually fix markers frame by frame. All of this makes the process unnecessarily long. Sometimes markers were not tracked as not enough cameras caught them. Vicon Nexus provides instruments to fix these blank trajectories as mentioned in chapter 4.

Data

Before the creation of this reporting tool the procedure was long and performed through different software, being not automated. During the Smart Track BTS analysis the operator had to manually select instants of running, leading to potential errors and imprecision in the parameters. This slowed the first part of our research to find the most relevant parameters.

8.0.2 Future research and improvements

To our knowledge, this was the first study of its kind to be conducted. Such combination of athletes, parameters investigated and in-vivo approach is not found in literature. Some limitations were inherently caused by these facts. What follows are proposals to improve the study and solve the problems above mentioned.

To obtain more consistent results subjects should be analyzed throughout the year, following their progress as they train, and not have them run on a single day. Due to the nature of athletics performance, a trial performed on December (loading season) will be different than a trial performed on May (competition season). Furthermore, an athlete able to come multiple time may respond better to running with different conditions, for example with cones on the ground. This could provide useful to compare different running techniques without having their performance hindered as it happened in this study.

The number of participants should increase to obtain results with greater statistical significance. It may help organize athletes by level from the first moment they are included in the study. Another idea is to use the system as a way to validate training programs: an athlete with clear weaknesses in block start may perform two sessions - for example 6 months apart - and

verify if there is an increase in start performance based on training efforts focused on explosive power.

Regarding the starting blocks an optimal solution would be using specially modified starting blocks with embedded load cells. These cells are placed on the block footplates and do not need any ground plates. This would allow for a more stable block and also increase the available plates for the subsequent steps, as the block could be placed before any force plate on the ground.

More data could be recorded and analyzed. This study focused on lower limbs and trunk, as arms movement was out of the scope of the study. While it is known that arms play a crucial role into balancing the legs' movement, further analysis could be carried out. The marker set used already placed relevant markers on the arms, and the MATLAB program could be extended to include upper limbs analysis.

MATLAB software could be further improved to allow comparisons of trials both between the same athlete and different ones, effectively making the data processing of chapter 7 completely automatic. This would bring the software to the next level. Another idea is to build a database that can be live-accessed by both researchers, coaches, and by the program itself, to maximize the analysis and comparison possibilities.

8.0.3 Further applicability to para athletes

Lastly, as discussed in the previous chapter, Paralympic athletes can be analyzed using the exact same piece of software. This image 8.1 shows a basic mapping performed by the author of this work. This enabled the MATLAB app to provide reports for athletes with trans-femoral and trans-tibial prostheses over trial performed months before it even existed, thanks to a compatible marker set. This mapping is not final, but rather functional to proving that Paralympic quick analysis can be achieved with this lighter marker set.

This shows the potential of the program, able to support different athletes and different marker set as long as either the original marker set is a subset of the full marker set applied to para athletes, or as long as markers on affected limbs are traced back to the original 22 markers used in the able-bodied athlete analysis. In particular, kinetic analysis can be performed regardless of the marker set used, with the exception of foot markers, used to determine foot position and order when hitting the ground. Kinematic analysis requires a thorough discussion on how it's best to map the studies parameters to para athletes. Coaches, researches and prostheses manufacturers should come together in defining the crucial elements to analyze in this specific field.

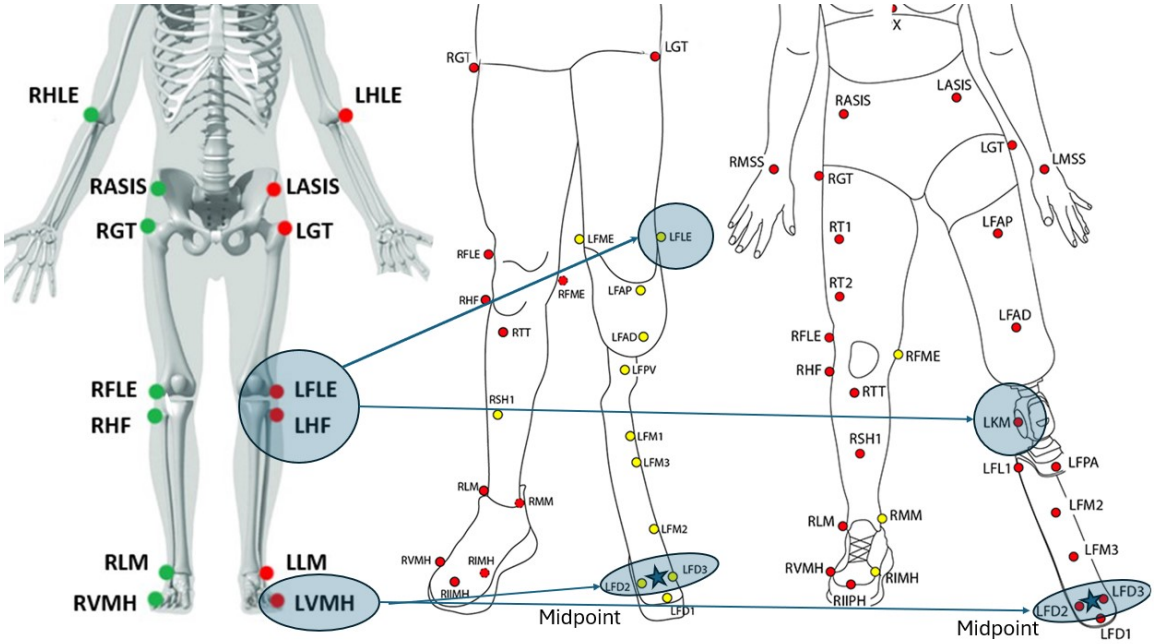

Figure 8.1: Mapping knee and foot markers between Normo, TT and TF athletes.

Bibliography

[1] Tom D. Brutsaert and Esteban J. Parra. What makes a champion? explaining variation in human athletic performance. *Respiratory Physiology and Neurobiology*, 151:109–123, 2006.

[2] Krzysztof Maćkała, Marek Fostiak, and Kacper Kowalski. Selected determinants of acceleration in the 100m sprint. *Journal of Human Kinetics*, 45:135–148, 2015.

[3] Vlatko Vucetic, Branka Matkovic, and Davor Sentija. Morphological differences of elite croatian track-and-field athletes. *Collegium antropologicum*, 32:863–8, 10 2008.

[4] Jean-Benoît Morin et al. Mechanical determinants of 100-m sprint running performance. *European Journal of Applied Physiology*, 45:135–148, 2012.

[5] Aditi Majumdar and Robert Robergs. The science of speed: Determinants of performance in the 100 m sprint. *International Journal of Sports Science and Coaching*, 6(3):479–493, 2011.

[6] Aanusz Iskr. Marzena Paruzel-Dyja, Anna Walaszczyk. Elite male and female sprinters' body build, stride length and stride frequency. *Studies in physical culture and tourism*, 13:33–37, 2006.

[7] H. Kunz and A. Kaufmann. Biomechanical analysis of sprinting: decathletes versus champions. *British journal of sports medicine*, 15:177–181, 1981.

[8] Jean-Benoît Morin et al. Technical ability of force application as a determinant factor of sprint performance. *Medicine and Science in Sports and Exercise*, 43(9):1680–1688, 2011.

[9] Timothy J. Suchomel et al. The importance of muscular strength in athletic performance. *Sports Medicine*, 46:1419–1449, 2016.

[10] James wild et al. A biomechanical comparison of accelerative and maximum velocity sprinting: Specific strength training considerations. *Professional Strength and Conditioning*, 21:23–37, 2013.

[11] Thomas A. Haugen and Felix Breitscha¨and Stephen Seiler. Sprint mechanical variables in elite athletes: Are force-velocity profiles sport specific or individual? *PLoS ONE*, 14, 2019.

[12] Thomas Haugen1 et al. The training and development of elite sprint performance: an integration of scientific and best practice literature. *Sports Medicine - Open*, 5:5–44, 2019.

[13] Matthieu Milloz, Kevin Hayes, and Andrew J. Harrison. Technical ability of force application as a determinant factor of sprint performance. *Sports Medicine*, 51:21–31, 2021.

[14] Jean Slawinski et al. Kinematic and kinetic comparisons of elite and well-trained sprinters during sprint start. *Journal of Strength and Conditioning Research*, 24(4):896–905, 2012.

[15] Neil Edward Bezodis, Stefen Willwacher, and Aki Ilkka Tapio Salo. The biomechanics of the track and field sprint start: A narrative review. *Sports Med*, 49:1345–1364, 2019.

[16] Valentina Cavedon et al. Anthropometry-driven block setting improves starting block performance in sprinters. *PLoS ONE*, 14(3):1345–1364, 2019.

[17] Maria João Valamatos et al. Biomechanical performance factors in the track and field sprint start: A systematic review. *International journal of Environmental research and Public Health*, 19:1–74, 2022.

[18] Ryu Nagahara et al. Association of sprint performance with ground reaction forces during acceleration and maximal speed phases in a single sprint. *Journal of Applied Biomechanics*, 34:104–110, 2018.

[19] Ryu Nagahara et al. Kinematics of transition during human accelerated sprinting. *Biology Open*, 3:689–699, 2014.

[20] G. Rabita et al. Sprint mechanics in world-class athletes: a new insight into the limits of human locomotion. *Scand J Med Sci Sports*, 25:583–594, 2015.

[21] F. Kugler and L. Janshen. Body position determines propulsive forces in accelerated running. *PLoS ONE*, 43:343–348, 2010.

[22] Jean-Benoit Morin, Pascal Edouard, and Pierre Samozino. The training and development of elite sprint performance: an integration of scientific and best practice literature. *New studies in athletics*, 3:87–103, 2013.

[23] Jiabin Yu et al. Biomechanical insights into differences between the mid-acceleration and maximum velocity phases of sprinting. *Journal of Strength and Conditioning Research*, 30(7):1906–1916, 2016.

[24] Peter G et al. Weyand. Faster top running speeds are achieved with greater ground forces not more rapid leg movements. *Journal of Applied Physiology*, 89:1991–1999, 2000.

[25] Kenji Miyashiro et al. Kinematics of maximal speed sprinting with different running speed, leg length, and step characteristics. *Front. Sports Act. Living*, 1, 2019.

[26] Kenneth P. Clark. Determinants of top speed sprinting: Minimum requirements for maximum velocity. *Applied Sciences*, 12:82–89, 2022.

[27] Jean-Benoît Morin et al. Acceleration capability in elite sprinters and ground impulse: Push more, brake less? *Journal of Biomechanics*, 48:3149–3154, 2015.

[28] Jonas Dodoo. Speed solutions. Accessed: 2024-10.

[29] Isacco Costa. Biomechanical analysis of running in elite sprinters after opensim musculoskeletal modeling. Master's thesis, University of Padua, 2023.

[30] physio pedia.com. physio-pedia.com. Accessed: 2024-9.

[31] Smirniotou et al. Strength-power parameters as predictors of sprinting performance. *Sports Med Phys Fitness*, 48:447–454, 2008.

[32] M.J.Harland and J.R. Steele. Biomechanics of the sprint start. *Sports Medicine*, 23:11–20, 1997.

[33] Ralph Mann. *The Mechanics of Sprinting and Hurdling*. Independently published, 2022.

[34] Edmund Cramp. C3d standard. Accessed: 2024.

[35] Addison-Wesley, Reading, MA. *VICON Plug-in Gait Reference Guide*, 2016.

[36] Inc. The MathWorks. Matlab documentation. Accessed: 2024.

[37] Emma Ghezzo. Investigation of correlation between élite sprinter ranking and kinematic and kinetic biomechanical parameters during starting and sprinting. Master's thesis, University of Padua, 2024.

[38] Ling Wei Lei. Analisi cinematica e dinamica della partenza ai blocchi e della corsa nella fase lanciata in velocisti nell'atletica leggera, 2024.

Ringraziamenti

Giunge al termine un percorso lungo, a tratti difficile. Sono una persona diversa da quando ho iniziato ed è merito di molte cose; più di tutto, però, delle persone.

Ringrazio il Professor Petrone per avermi seguito con cura e attenzione come relatore; per l'opportunità di fare ricerca nello sport che più mi appassiona; per l'impegno che dedica costantemente ai progetti seguiti e per avermi trasmesso l'importanza della cura dei dettagli.

Ringrazio il Professor Marcolin per avermi seguito come Correlatore, per la costante presenza durante i test al Palaindoor e per la completa disponibilità nel supportare il mio lavoro.

Ringrazio Emma e Davide, compagni di tesi, per aver reso il tutto più leggero, e i compagni di Lab con cui ho condiviso questo percorso.

Ringrazio Coach Airale, per avermi insegnato la vera atletica e per aver creduto in me.

Ringrazio i *Pancini*, perchè amici così dove li trovo?

Ringrazio il *Privè che si è laureato*, perchè ci siamo laureati tutti di nuovo, in luoghi diversi.

Ringrazio *Pirkuc*, perchè è la prova che le vere amicizie durano negli anni.

Un rigraziamento tardivo a Mattia, Riccardo, Paolo e Andrea, che agli inizi mi accolsero a Padova. Ringrazio dunque l'appartamento di Padova, diventato presto ben più di un luogo in cui dormire da fuorisede. Ringrazio chiunque l'abbia condiviso con me, conoscendolo come l'Interno 3, Casa Italia o Ristorante Chef Cina.

Ringrazio il mio portatile, che ha quasi tirato le cuoia tagliando il traguardo. #finoallafine

Ringrazio chi ha creduto in me, chi ha continuato a chiedermi come andavano gli studi e chi ha supportato quelle scelte che, quando non cambiano la vita, la indirizzano comunque con decisione.

Ringrazio, da ultimo, la mia famiglia sopra a tutto. E' grazie a loro se ho avuto l'opportunità di realizzarmi. Probabilmente tante parole faticherebbero a spiegare quello che vorrei dire, quindi ne scelgo di chiare: il sentimento che più provo è gratitudine per quello che mi è stato dato. Dal primo giorno ad oggi, dopo 10.000 giorni, so che sono stato amato. In particolare: grazie Enrico, Giorgia, Chiara, Walter, Ofelia, Luigi, Dima.

Grazie a chiunque non ho nominato, ma legge o ascolta queste parole: capisco solo ora quel "troppe persone da ringraziare" che tante volte ho letto altrove.

E grazie a me, per non aver mollato.

Appendix A

Full reports

To help visualize and fully understand the report structure, in this appendix are included two full reports (Block Start, TSSR) of Subject 14, the author of this thesis.

Block Start Report

S14, High level athlete, trial OSN 30

Padova - UNIPD

30-Nov-2024

Capitolo 1. Kinematic Parameters: Tabular data

Kinematic Parameters: Block Clearance

Variable Name	Left Leg	Right Leg	Difference (%)
Speed at Block Clearance (m/s)	3.27	-	
Distance: block to first FootStrike (cm)	-	66.58	
Distance: block to first FS norm (cm/leg)	-	79.06	
Push angle at block clearance (°)	35.82	-	
Thigh-Shank Angle at Block Clearance (°)	88.76	-	
Thigh-Trunk Angle at Block Clearance (°)	197.47	-	
Thigh to Horizontal Angle at BC (°)	-142.16	-	
Shank to Vertical Angle at BC (°)	-53.55	-	

The above table includes kinematic data exclusively related to block clearance. Data is shown on the column of the front leg, meaning the last leg to leave the block footplates. The other leg only shows data about the distance covered with the other leg.

Kinematic parameters: first step of each leg.

Variable Name	Left Leg	Right Leg	Difference (%)
Step Frequency (Hz)	4.1	4.1	0
Speed at Foot Strike (m/s)	4.29	3.41	22.9
Contact Time (ms)	164	180	9.3
Flight Time (ms)	80	56	35.3
Step Length (cm)	1.22	1.03	16.9
Step Length Normalized (cm/leg)	1.45	1.22	17.2
Stride Length (cm)	2.65	2.26	15.9
Stride Length Normalized	3.15	2.68	16.1
Shank angle at Foot Strike (°)	50.23	39.19	24.7
Trunk Angle at Foot Strike (°)	43.11	33.68	24.6
Push Angle at Foot Off (°)	41.1	41	0.2
Thigh-Trunk Angle at Foot Off (°)	202.52	200.27	1.1

The above table contains the kinematic parameters of the first two steps of the trial. Step number 1: Right

Kinematic parameters: last step of each leg.

Variable Name	Left Leg	Right Leg	Difference (%)
Step Frequency (Hz)	4.1	4.1	0
Speed at Foot Strike (m/s)	5.87	5.09	14.2
Contact Time (ms)	128	140	9
Flight Time (ms)	80	112	33.3
Step Length (cm)	1.22	1.42	15.2
Step Length Normalized	1.45	1.69	15.3

Stride Length (cm)	2.65	2.26	15.9
Stride Length Normalized	3.15	2.68	16.1
Shank angle at Foot Strike (°)	66.08	54.65	18.9
Trunk Angle at Foot Strike (°)	41.93	43.3	3.2
Push Angle at Foot Off (°)	41.34	42.69	3.2
Thigh-Trunk Angle at Foot Off (°)	202.36	199.03	1.7

The above table contains the kinematic parameters of the last two steps of the trial. Left is step 4, Right is step 3.

Capitolo 2. Speed Data

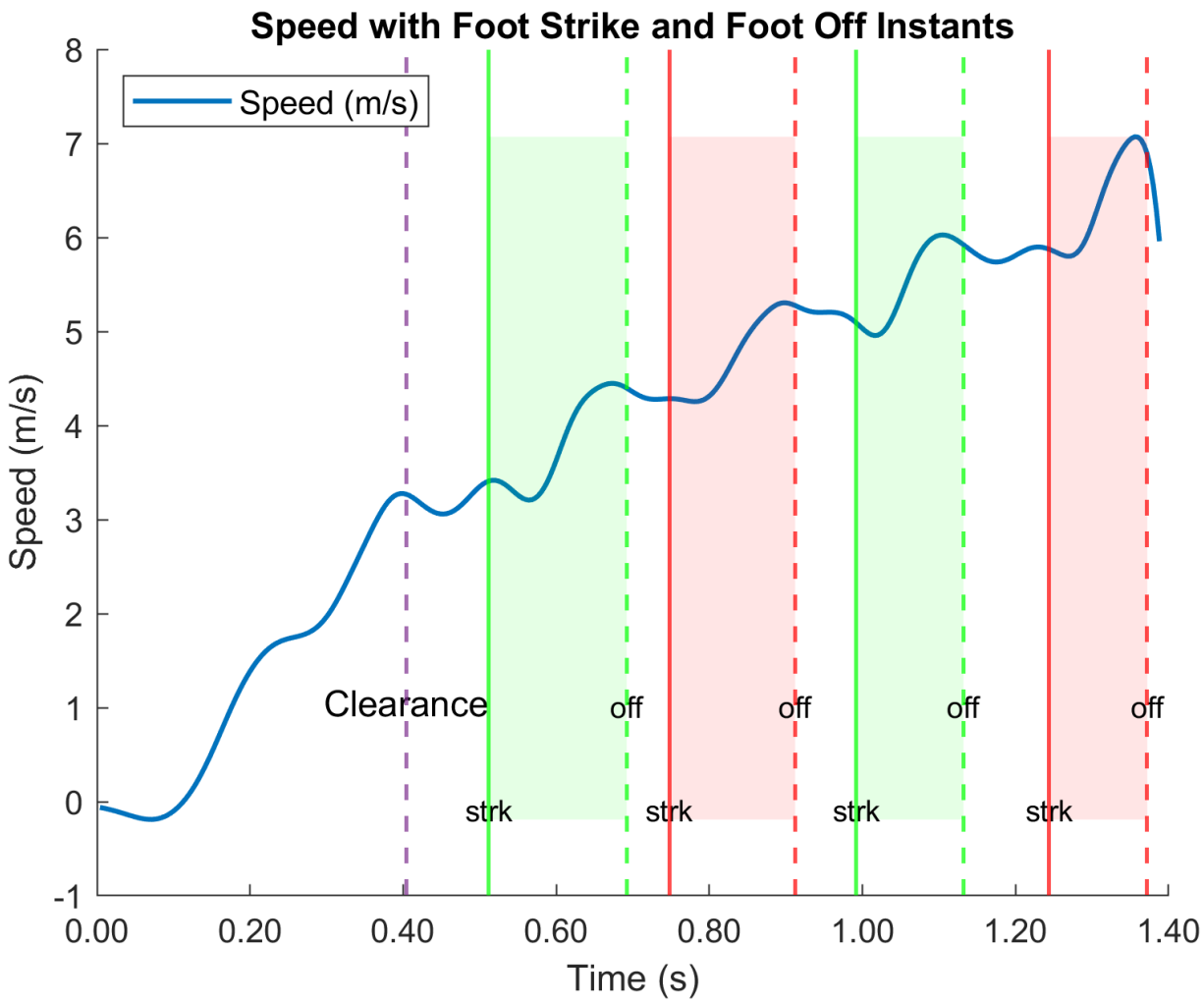

This plot shows the speed curve. Foot strike (continuous line) and Foot Off (dashed line) instants are added to the plot to better visualize the running cycle. A shade is added between the lines to represent the time during which the foot is in contact with the ground. Green color is used for right foot, while red for left leg. Note: Spikes in the speed curve may be issue-related to the tracking of Sacrum Marker.

Capitolo 3. GRF and Impulses: Starting block

Blocks GRF, Block Impulses. Leg in front: Left. The left impulse is 2.97 times the right impulse.

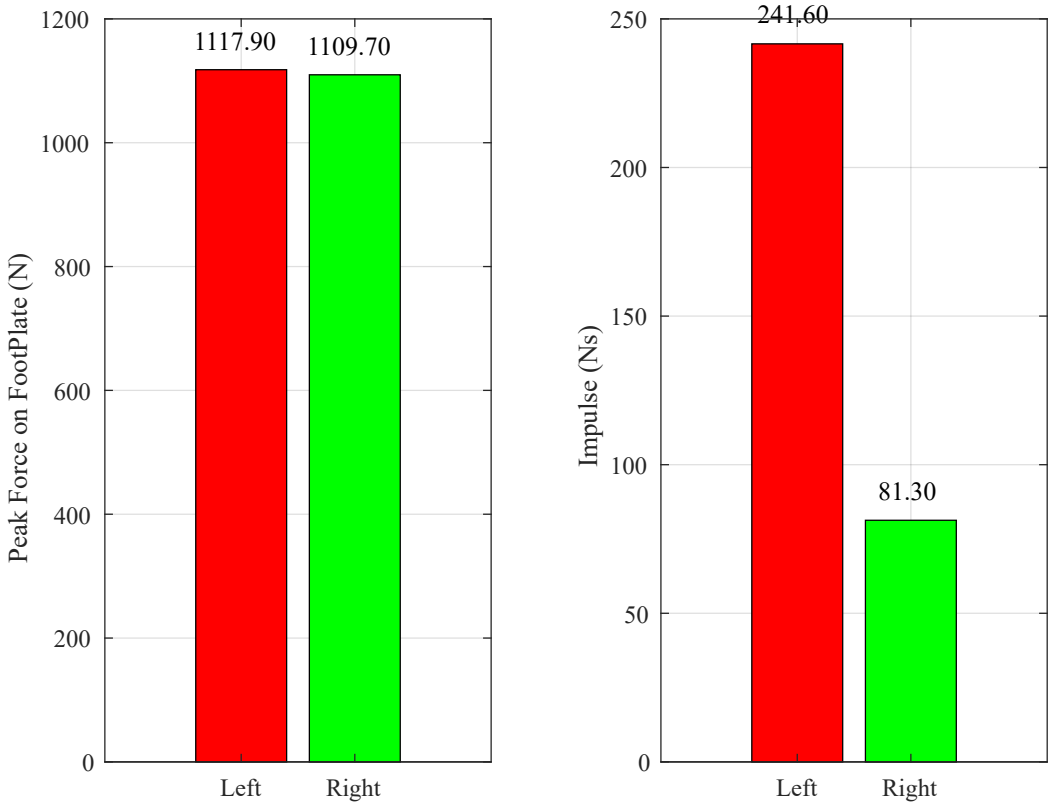

This plot shows: on the left, the vertical Ground Reaction Force (GRF) components for both legs on the block. On the right, the impulse generated by both legs on the block.

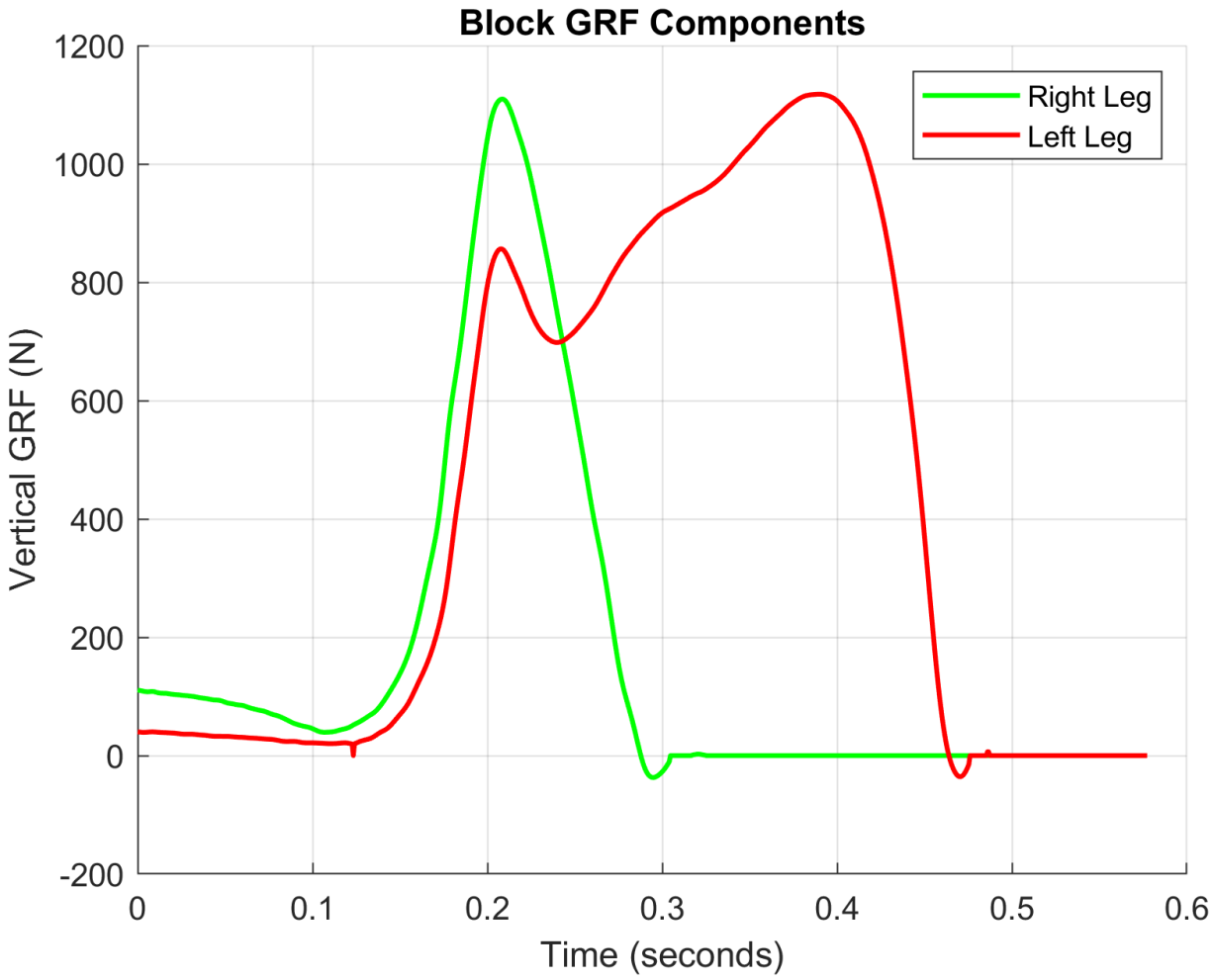

This plot of Ground Reaction Force (GRF) shows the force exerted on the Right (green) and Left (red) footplates of the block. The front foot is fixed in place for a longer period than the back foot, and it can be seen from this plot.

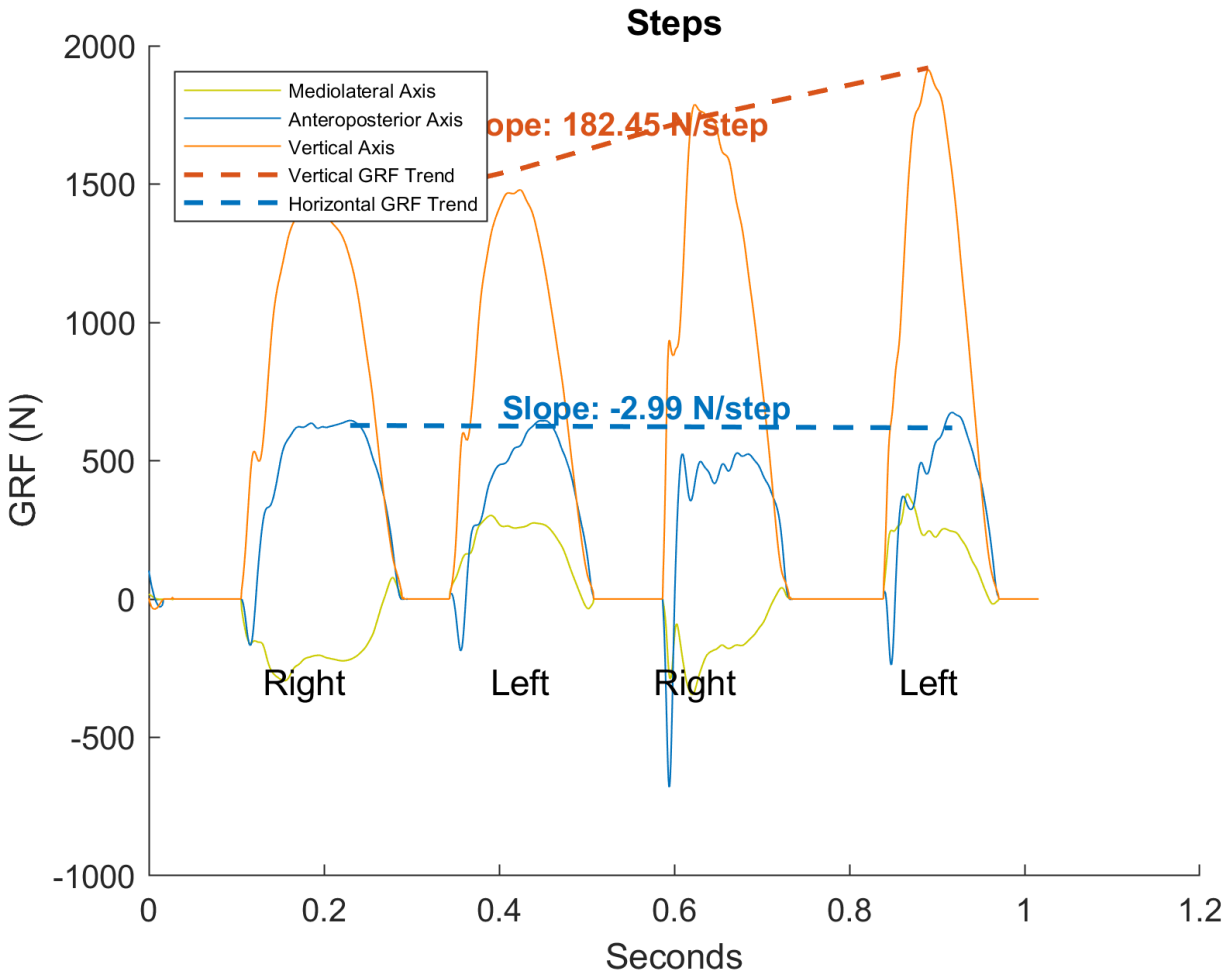

This plot shows the GRF (N) components for the steps after block clearance. Two trend lines are drawn to show the trend regarding peak GRF generated at each step, both in Vertical and Horizontal axis. Note: maximum GRF alone is not enough to analyze the steps: the following graph about impulses considers the whole force applied over the contact time.

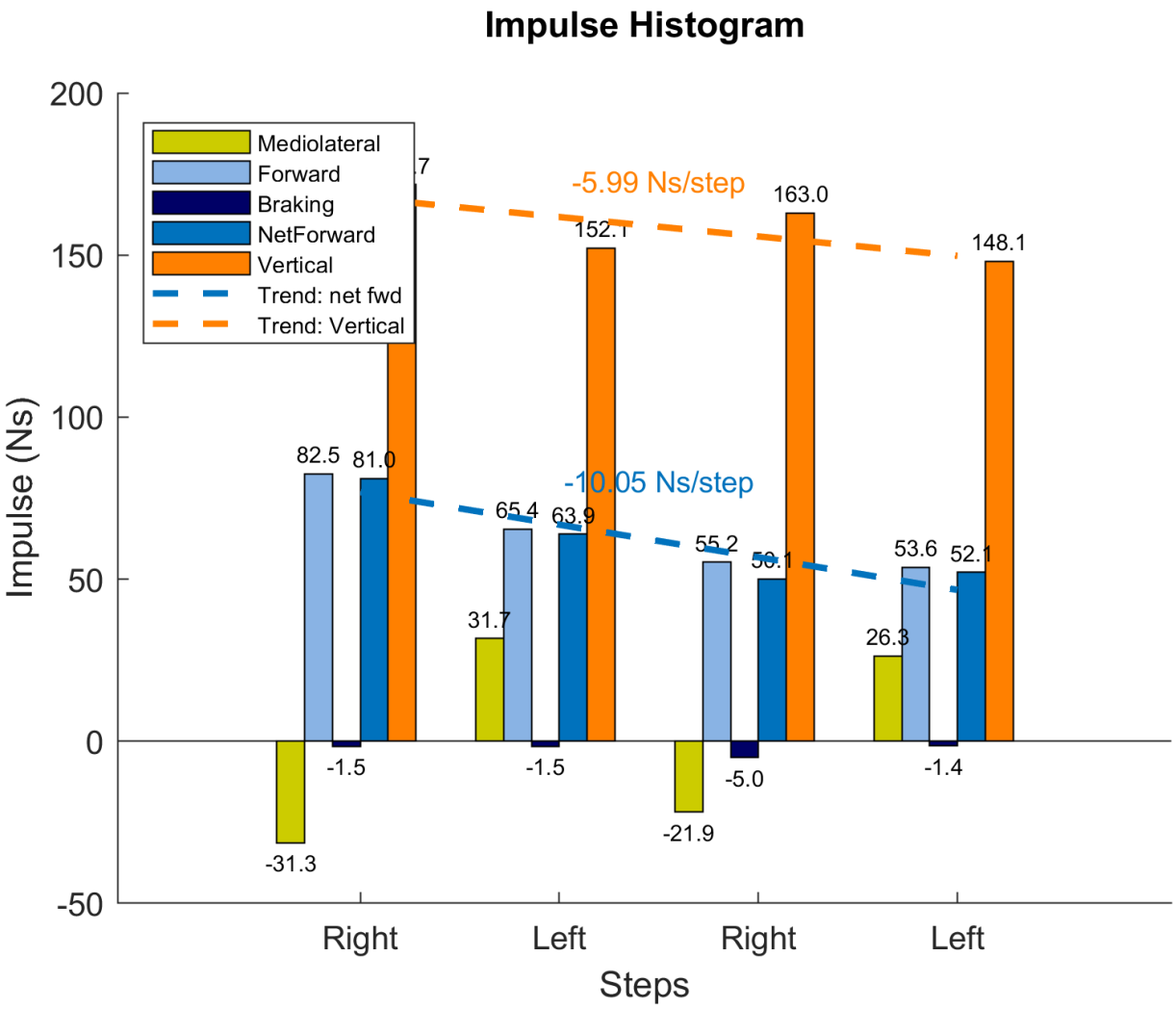

This plot shows the Impulse (Ns) for the steps after block clearance. Two trend lines are drawn to show the trend regarding Impulses generated at each step, both in Vertical and Net-Forward direction.

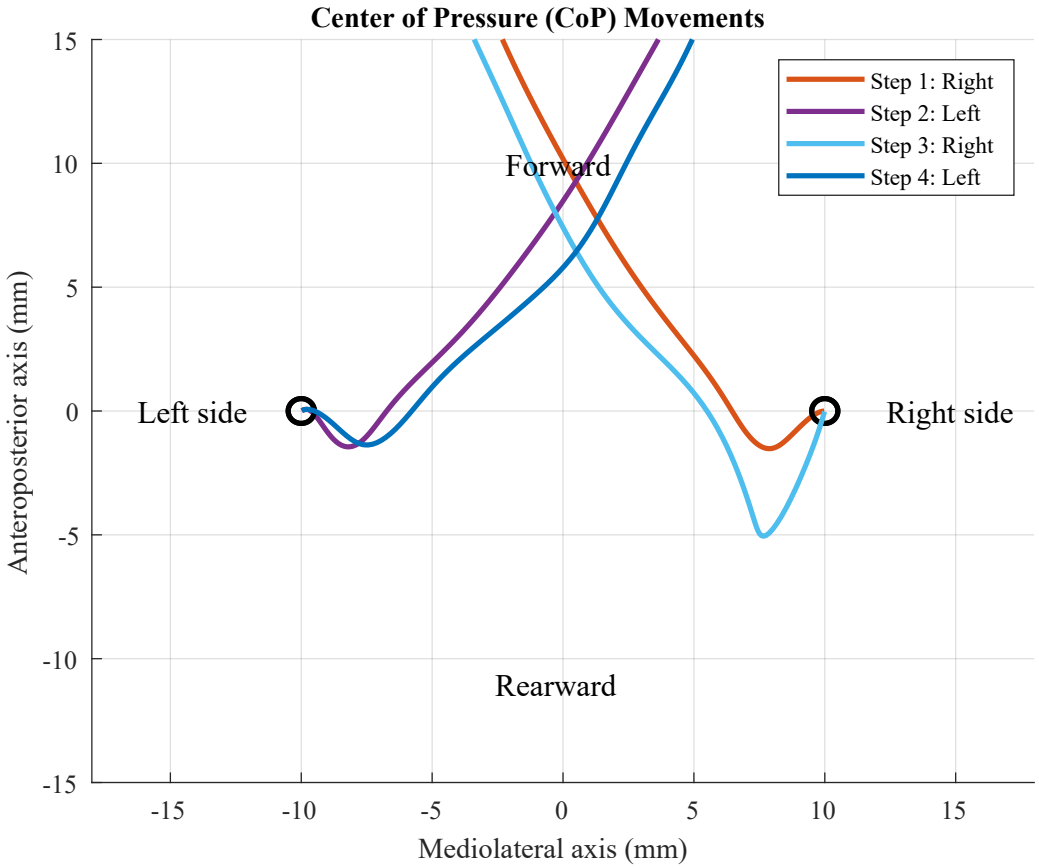

This Plot shows a vertical view of the CoP for each of the steps after block clearance.Right steps start on the right side of the plot, in the black circle. Left steps start on the left side of the plot. This graph can be used to compare the center of pressure between steps, especially if anomalies are found between steps or impulses.

Capitolo 4. Tables: Block Parameters and Steps Parameters

Impulses: every step.

Leg	Mediolateral (Ns)	Propulsive (Ns)	Braking (Ns)	Resulting (Ns)	Vertical (Ns)
Right	-31.30	82.50	-1.50	81.00	171.70
Left	31.70	65.40	-1.50	63.90	152.10
Right	-21.90	55.20	-5.00	50.10	163.00
Left	26.30	53.60	-1.40	52.10	148.10

This table shows the impulses for each step, in order. Mediolateral, Anteroposterior and Vertical components are shown. The Anteroposterior component is split in 3: propulsive, braking, resulting. All Impulses are expressed in Newton-Seconds (Ns).

GRF peaks: every step.

Leg	Mediolateral GRF (N)	Anteroposterior GRF (N)	Vertical GRF (N)
Right	-294.90	645.40	1406.80
Left	302.30	644.70	1478.90
Right	-345.50	528.20	1787.40
Left	380.50	674.30	1912.20

This table shows the GRF peaks for each step, in order. Mediolateral, Anteroposterior and Vertical components are shown.All GRF are expressed in Newton (N).

Ratios: horizontal impulse with respect to vertical impulse.

Leg	Ratio
Right	0.47
Left	0.42
Right	0.31
Left	0.35

In this table are shown the ratios between horizontal net impulse and vertical impulse. It is expected to see a decrease in the ratio as the steps follow one another: the athlete moves from the block position into a more vertical, upright position after each step.

TSSR Report

S14, High level athlete, trial OSN 44

Padova - UNIPD

30-Nov-2024

Capitolo 1. Main parameters, steps GRF and Impulses

Main kinematic parameters

Variable Name	Left leg	Right leg	Difference (%)
Speed (m/s)	9.82	9.82	
Step Frequency (Hz)	4.42	4.42	
Contact time (ms)	92	88	4.4
Flight time (ms)	140	132	5.9
Step length (m)	2.25	2.19	2.7
Stride length (m)	NaN	4.44	NaN
Hip displacement (cm)	53.59	50.39	6.2
Support angle (°)	149.5	154.54	3.3
Pelvis excursion (cm)	6.59	6.59	
Leg angular velocity (°/s)	NaN	367.11	NaN

The above table contains the most relevant parameters of the trial, chosen among the full set. The full set can be found at the end of this report.

Steps: GRF (N)

Leg	Mediolateral (N)	Anteroposterior (N)	Vertical (N)
Right	-403.70	611.60	3088.70
Left	414.10	568.30	2927.70
Right	-401.00	623.00	2974.20

This table shows the GRF peaks for each step, in order. Mediolateral, Anteroposterior and Vertical components are shown. All GRF are expressed in Newton (N).

Steps: Impulses (Ns)

Leg	Mediolateral (Ns)	Propulsive (Ns)	Braking (Ns)	Resulting (Ns)	Vertical (Ns)
Right	-8.40	19.70	-12.00	7.60	160.40
Left	4.70	19.40	-14.20	5.20	157.20
Right	-9.30	19.60	-11.80	7.80	149.90

This table shows the impulses for each step, in order. Mediolateral, Anteroposterior and Vertical components are shown. The Anteroposterior component is split in 3: propulsive, braking, resulting. All Impulses are expressed in Newton-Seconds (Ns).

Capitolo 2. Speed

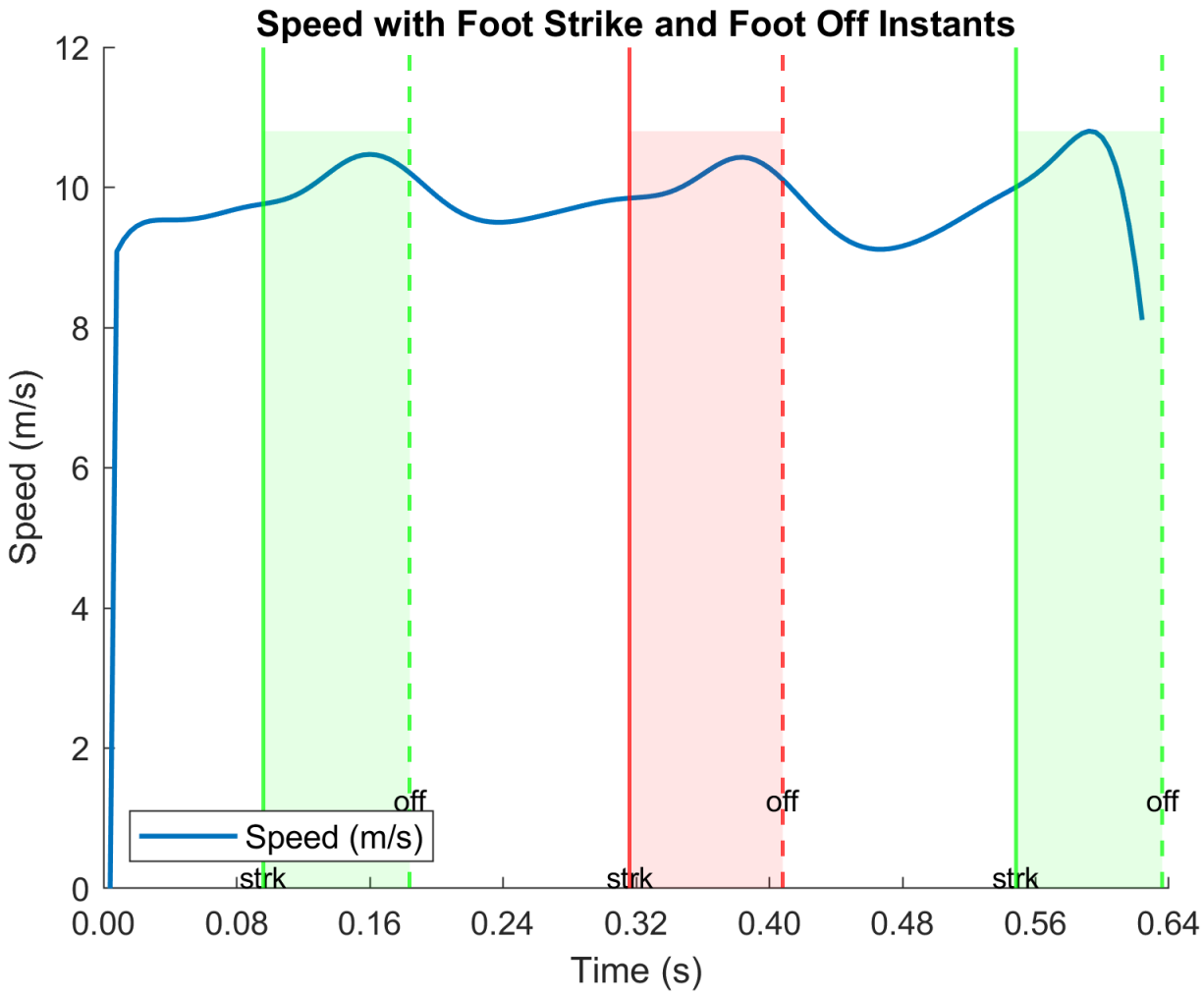

This plot shows the speed curve. Foot strike (continuous line) and Foot Off (dashed line) instants are added to the plot to better visualize the running cycle. A shade is added between the lines to represent the time during which the foot is in contact with the ground. Green color is used for right foot, while red for left leg. Note: Spikes in the speed curve may be issue-related to the tracking of Sacrum Marker (S). Below, the plots show the GRF (N) components for the steps after block clearance. Two trend lines are drawn to show the trend regarding peak GRF generated at each step, both in Vertical and Horizontal axis. Note: maximum GRF alone is not enough to analyze the steps: the following graph about impulses considers the whole force applied over the contact time. Then, the second plot shows the Impulse (Ns) for the steps after block clearance. Two trend lines are drawn to show the trend regarding Impulses generated at each step, both in Vertical and Net-Forward direction.

Capitolo 3. GRF and Impulses

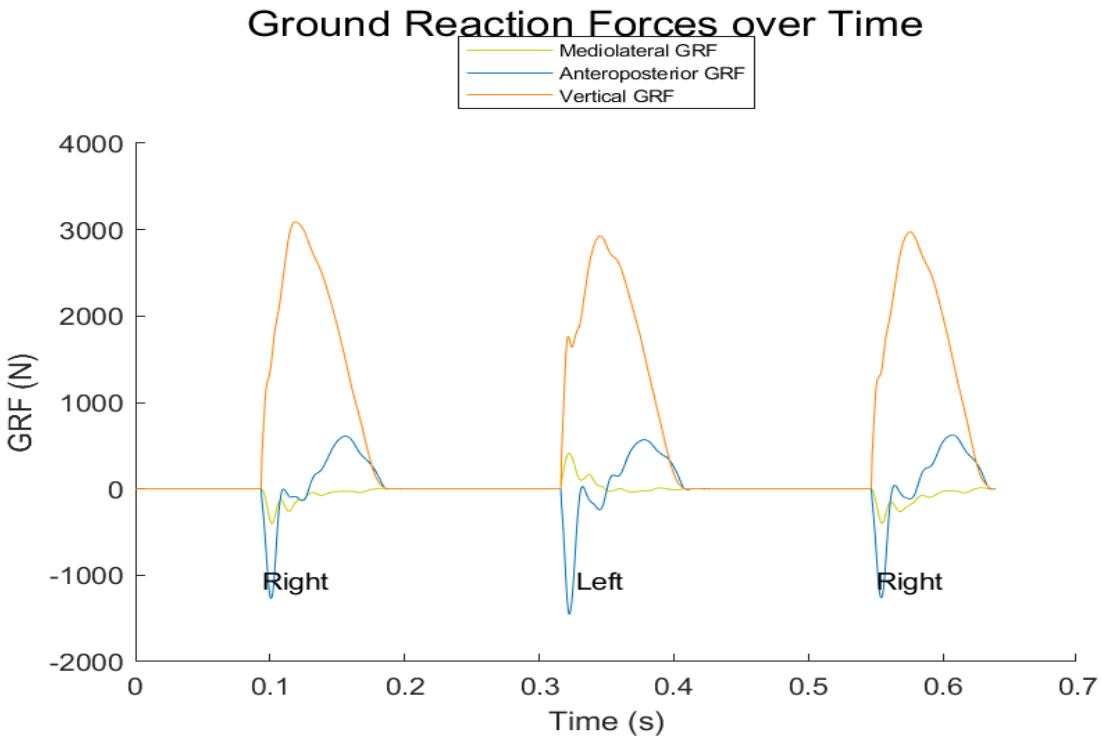

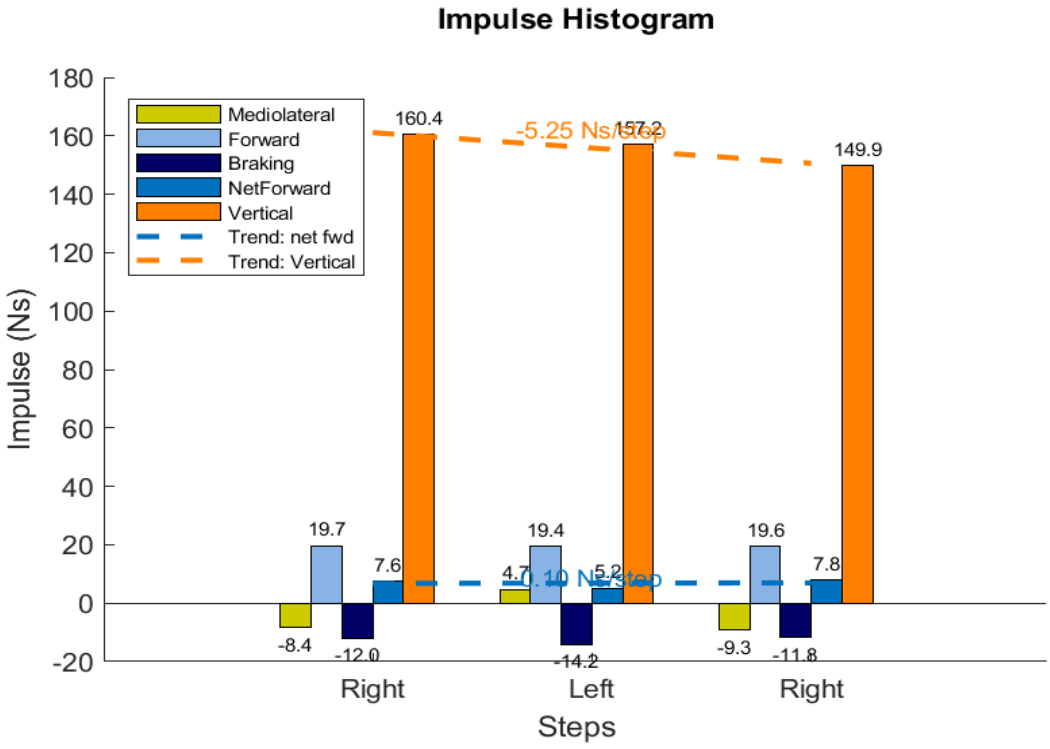

Capitolo 4. Center of Pressure (CoP) Movements

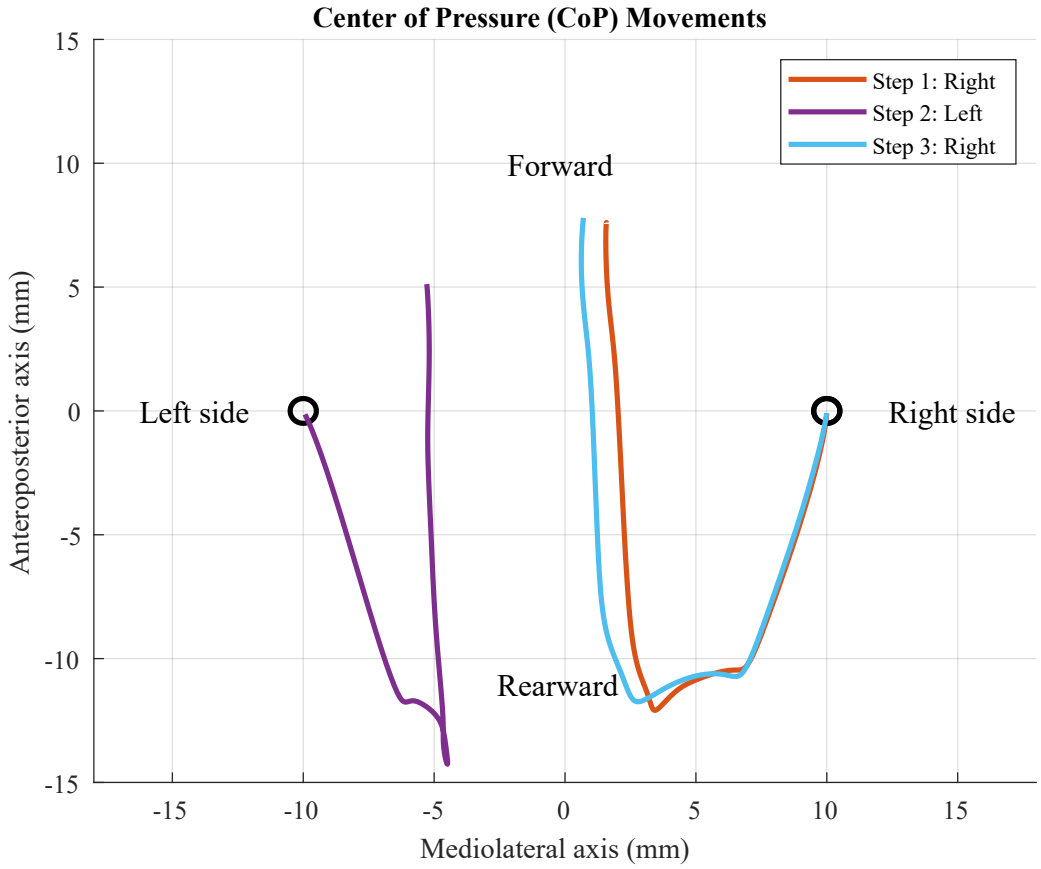

This Plot shows a vertical view of the CoP for each of the steps after block clearance. Right steps start on the right side of the plot. Left steps start on the left side of the plot. This graph can be used to compare the consistency of CoP between steps, especially if anomalies are found on steps or impulses. Below, the averaged kinetic parameters for each leg.

Kinetic Parameters - Averaged

Kinetic Variables	Left Leg	Right Leg	Difference (%)
Peak Propulsive GRF (N)	568.3	617.3	8.3
Peak Vertical GRF (N)	2927.7	3031.45	3.5
Peak lateral GRF (N)	414.1	-402.35	13897
Vertical Impulse (Ns)	157.2	155.15	1.3
Propulsive Impulse (Ns)	19.4	19.65	1.3
Braking Impulse (Ns)	-14.2	-11.9	17.6
Net Forward Impulse (Ns)	5.2	7.7	38.8
Lateral Impulse (Ns)	4.7	-8.85	653
Propulsive ratio (Horiz/vert)	0.033	0.05	41

Capitolo 5. Full Kinematic parameters: Spatial, Temporal, Angular.

The following 3 tables contain the Spatial, Temporal, and Angular parameters divided by leg, with the absolute distance shown as percentage (%) on the last column. Note: "NaN" is shown when not enough steps were captured to compute the data.

Spatial Parameters

Variable Name	Left leg	Right leg	Difference (%)
Hip Displacement Normalized (cm/leg)	0.62	0.58	6.7
Hip Displacement (cm)	53.59	50.39	6.1
Maximum Sacrum Position (cm)	100.41	100.41	
Minimum Sacrum Position (cm)	93.82	93.82	
Range of Sacrum Motion (cm)	6.59	6.59	
Step Length (m)	2.25	2.19	2.7
Step Length Normalized (m/leg)	2.61	2.54	2.7
Stride Length (m)	NaN	4.44	NaN
Stride Length Normalized (m/leg)	NaN	5.15	NaN

Temporal Parameters

Variable Name	Left leg	Right leg	Difference (%)
Average Speed (m/s)	9.82	9.82	
Contact Time (ms)	92	88	4.40%
Fly Time (ms)	140	132	5.90%
Step Frequency (Hz)	4.42	4.42	

Angular parameters

Variable Name	Left leg	Right leg	Difference (%)
Ankle Angle (°)	89.63	85.34	4.9
Early Extension Angle (°)	-39.86	-47.64	17.8
Early Extension TAV (°/s)	-332.18	-384.18	14.5
Early Flexion Angle (°)	66.77	47.82	33.1
Early Flexion TAV (°/s)	439.29	323.11	30.5
Full Flexion Angle (°)	NaN	88.11	NaN
Full Flexion TAV (°/s)	NaN	367.11	NaN
Push Angle (°)	50.79	52.67	3.6
Shank Angle (°)	-6.01	-12	66.5
Support Angle (°)	149.5	154.54	3.3
Thigh Switch Range (°)	92.96	89.91	3.3
Thigh to Horizontal Angle (°)	-27.3	-21.78	22.5
Thigh to Vertical Angle (°)	25.09	19.9	23.1